The 7th Antarctic Meteorological Observation, Modeling, and Forecasting Workshop

9–11 July 2012

National Center for Atmospheric Research
Boulder, Colorado, USA

NCAR NSF AMPS CIRES ATOC

Preface

The National Center for Atmospheric Research (NCAR) and the University of Colorado welcome you to the 7th Antarctic Meteorological Observation, Modeling, and Forecasting (AMOMF) Workshop in Boulder, Colorado, USA. The workshop brings together those with both research and operational/logistical interests in Antarctic meteorology and weather forecasting. It serves as an international forum for current results and ideas in Antarctic meteorology, numerical weather prediction, and weather forecasting. While the workshop has a meteorological focus, other scientific disciplines with related Antarctic interests and results are welcome.

The AMOMF Workshop's history stems from annual meetings on the activities of the Antarctic Meteorological Research Center (AMRC), Antarctic Automated Weather Station (AWS), and Antarctic Mesoscale Prediction System (AMPS). Thus, the workshop includes discussions on the relationships between the AMPS/AMRC/AWS programs, other American efforts, and international activities and Antarctic forecasting, logistical support, and science. Submissions of interest to these programs, to Antarctic weather researchers and forecasters, and to support for international Antarctic efforts have been welcome. Over the years, the workshop participants have benefitted from this dialog on the shared issues and goals of the Antarctic meteorology and related communities.

We thank all of those who have submitted papers and extended abstracts and who will attend the workshop. We look forward to active participation by all and anticipate that the sessions will be informative and productive.

Special recognition is due to Ms. Kris Marwitz and Ms. Michelle Menard of NCAR for their handling of logistics and for producing the preprint volume.

The 7th Antarctic Meteorological Observation, Modeling, and Forecasting Workshop is organized by NCAR and the University of Colorado. It is hosted this year by the Mesoscale and Microscale Meteorology Division of NCAR and sponsored by the National Science Foundation Office of Polar Programs.

Jordan G. Powers, National Center for Atmospheric Research
John J. Cassano, University of Colorado
Workshop Organizers

9 July 2012

7th Antarctic Meteorological Observation, Modeling, and Forecasting Workshop

National Center for Atmospheric Research
Boulder, Colorado, USA
9–11 July 2012

Monday, July 9, 2012

0900–0910 Opening Remarks and Information
Jordan G. Powers
National Center for Atmospheric Research

0910–0940 Our Antarctic Community— Remembrances
Chairperson: Jordan G. Powers

Speakers Note: In all regular sessions, talks are allotted 20 minutes. Additional scheduled time in sessions is reserved for discussion.

0940–1020 Antarctic Numerical Modeling 1
Chairperson: John J. Cassano

Initial Verification of Access-P: The Polar Version of the Bureau of Meteorology's Atmospheric Forecasting Model
Phillip A Reid
Australian Bureau of Meteorology, Centre for Australian Weather and Climate Research

AMPS Update— July 2012
Kevin W. Manning and Jordan G. Powers
National Center for Atmospheric Research

1020–1040 Break

1040–1200 Antarctic Numerical Modeling 1 (cont'd)

Current Status and Future Plans for OSU AMPS Database
Sheng-Hung Wang, David H. Bromwich, and Julien P. Nicolas
Polar Meteorology Group, Byrd Polar Research Center, The Ohio State University

Verification of AMPS Wind Forecasts for the DROMLAN Area during Antarctic Summer Season 2011–12
Michael Knobelsdorf
German Weather Service/Deutscher Wetterdienst

Antarctic Numerical Modeling 2
Chairperson: Mark W. Seefeldt

A Comprehensive Evaluation of Polar WRF Forecast Performance in Antarctica
David H. Bromwich[1,2], Francis O. Otieno[1], Keith M. Hines[1], Kevin W. Manning[3], and Elad Shilo[4]
[1]Polar Meteorology Group, Byrd Polar Research Center, The Ohio State University
[2]Atmospheric Sciences Program, Department of Geography, The Ohio State University
[3]National Center for Atmospheric Research
[4]Israeli Meteorological Service

Clouds over the Larsen Ice Shelf: Observations Compared to WRF
Tom Lachlan-Cope
British Antarctic Survey

1200–1330 Lunch

1300–1350 Antarctic Numerical Modeling 2 (cont'd)

Evaluation of WRF Ensemble-Based Variational (EnVar) Data Assimilation Scheme for an Antarctic Cyclone Study
Chengsi Liu
University of South Florida

1350–1510 Antarctic Observational and Logistical Efforts 1
Chairperson: Chester Clogston

BAS Antarctic Peninsula Automatic Weather Station Update 2011/12
Steven R. Colwell
British Antarctic Survey

USAP Antarctic Automatic Weather Station Program Status and Field Report
Lee J. Welhouse[1], Matthew A. Lazzara[1], Jonathan E. Thom[1], Linda M. Keller[2], George A. Weidner[2], John J. Cassano[3], and Alice DuVivier[3]
[1]Antarctic Meteorological Research Center, Space Science and Engineering Center
[2]Department of Atmospheric and Oceanic Sciences, University of Wisconsin–Madison
[3]Department of Atmospheric and Oceanic Sciences, University of Colorado

Meteorological Observations at Aboa, Antarctica during Austral Summer 2010–2011
Priit Tisler[1], Rostislav Kouznetsov[1,2], Timo Palo[1,3], Timo Vihma[1], and Tiina Kilpeläinen[1,4]
[1] Finnish Meteorological Institute
[2] A.M. Obukhov Institute of Atmospheric Physics
[3] University of Tartu
[4] University of Helsinki

1510–1530 Break

1530–1615 Antarctic Observational and Logistical Efforts 1 (cont'd)

Two Summer Seasons at Union Glacier: 2010–2011/2011–2012
Marc DeKeyser
Antarctic Logistics and Expeditions

The British Antarctic Survey's New Halley VI Station
Steven R. Colwell
British Antarctic Survey

1615–1700 Poster Session

1700 Adjourn

Tuesday, July 10, 2012

0900–1030 Antarctic Observational and Logistical Efforts 2
Chairperson: Steven R. Colwell

Observing the Antarctic Atmosphere with Small Unmanned Meteorological Observers (SUMO)
John. J. Cassano
Cooperative Institute for Research in Environmental Sciences/Department of Atmospheric and Oceanic Science
University of Colorado

Augmentation of the Ross Island Region AWS Network with New Autonomous Sensors for Measuring Atmospheric Composition in Antarctica
L.E. Kalnajs
Laboratory for Atmospheric and Space Physics
University of Colorado

Power, Data Telemetry, and Ideas for Additional Sensors on Automatic Weather Stations
Jonathan E. Thom, Lee J. Welhouse, and Matthew A. Lazzara
Antarctic Meteorological Research Center
Space Science and Engineering Center
University of Wisconsin–Madison

Antarctic Automatic Weather Station Temperature Measurements: How Good Are They?
George A. Weidner[2], Jonathan E. Thom[1,2], Lee J. Welhouse[1], Matthew A. Lazzara[1], Linda M. Keller[2], and David E. Mikolajczyk[1]
[1]Antarctic Meteorological Research Center, Space Science and Engineering Center, University of Wisconsin–Madison
[2]Department of Atmospheric and Oceanic Sciences, University of Wisconsin–Madison

1030–1050 Break

1050–1200 Antarctic Observational and Modeling Studies 1
Chairperson: David H. Bromwich

Investigating a Unique Summertime Precipitation Event in the McMurdo Dry Valleys (MDV), Antarctica
Tanja Dallafior, Marwan Katurji, Iman Soltanzadeh, and Peyman Zawar-Reza
Centre for Atmospheric Research, University of Canterbury

High-Resolution Numerical Analysis of Up-Valley Summer Flow in Miers Valley
Iman Soltanzadeh, Peyman Zawar-Reza, Marwan Katurji, and Tanja Dallafior
Centre for Atmospheric Research, University of Canterbury

Characterizing and Predicting Surface Melt in Antarctica
David B. Reusch[1], Derrick J. Lampkin[2], and David P. Schneider[3]
[1]New Mexico Institute of Mining and Technology
[2]The Pennsylvania State University
[3]National Center for Atmospheric Research

1200–1330 Lunch

1330–1500 Antarctic Observational and Modeling Studies 1 (cont'd)

The Synoptic Settings of Strong Wind Events at McMurdo Station
Jordan G. Powers
National Center for Atmospheric Research

Analysis of High Winds over the Ross Ice Shelf, Antarctica: Barrier Winds along the Transantarctic Mountains
Melissa A. Nigro and John J. Cassano
Cooperative Institute for Research in Environmental Sciences / Department of Atmospheric and Oceanic Sciences, University of Colorado

Antarctic Observational and Modeling Studies 2
Chairperson: Matthew A. Lazzara

Air-Sea Fluxes in Terra Nova Bay, Antarctica from In Situ Aircraft Measurements
Shelley L. Knuth and John J. Cassano
Department of Atmospheric and Oceanic Sciences/Cooperative Institute for Environmental Studies, University of Colorado

The Application of Automatic Weather Station (AWS) Observations and Antarctic Mesoscale Prediction System (AMPS) Data to the Analysis of Surface Level Ozone Observations in the Ross Island Region
Mark Seefeldt[1,2], Michael Tice[1], Allison Burg[1], Lars Kalnajs[3], and Matthew Lazzara[4]
[1]Department of Engineering—Physics—Systems, Providence College
[2]Cooperative Institute for Research in Environmental Sciences, University of Colorado
[3]Laboratory for Atmospheric and Space Physics, University of Colorado
[4]Antarctic Meteorology Research Center, University of Wisconsin–Madison

1500–1520 Break

1520–1600 Antarctic Observational and Modeling Studies 2 (cont'd)

A Study of Winter Static Stability Regimes in the Dry Valleys using Pseudo-vertical Profiles of Temperature
Peyman Zawar-Reza[1], Marwan Katurji[1,2], Bob Noonan[1], Iman Soltanzadeh[1], Tanja Dallafior[1,3], and Sharon Zhong[2]
[1]Centre for Atmospheric Research, University of Canterbury
[2]Department of Geography, Michigan State University
[3]Institute for Atmospheric and Climate Science, Eidgenössische Technische Hochschule (ETH) Zürich

Synoptic Control of the Atmospheric Meridional Moisture Transport into the Antarctic Interior: A New Approach
Maria Tsukernik
Brown University

1600–1700 SCAR Expert Group on Operational Meteorology in the Antarctic (EGOMA) Open Meeting
Chairperson: Steven R. Colwell

GCOS, SCAR, and EC–PORS
Steven R. Colwell
British Antarctic Survey

General Discussion and Participant Input

1700 Adjourn

Wednesday, July 11, 2012

0900–1030 Antarctic Observational and Modeling Studies 3
Chairperson: Kevin W. Manning

The Use of AMPS in Ice Core Studies— Solved and Unsolved Problems
Elisabeth Schlosser[1], Jordan G. Powers[2], Michael G. Duda[2], and Kevin W. Manning[2]
[1]Institute of Meteorology and Geophysics, University of Innsbruck
[2]National Center of Atmospheric Research

The Role of Atmospheric Rivers in Accumulation in Dronning Maud Land, East Antarctica
I. V. Gorodetskaya[1], N. P. M. van Lipzig[1], F. M. Ralph[2], G. A. Wick[2], M. Tsukernik[3], A. W. Delcloo[4], and A. Mangold[4]
[1]Catholic University of Leuven
[2]National Oceanic and Atmospheric Administration
[3]Brown University
[4]Royal Meteorological Institute of Belgium

Insight into Antarctic Precipitable Water from AMPS Forecasts and New Ground-Based GPS Measurements
Julien P. Nicolas[1], David H. Bromwich[1], and Ian D. Thomas[2]
[1]Polar Meteorology Group, Byrd Polar Research Center and Atmospheric Sciences Program, Department of Geography, The Ohio State University
[2]School of Civil Engineering and Geosciences, Newcastle University

Upcoming East Antarctic Sea Ice Weather Buoy Deployments
Katherine Leonard[1] and Ted Maksym[2]
University of Colorado and École Polytechnique Fédérale de Lausanne
Woods Hole Oceanographic Institute

1030–1050 Break

1050–1200 Open Session: Community Discussions
Chairperson: Jordan G. Powers

AMPS User Feedback

Logistical Needs and Issues

Observational Programs Needs and Issues

1200 Workshop Adjourn

Posters

Regional Climate Research in the Antarctic Peninsula Region and Scheme of the Long-Range Forecast of Mean Monthly Air Temperature
Vazira Martazinova and Vladislav Tymofeyev
Ukrainian Research Hydrometeorological Institute

Evaluation of the Antarctic Mesoscale Prediction System (AMPS) in the Ross Island Region Based on a Comparison to Automatic Weather Station (AWS) Observations
Michael Tice[1] and Mark Seefeldt[1,2]
[1]Department of Engineering—Physics—Systems, Providence College
[2]Cooperative Institute for Research in Environmental Sciences, University of Colorado

An Analysis of 10-years (2001–2010) of Automatic Weather Station (AWS) Observations in the Ross Island Region
Allison Burg[1] and Mark Seefeldt[1,2]
[1]Department of Engineering—Physics—Systems, Providence College
[2]Cooperative Institute for Research in Environmental Sciences, University of Colorado

Validation of the Diurnal Cycles in Atmospheric Reanalyses over Antarctic Sea Ice
Esa-Matti Tastula[1], Timo Vihma[2], Edgar L Andreas[3], and Boris Galperin[4]
[1]University of South Florida
[2]Finnish Meteorological Institute
[3]Northwest Research Associates
[4]University of South Florida

INITIAL VERIFICATION OF ACCESS-P: THE POLAR VERSION OF THE BUREAU OF METEOROLOGY'S ATMOSPHERIC FORECASTING MODEL

Phillip A Reid[1]
Australian Bureau of Meteorology, CAWCR

Abstract

During summer of 2011/12 the Australian Bureau of Meteorology implemented a new limited area Numerical Weather Prediction model for Antarctic weather forecasts: the Australian Community Climate and Earth-System Simulator – Polar (ACCESS-P). This study will introduce the model and present an initial spatial and station-based verification of screen temperature, surface pressure and 10 metre winds for December 2011 through February 2012. Results suggest a semi-diurnal error in screen temperature associated with sea ice coverage, with a positive forecast temperature bias during night time conditions. Errors in forecast 10 metre wind and surface pressure were relatively consistent through the season; however simulated screen temperatures were systematically worse later in the season. Ongoing verification will provide an objective method of assessing forecast performance upon implementing improvements within the model.

1. Introduction

Australia's Bureau of Meteorology (Bureau) operates summertime forecasting offices in the two main Antarctic Stations of Casey and Davis for the support of Antarctic operations, aviation and research field parties. The Bureau has been providing high resolution numerical weather prediction (NWP) output for forecasting support over the last 10 years, initially from an Antarctic version of the Bureau's LAPS (Limited Area Prediction System (Adams, 2004), with an East Antarctic domain running from July 2001, followed by a polar-stereographic version (polarLAPS) covering Antarctica and much of the Southern Ocean in October 2005. Due to a change in computing platform and NWP global and regional model in 2010 the polar LAPS model ceased running.

ACCESS-P (Australian Community Climate Earth System Simulator – Polar) replaces polarLAPS and nests within the Bureau global ACCESS model. The ACCESS systems are based on the UK Met Office Unified Model/Variational Assimilation (UM/VAR) system and are run operationally globally (ACCESS-G) and on a number of sub-domains relevant to the Australian community.

Currently ACCESS-P runs in a semi-operational (research) environment and nests within the most recent developmental version of ACCESS-G (APS1 – Australian Parallel Suite 1). Running ACCESS-P within a developmental global model has caused some discontinuities in model results (forecast guidance), and these will be discussed in this paper. In late 2012 APS1 will move from developmental to operational and hence will provide a more consistent basis for subsequent nested models, including ACCESS-P.

ACCESS-P runs on a rotated pole 25km grid and nests within a global model of 40km resolution. Vertical resolution is 70 hybrid levels. Model runs provide 72 hour forecasts starting at 00Z and 12Z. The model is atmosphere only. Further information about the original ACCESS implementation (APS0) can be found in the NMOC Operations Bulletin No.83 (NMOC, 2010).

This paper presents an initial verification of several variables from the ACCESS-P model for the summertime forecast period of December 2011 through February 2012. Results are shown as: spatial maps; plots of area averaged monthly mean values; plots of daily 24 hour forecast errors; and finally a comparison of model analysis versus station based observations. Aims for this study, although not fully realised at this stage, are to:

- Look for and understand any systematic errors that may exist in the model.
- Look for weaknesses in the model's performance in order to understand how best to optimise the system for the polar applications (model improvements).
- Provide a basis against which to compare future model enhancements.
- Promote discussion and an exchange of ideas regarding Antarctic modelling and forecast verification in the wider community.

The analysis performed here uses the usual standard verification tools, predominantly root

[1] *Corresponding author address:* Bureau of Meteorology (CAWCR), GPO Box 727, Hobart, Tasmania, 7001, Australia. p.reid@bom.gov.au

mean square error (RMSE) and mean error (ME: forecast minus analysis). Observations from Casey station (latitude -66.282°, longitude 110.527°, height of 40 metres) are compared with interpolated analyses. Model data are interpolated to station latitude and longitude via distance weighting and screen temperature is corrected using a simple lapse rate of 1°C per 100m.

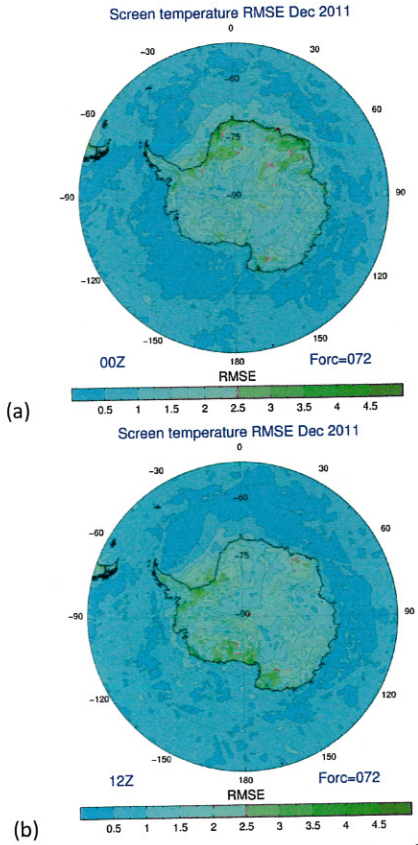

Figure 1 ACCESS-P screen temperature RMSE (°C) for: (a) December 2011 00Z 72 hour forecast, (b) December 2011 12Z 72 hour forecast.

2. Results

Spatial analysis

The spatial pattern of screen temperature RMSE (analysis compared to the respective 72 hour forecasts) for December 2011 (**Figure 1**) shows a semi-diurnal pattern, with larger errors shown to occur on the night-time side of the Antarctic continent. This is consistent in spatial pattern through each of the 2011/12 summer months. The mean error of the same forecasts (**Figure 2**) shows a warm semi-diurnal bias over sea ice areas for December 2011 (compare with the sea ice map at http://www.cawcr.gov.au/staff/preid/seaice/images/seaice_gsfc/monthly_seaice_ssta_201112.png).

This pattern does not show up in subsequent summer months as sea ice has substantially retreated by the end of December. Both these results (biases within the RMSE and ME of screen temperature) are consistent with those from ACCESS-G (not shown) suggesting that the problem exists within the global model. Examination of screen temperature RMSE from ACCESS-G (not shown) reveals a similar semi-diurnal bias over southern Africa, although the bias there occurs during daylight hours.

A semi-diurnal bias is not evident, or at least is not consistent across all three months, in RMSE for 10 metre winds (**Figure 3**), or for surface pressure (not shown).

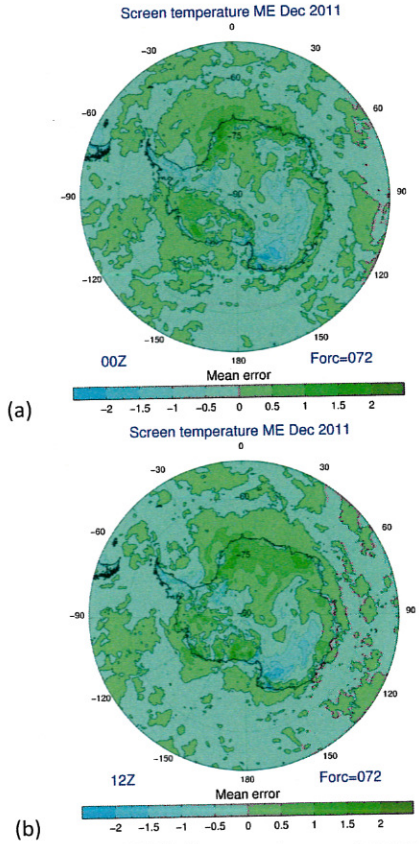

Figure 2 ACCESS-P screen temperature mean error (ME = forecast – analysis) (°C) for: (a) December 2011 00Z 72 hour forecast, (b) December 2011 12Z 72 hour forecast.

Monthly mean forecasts

Figure 4 shows the monthly mean 00Z screen temperature RMSE averaged over the simulated Antarctic continent (all grid points south of 60°S and with topography greater than 100m). Note the considerably larger RMSE in screen temperature for February 2012 in comparison to the previous two

months. This is consistent across both ACCESS-P and ACCESS-G, within both 00Z and 12Z forecasts, and is also readily seen in the increased errors in the maps of February 2012 (similar to **Figure 1** but not shown here). Also curious is the sharp increase in 72 hour RMSE in February 2012 which is not evident in the previous two months.

Monthly average RMSE for both surface pressure (not shown) and wind speed (**Figure 5**) show a different pattern to that of screen temperature. For these variables December 2011 is the worst performing month. However, as was the case for screen temperatures, both variables show a distinct increase in forecast errors at 72 hours during February 2012.

Daily 24 hour forecasts

In an attempt to understand where errors in the forecast model may have been introduced, and to look for further systematic errors, **Figure 6** shows the daily RMSE for all 24 hour forecasts (00Z only) for the entire summer season.

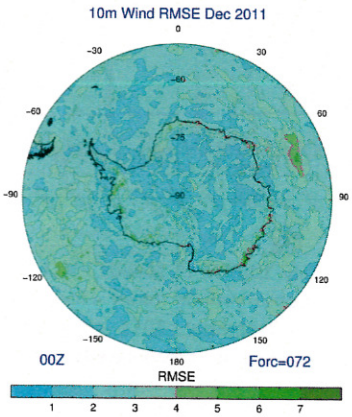

(a)

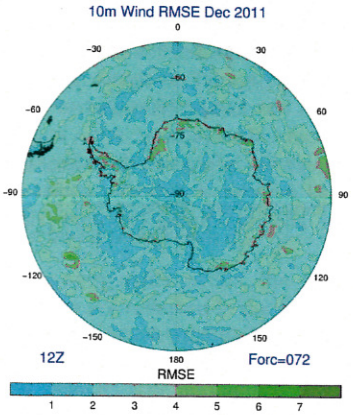

(b)

Figure 3 ACCESS-P wind speed RMSE (ms^{-1}) for: (a) December 2011 00Z 72 hour forecast, (b) December 2011 12Z 72 hour forecast.

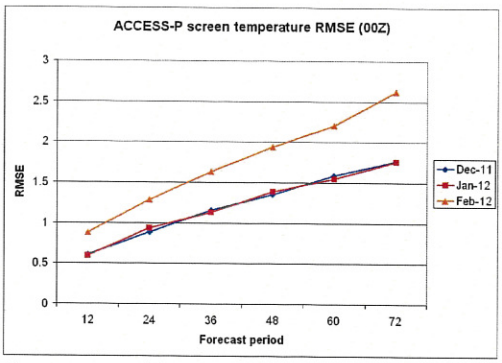

Figure 4 Monthly averages of screen temperature RMSE (°C) from ACCESS-P for all 00Z runs from 1 December 2011 through 29 February 2012. Area averaging is based on all grid points south of 60°S with model topography greater than 100m. Forecasts are compared to respective analysis.

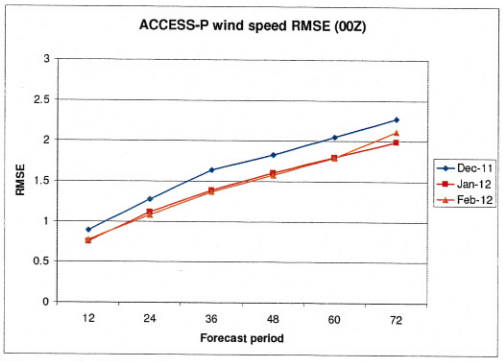

Figure 5 Monthly averages of wind speed RMSE (ms^{-1}) from ACCESS-P for all 00Z runs from 1 December 2011 through 29 February 2012. Area averaging is based on all grid points south of 60°S with model topography greater than 100m. Forecasts are compared to respective analysis.

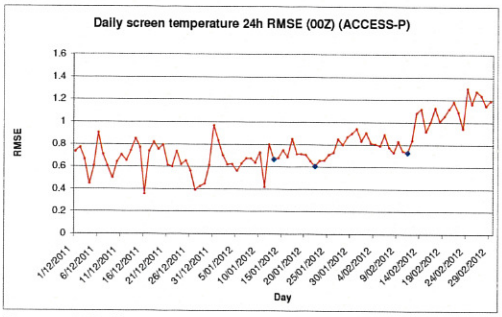

Figure 6 Daily screen temperature RMSE (°C) from ACCESS-P for all 00Z runs from 1 December 2011 through 29 February 2012. 24 hour forecasts are compared to respective analysis. Blue highlighted points are, from left to right, 13 January, 22 January and 11 February 2012.

From this we can see the screen temperature forecasts errors begin to increase from about the 22 January 2012 (as marked on the plot). Prior to mid-January daily RMSE varied considerably, with a reduction in its modulation from about the 13 January. On the 11 February there appears to be a sharp rise in RMSE.

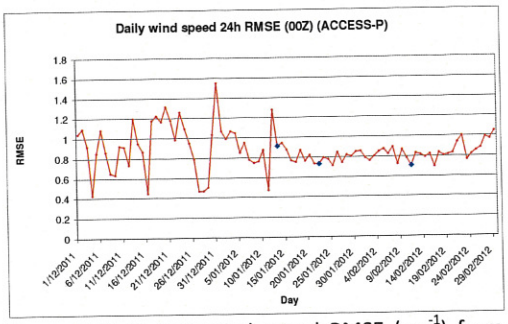

Figure 7 Daily 10m wind speed RMSE (ms^{-1}) from ACCESS-P for all 00Z runs from 1 December 2011 through 29 February 2012. 24 hour forecasts are compared to respective analysis. Blue highlighted points are, from left to right, 13 January, 22 January and 11 February 2012.

Daily values of RMSE for surface pressure (not shown) and wind speed (**Figure 7**) show that prior to mid-January 2012 daily errors were considerably variable, but in the latter half of summer variability decreased substantially. This seems somewhat consistent in timing with the RMSE results of screen temperature.

Observations versus analyses

So far the verification has focused on the performance of the model forecasts. Here we examine the model analysis by comparing it to Casey station observations.

Figure 8 shows the difference between screen temperatures from the analysis and observations for all 00Z and 12Z model runs. Model analysis underestimates Casey screen temperatures by as much as 5°C. Also apparent is a drift later in the season towards a more persistently cool analysis, although the analysis also seems to be more persistently cool during early December 2011 as well.

Interpolated wind analyses are compared to Casey wind speeds in **Figure 9**. Wind speeds from the model analysis are a reasonable representation of observations; however the analysis sometimes delays the onset of strong wind events by 12 hours and generally underestimates the observed wind speeds during strong wind events.

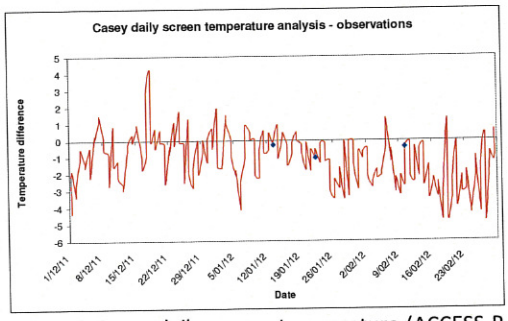

Figure 8 Casey daily screen temperature (ACCESS-P analysis minus observations) for all 00Z and 12Z from 1 December 2011 through 29 February 2012. Analysis is interpolated to Casey latitude and longitude and lapse rate adjusted. Blue highlighted points are, from left to right, 13 January, 22 January and 11 February 2012.

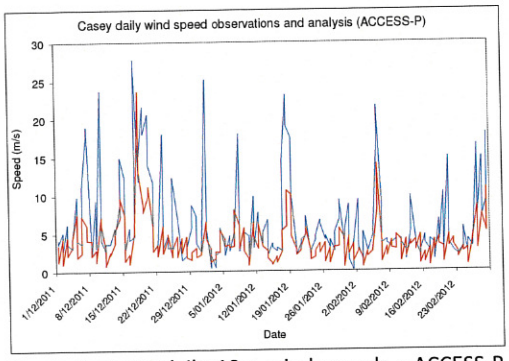

Figure 9 Casey daily 10m wind speeds - ACCESS-P analysis (red) and observations (blue) - for all 00Z and 12Z from 1 December 2011 through 29 February 2012. Analysis is interpolated to Casey latitude and longitude.

Given the variable nature of the observed wind speeds it is unclear whether there is any drift in the performance of the model analyses over the summer months. A box and whisker plot of screen temperatures from observations and analyses reveals that although the interpolated analyses have a cool bias for all months, a distinctly cooler bias developed in the analyses during February (**Figure 10**).

3. Discussion

This verification is at an early stage, so many of the model's idiosyncrasies shown above are not yet fully understood. It is apparent that changes were made in the global model (ACCESS-G) and that these contributed to ACCESS-P model performance, probably negatively when examining screen temperature alone.

A semi-diurnal bias in screen temperature forecasts, as measured using RMSE, is not uncommon (e.g. it is evident in ACCESS-G APS0, NMOC, 2010, their Figure 13). The warm semi-diurnal bias in screen temperature mean error (forecast minus analysis) over sea ice is perhaps evidence of the model's inability to correctly handle sea ice and associated fluxes. Corrections made to ACCESS-G sea ice on 19 January 2012 may be responsible for the model's degrading performance in both the analyses and forecasts after that period. It is possible that improved performance in some variables (surface pressure and wind speed) came at the expense of the performance in screen temperature.

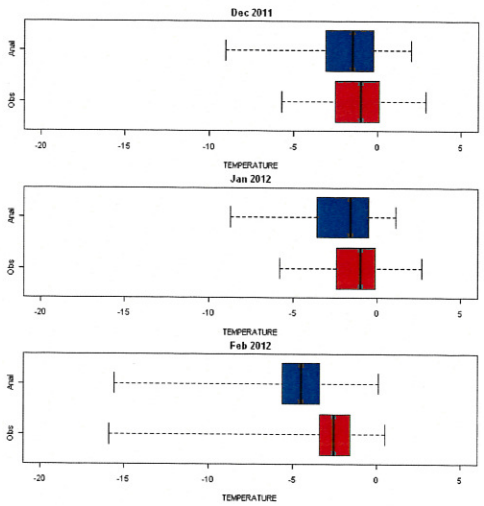

Figure 10 Box and whisker plot showing screen temperature observations and interpolated grid point analysis from ACCESS-P to Casey for December 2011 and January, February 2012. The summary statistics used to create the box and whisker plots are the median of the data, the lower and upper quartiles (25% and 75%) and the minimum and maximum values.

4. Conclusions

Errors in the model's performance, as shown above, are possibly the result of:

- Changes made within the global model. These are reflected in the discontinuities in the daily verification statistics.
- The model's non-polar-specific physics.
- The model's inability to handle a changing polar environment – sea ice retreat.

Given the uncertainty in where the errors lie, there is currently little sense in making wholesale changes to ACCESS-P until further analysis is complete and the model is nested within a stable operational environment.

Further model analysis will include an extension of the verification statistics to encompass the period September 2011 through May 2012. This may show how the model performed under sea ice retreat and advance conditions. An examination of low level model temperatures, rather than using screen temperature which is a diagnostic variable, may also be worthwhile.

Later in 2012 the Bureau will adopt APS1 as its operational forecast model. ACCESS-P will nest within that model providing it with an environment that is stable and where any changes that do occur are documented and verified.

Verification analysis of ACCESS-P will continue. Future verification statistics will include an analysis of not only a simulated Antarctic continent but also a simulated sea ice environment in order to track improvements in sea ice model performance.

References

Adams N. 2004 A numerical modeling study of the weather in East Antarctica and the surrounding Southern Ocean. *Weather and Forecasting,* Vol. 19, No. 4, 653-672.

NMOC Operations Bulletins, No 83, 2010: "Operational implementation of the ACCESS Numerical Weather Prediction systems", http://www.bom.gov.au/australia/charts/bulletins/apob83.pdf

AMPS Update – July 2012

Kevin W. Manning
Jordan G. Powers

Mesoscale and Microscale Meteorology Division
NCAR Earth System Laboratory
National Center for Atmospheric Research
Boulder, CO, 80307

1. The Antarctic Mesoscale Prediction System

The Antarctic Mesoscale Prediction System (AMPS) is a real-time, experimental, numerical weather prediction system for Antarctica, offering timely high-resolution NWP products in support of the United States Antarctic Program's weather forecasting and logistical needs. AMPS is a collaboration between the National Center for Atmospheric Research (NCAR) and they Byrd Polar Research Center (BPRC) of the Ohio State University, and is sponsored by the National Science Foundation. The targeted users for AMPS data are the USAP forecasters from the Space and Naval Warfare Systems Center Atlantic, based in Charleston, SC and McMurdo Station, Antarctica.

McMurdo Station is the the primary hub of USAP operations in Antarctica, so AMPS offers its highest-resolution products (on a 1.7-km grid) over the Ross Island and McMurdo Station region. Due to the continental coverage of AMPS' larger grids, as well as the ready availability of AMPS text, graphical, and GRIB-formatted products through the project's web page (http://www.mmm.ucar.edu/rt/amps), forecasters for other national Antarctic programs have found the AMPS data to be useful for their needs.

AMPS also maintains a long-term archive (offline) of AMPS model output. These archived forecasts have been used by Antarctic researchers in a variety of projects, ranging from case studies of high-impact weather situations, to seasonal and multi-year climatological studies.

2. New this year

The model currently used in AMPS is based on the WRF V3.2.1 release, with polar modifications. This version was implemented in AMPS in April of 2011. The AMPS team has kept this configuration stable this past year, with no significant changes to the WRF model. At the data assimilation step, we have made some adjustments to the WRFDA[1] handling of AMSU radiances in order to maintain the stability of the bias-correction terms for satellite radiances.

In support of forecasting for field activities in the Pine Island Glacier (PIG) region, we implemented a one-way nest for PIG, beginning 29 Nov 2011. This nest provides locally higher-resolution (5-km grid) model data than the AMPS continental-scale, 15-km grid (Fig. 1).

Following up on the following plotting window we implemented last year to follow the *R/V Nathaniel B. Palmer*, we have added a window to follow *R/V Laurence M. Gould*. These windows plot sub-regions of the AMPS 15-km grid (or 45-km grid, depending on the location of the vessel), centered on the ship.

3. Recent Tests

It is important for AMPS to keep up-to-date with recent releases of the WRF model, both to implement fixes to problems found in the WRF code and to take advantage of new features introduced into WRF. Additionally, new developments in the polar modifications may be available for more recent WRF releases.

To that end, we have tested WRF V3.3.1 (with polar modifications) in the AMPS configuration. Verification results based on comparisons to surface AWS observations showed little difference between version 3.3.1 and the V3.2.1 currently used in AMPS,. The only consistent difference was slightly higher temperatures (on the order of tenths of K) in V3.3.1. These results suggest no immediate need to upgrade, but no real reason to avoid upgrading, either.

[1] WRFDA is the data assimilation package for WRF.

We have also tested in the AMPS configuration the MYNN surface layer and PBL schemes within version 3.3.1. These results showed a slight improvement in the near-surface wind speed bias (i.e., weaker surface winds overall) and suggest that a switch to using MYNN surface layer and PBL schemes should be considered. We have tested the use of soundings retrieved from the AIRS (Atmospheric Infrared Sounder) satellite data in the AMPS data assimilation step . Results were mixed, but indicate an overall degradation of the forecast when we assimilate the AIRS soundings. Therefore, assimilation of AIRS data is not planned, though further investigation may be in order.

4. Upcoming

In the summer or autumn of 2012, we will acquire new computing hardware for AMPS. The new computer, to be called "Erebus" and to be hosted at the NCAR-Wyoming Supercomputing Center in Cheyenne, Wyoming, represents approximately 15 to 20 times the current computing capacity of AMPS.

This new computing capacity will offer new possibilities for AMPS. AMPS will likely move to higher-resolution forecast grids. Other possibilities include larger-area grids, ensemble forecast products, or more comprehensive testing, in the Antarctic environment, of model physics parameterizations and modifications. In more experimental areas, we may begin to test computationally-intensive tasks such as more sophisticated data assimilation techniques or coupled atmosphere/ocean/ice modeling.

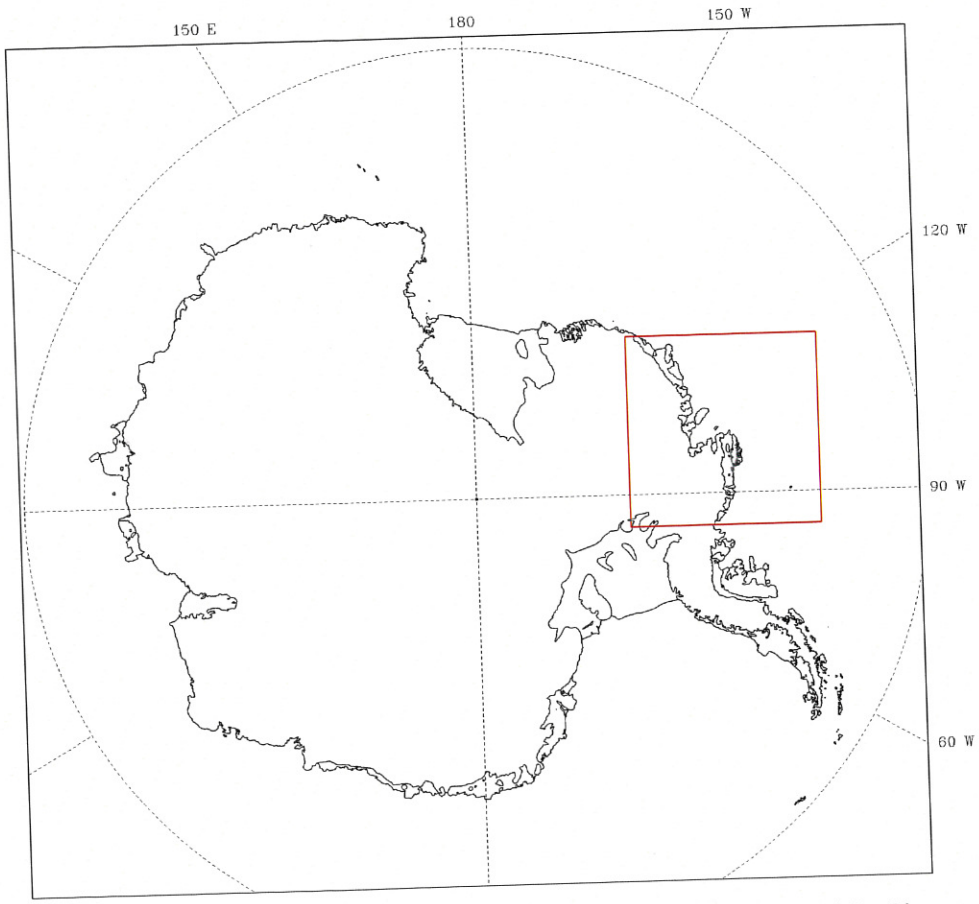

Fig 1. AMPS domain 2 (15-km continental grid), showing the location of the Pine Island Glacier one-way nest in red.

Current Status and Future Plans for the OSU AMPS Database

Sheng-Hung Wang[1], David. H. Bromwich[1,2], and Julien P. Nicolas[1,2]

[1]Polar Meteorology Group, Byrd Polar Research Center, The Ohio State University, Columbus, OH
[2]Atmospheric Sciences Program, Department of Geography, The Ohio State University, Columbus, OH

The Ohio State Polar Meteorology Group (PMG) has built a new data server to support the AMPS project. It has two 12-core processors, 128 GB of RAM, and supports up to 48 TB of data storage. PMG will copy AMPS daily 00 UTC analysis and forecast grib outputs for domains 2-6 starting from 2011 and backward process them. The primary purpose of the AMPS database at OSU is to provide an easily accessible subset of AMPS output that focuses on most frequently used variables and that approximates observed conditions. We will provide data in NetCDF format. In addition, we will compute and plot monthly means for selected variables. We will provide some support for additional processing as a result of user requests. The revamped AMPS database web page is under construction.

Verification of AMPS wind forecasts for the DROMLAN area during Antarctic summer season 2011-12

Michael Knobelsdorf, meteorologist, German Weather Service

Abstract

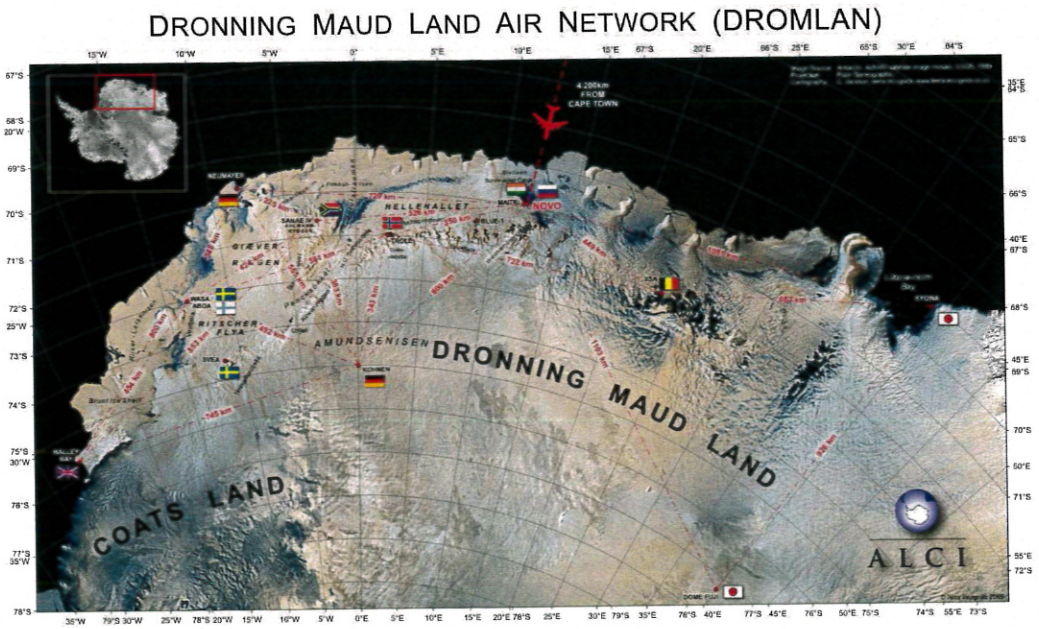

Figure 1: Antarctic DROMLAN-area

Since 2002 the German Alfred Wegener Institute (AWI) is involved in the international DROMLAN project providing weather forecasts for the entire wide Dronning Maud Land from the British Halley-Station in the west to the Japanese Syowa-Station in the east (figure 1). The German-Weather-Service (DWD) as a contractor is responsible to send meteorologists on duty during annual Antarctic summer season from November to February. The forecast base is the German station Neumayer III at the Exström-Shelf Ice nearby the north-eastern Weddell Sea at 70°40'S 008°16'W.

The meteorologists make daily forecasts for research-stations, research vessels off the DROMLAN coast, land expeditions and especially for the entire air traffic inside the DROMLAN area as well as for intercontinental flights from Cape Town to the Dronning Maud Land. The handling of the frequently bad Antarctic weather is a daily great challenge. This requires longtime experience and good meteorological data bases. Sparse weather observations on sea and ice, high resolution satellite pictures, global model forecasts, regional model forecasts and ensemble prediction systems should be combined, weighted and interpretated for the best possible forecast. There is a special focus on key parameters like contrast and horizon derived from wind speed, cloud base, cloud cover and precipitation.

Since many years the AMPS is one of the most important meteorological data bases for our

forecasts: There is a close collaboration between our forecasters and AMPS modelers with optimized grid points, meteograms and cross sections. Parallel to our daily work in Antarctica we can verify the AMPS-forecasts especially in respect to real regional weather conditions around the airfields at DROMLAN area. During last season 2011/12 we compared wind forecasts from 00UTC AMPS model runs with real weather observations at seven DROMLAN airfields at 06, 12 and 18UTC. We got statistics being representative only for last summer season at DROMLAN area. Altogether we can confirm a high quality of model wind forecasts especially for stations like Neumayer III, Novolazarevskaja, Syowa and Halley with only some weaknesses depending on daytime and wind forces. Wind forecasts for the South-African station SANAE displayed problems especially in the mornings. Apart from that there were many ongoing problems with wind forecasts at the Belgium station Princess Elisabeth and especially at the Norwegian station Troll which can be explained by orography and unknown regional wind systems.

This talk will present these detailed statistics with observed mean overestimations and underestimations, backing and veering of model wind forecasts compared to wind observations. We will make some proposals for solution and we hope these results can perform a contribution to the further improvement of the AMPS model.

A COMPREHENSIVE EVALUATION OF POLAR WRF FORECAST PERFORMANCE IN ANTARCTICA

David H. Bromwich[*,1,2], Francis O. Otieno[1], Keith M. Hines[1], Kevin W. Manning[3], and Elad Shilo[4]

[1]Polar Meteorology Group, Byrd Polar Research Center, The Ohio State University
108 Scott Hall, 1090 Carmack Road Columbus, OH 43210

[2]Atmospheric Sciences Program, Department of Geography, The Ohio State University, Columbus, OH

[3]National Center for Atmospheric Research,
3450 Mitchell Lane, Boulder, CO, 80307-3000

[4]Israeli Meteorological Service, Bet Dagan 50250, Israel

1. Introduction

Critical forecasts in support of the US Antarctic Program (USAP) are now routinely made by the Antarctic Mesoscale Prediction System (AMPS; Powers et al. 2012) using the Polar Weather Research and Forecasting model (Polar WRF) which is based on an earlier mesoscale, model (Polar MM5; Bromwich et al. 2001). The forecasts are needed for the safety of those working in Antarctica and in planning transport logistics for USAP activities. With the increasing number of visitors to the continent (IAATO 2010), forecasts may be needed in the future for a large-scale evacuation from the continent. The model, originally developed for Northern Hemisphere (NH) mid-latitudes applications has been tested more extensively in Arctic (Bromwich et al. 2009; Hines and Bromwich 2008; Hines et al. 2011; Cassano et al. 2011) compared to Antarctic environments. Scarcity of long term observations in Antarctica and potentially large changes in the ice sheet surface mass balance (Velicogna 2009) are now expanding the application of Polar WRF beyond AMPS forecasts. Long term simulations could provide model data needed to diagnose variations in climate such as those depicted in the EPICA (2004) ice cores. These applications require a comprehensive evaluation of Polar WRF performance since the model on which it is based was not targeted to the environment in which it is now being applied. Rapid and continuous refinements to both the Standard and Polar WRF models also create a challenge for both AMPS and applications requiring an understanding of long-term trends. Improvements in models to address emerging challenges have been also been called for in a recent National Research Council (*NRC*, 2011) report.

This study expands on the Arctic evaluations (Wilson et al. 2011, 2012) completed by the Polar Meteorology Group at The Ohio State University (OSU) to all of Antarctica on an annual time scale. The focus is on three factors that influence forecast skill: model improvements, uncertainty in driving data, and interannual variations in the large-scale atmospheric circulation. Four recent bug-fixed versions of Polar WRF (releases 3.0.1, 3.1.1, 3.2.1, and 3.3.1) are chosen to assess the impact of model developments. Improvements that only ease user application or enhance computational efficiency are not considered. Influence of the uncertainty in the initial and lateral boundary conditions is examined by comparing forecasts made using the reanalysis from the European Centre for Medium-Range Weather Forecasts (ECMWF; ERA-Interim, *Dee et al.* 2011) which represents a major advance over previous ECMWF reanalyses with those made using the final analysis from NCEP operational global analysis data (GFS-FNL). Influence of changes in the large scale atmospheric circulation on model skill is evaluated by comparing forecasts using ERA-Interim for 1993 and 2007. Strictly speaking, there were more measurements assimilated in 2007, compounding differences due to interannual variations with those due to analysis quality.

*Corresponding author address:
David H. Bromwich, Byrd Polar Research Center, The Ohio State University, 108 Scott Hall, 1090 Carmack Road Columbus, OH 43210
email: bromwich.1@osu.edu

2. Model, experiments, and data

2.1 Model description

Polar WRF uses fully compressible Euler nonhydrostatic equations on a horizontal Arakawa C-grid staggering and a vertical terrain-following hydrostatic-pressure coordinate (*Skamarock et al.* 2009). In this study reflection of gravity waves from the upper boundary is controlled using increased diffusion and damping of the vertical velocity over an 8 km depth from the model top. Table 1 presents a summary of the physics packages used in assessing the impact of model improvements. While all the experiments in Table 1 used WRF Single moment 5-class microphysics, some more recent analysis at OSU using the Morrison microphysics shows decreases in the biases discussed in the results section. AMPS uses the WSM5 hence the level of skill found here provides a benchmark for the comparable resolution AMPS experimental forecasts.

Table 1: WRF Configuration and physics options

Version	Polar WRF3.0.1/3.1.1/3.2.1/3.3.1
Microphysics	WRF Single moment 5 class
Longwave	Rapid Radiative Transfer Model RRTM in 3.0.1, 3.1.1, and RRTMG or CAM in 3.2.1, 3.3.1
Shortwave	Goddard Shortwave in 3.0.1 and 3.1.1; RRTMG in 3.2.1 and 3.3.1
Land surface	Noah Land Surface Model (LSM)
Planetary Boundary Layer	Mellor Yamada-Janjic (MYJ) or the Mellor Yamada Nakanishi and Niino (MYNN)
Surface layer	Monin-Obukhov (Janjic-eta) scheme
Cum. Param.	Grell-Devenyi
Resolution	60 km
Lat/Lon	121x121
Relaxation zone	10 grid points
Vertical Levels	39 eta levels
Time step	120s
Model Top	Set at 10 mb with damping over 8 km from model top
Base State Temperature	273.16 K
SST	NCEP Real-time, global (RTG-SST) in 2007 ; NOAA optimally interpolated OI SST for 1993
Sea ice	NSIDC 25 km fractional sea ice
Lateral Boundary data	GFS-FNL or ERA-INT

2.2 Experiments

Three full year experiments using GFS-FNL analysis are each conducted with a different version of Polar WRF for 2007. A total of seven sensitivity experiments aimed at evaluating the impact of driving data uncertainty, schemes used in shortwave and longwave radiation and planetary boundary layer are also performed for January (*summer*) and July (*winter*) 2007. Integrations are carried out in forecast mode over 48-hr durations but only the last 24 hours are used in the analysis to allow for model spin-up. Adjacent non-overlapping segments are then joined to make a complete annual time series.

A single domain, very similar to AMPS grid 2, centered at the South Pole with 39-vertical levels at a horizontal resolution of 60 km is used. The impact of this coarse resolution on the statistics is minimized by emphasizing only stations that are properly represented and depict synoptic behavior. Elevation, fractional sea ice and sea-surface temperatures (SST) are respectively specified from the 200 m Radarsat Antarctic Mapping Project Digital Elevation Model (RAMP-DEM; *Liu et al.,* 2001), the DMSP Special Sensor Microwave Imagers (SMM/I) available from the National Snow Ice data Center (NSIDC; *Comiso,* 2007) and either the NCEP 0.5 degree real-time global (RTG, SST; *Gemmill et al.,* 2007) analyses for 2007 or the NOAA weekly 1.0 degree Optimum Interpolated observations (OI, *Reynolds et al.,* 2007) for 1993 (prior to RTG SSTs). Except for terrain, the daily lower boundary conditions are linearly interpolated for temporal updates every 6 hours throughout the forecast. Other model modifications include increases in the maximum albedo from the Standard-WRF value over glaciers of 0.7 to 0.8. Monthly and annual mean analysis 2 m temperature above the ice/snow surface are used to specify the bottom and top snowpack temperatures in the Noah LSM with a linear interpolation for intermediate depths.

2.3 Observational data

Observations from synoptic stations are retrieved from the National Climate Data Center (NCDC) archives and augmented by Automatic Weather Station (AWS) observations from the University of Wisconsin's Antarctic Meteorological Research Center (AMRC), the Italian Antarctic Research Program and the Australian Antarctic Data Center. Forecast 10 m wind speeds are adjusted using the logarithmic wind profile down to 3 m to better match AWS measurements. Observed surface downwelling shortwave and longwave radiation for surface energy budget analysis are obtained from the Baseline Surface Radiation Network (BSRN; *Ohmura et al.,* 1998) of Antarctic Stations (*Dutton* 2008; *Vitale,* 2009;

Yamanouchi, 2010*; König-Langlo,* 2011). Upper air measurements are from the archives of the British Antarctic Survey (BAS) and the Integrated Global Radiosonde Archive (IGRA; *Duree et al.* 2006). The extreme climate and challenging logistical access of Antarctica inevitably produce some unusable measurements. Following basic visual examinations of observed time series from the archives above, the availability (>50%) and representativeness (< ±3σ) are verified more objectively and duplicate data arising from close proximity between many of the AWS to existing synoptic stations are removed. For temperature and pressure adjustments are made using the dry adiabatic lapse rate (9.8 °C/km) and the hypsometric relationship before any of the statistical analysis

3 Results

3.1 Surface conditions

Average statistics over the stations are shown in Figures 1 and 2 respectively for 2m air temperature and 10 m wind speed. Correlations of 2 m air temperature exceed 0.7 for most of the year except in January when values ~0.55 indicate difficulties with the diurnal cycle at the peak of summer. The biases show distinct differences between the winter and summer seasons. All model versions have a cold near surface temperature bias in summer with January peaks below -2 ºC. During winter on the other hand a warm bias prevails, again for all three versions. The temporal correlation patterns for 2 m dew point temperature forecasts are very similar to those found in the 2 m air temperature above but the magnitude remains below 0.7 throughout the year. Very low amounts of moisture on the continent together with difficulties in making these observations contribute to the larger dewpoint RMSEs.

No single model version consistently outperforms all the others in forecasts of surface pressure which are generally higher than observed. Correlations for forecast monthly wind speed exceed ~0.50 throughout the year with no well-defined difference between winter and summer (Figure 2). The peak winter wind speed bias is likely related to seasonal variation in absolute wind speeds, with higher speeds producing the larger biases. Largest errors occur at the coast and can exceed 9 ms^{-1}. The biases highlight the difficult challenge for any Antarctic verification effort as many of the observations are located along the coast where evaluation of the model skill is the most challenging.

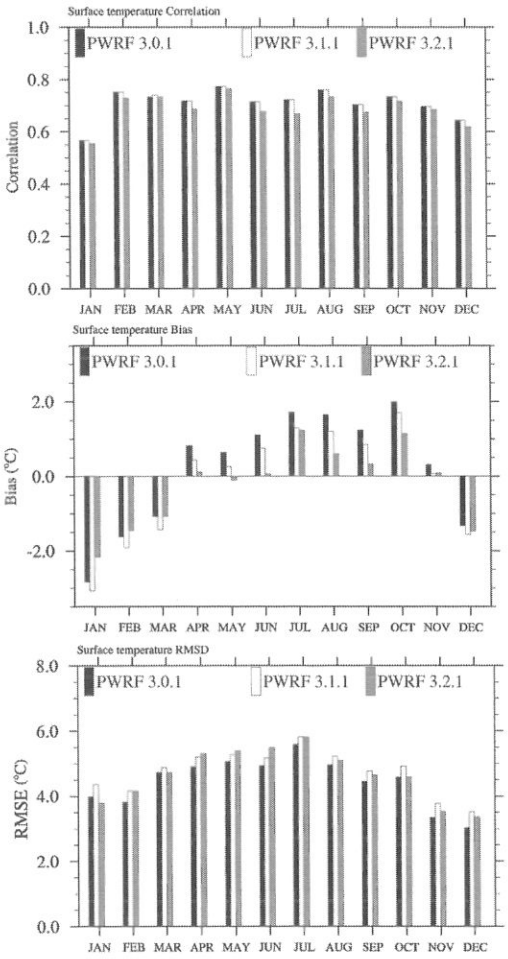

Fig. 1: Domain averaged monthly 2m air temperature statistics; lowest correlations are found in January (n=25).

3.2 Downwelling surface radiation

Less than 400 Wm^{-2} of January forecast downwelling shortwave radiation (SWDOWN) reaches the surface at Neumayer (*a lower latitude station; top panel in Figure 3*) on average compared to more than that at Amundsen-Scott (*higher latitude bottom panel*). These forecasts are consistent with the observations which also show Amundsen-Scott with ~410 Wm^{-2} of incident SWDOWN and only 310 Wm^{-2} at Neumayer. Therefore Polar WRF exhibits a positive SWDOWN bias. The average from ten additional sites matching the locations of established coastal stations (Halley, Dumont, Casey, Mirnyj, Mawson, Rothera, Belgrano, Silvia, Mt Siple and McMurdo)

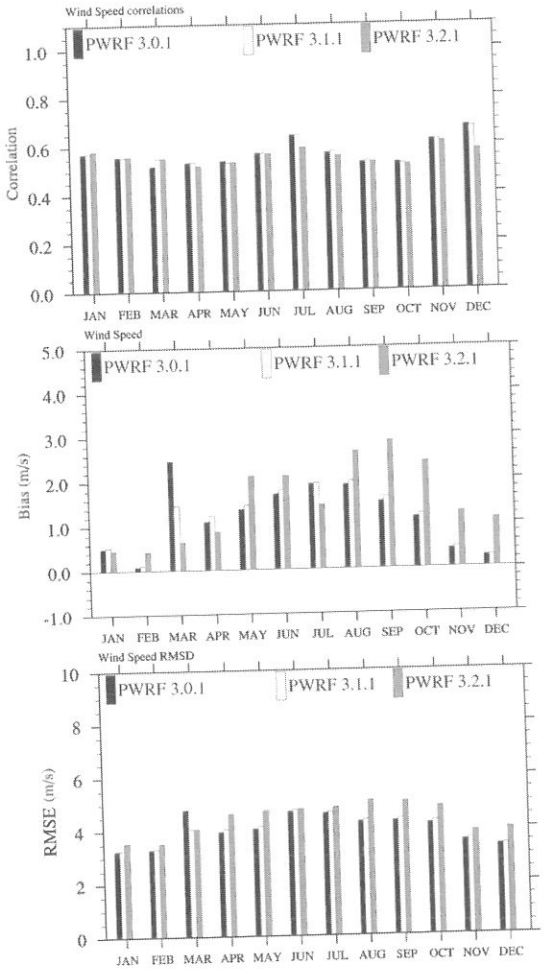

Fig. 2: Monthly mean wind speed statistics from 25 stations.

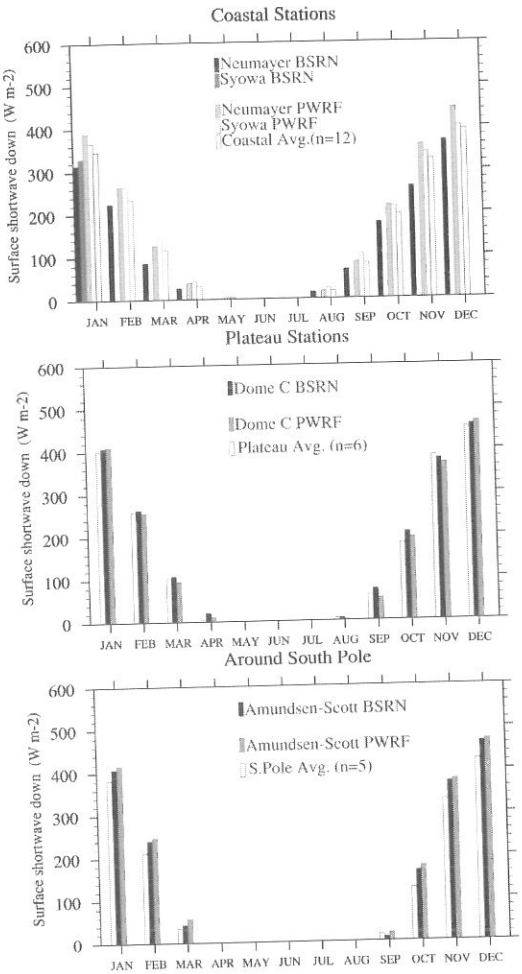

Fig. 3: Mean monthly incident shortwave at the surface for 2007; the average is computed from locations of similar characteristics from the forecasts.

Table 2: Correlations, biases and RMSE from Polar WRF 3.1.1 hourly averages for downwelling shortwave and longwave. Statistics for downwelling shortwave are for the periods Sep 21st through Dec 31st and Jan. 1 to Mar 21st

	Shortwave		Longwave	
	CORR			
	1993	**2007**	**1993**	**2007**
Neumayer	0.94	0.95	0.65	0.77
Dome C	-	0.98	-	0.79
South Pole	0.70	0.97	-	0.63
	BIAS			
Neumayer	47.8	32.5	-18.8	-9.4
Dome C	-	19.9	-	6.2
South Pole	53.3	66.0	-	-23.4
	RMSE			
Neumayer	108.0	90.9	40.6	35.8
Dome C	-	51.1	-	21.3
South Pole	73.8	46.8	-	29.2

is also higher than the observations at Neumayer and Syowa. Therefore on average excessive forecasts of downwelling surface shortwave radiation at Neumayer and Syowa are characteristic of Antarctic coastal locations. Variability in the forecast SWDOWN decreases more rapidly than in observations during the fall seasons and this can also contribute (*higher averages*) to the excess SWDOWN during this part of the year. Table 2 shows that excessive SWDOWN from Polar WRF311 occurs in both 1993 and 2007. We hypothesize that inadequate cloud representation (lower amounts or smaller optical thickness) is responsible for the forecasts of excess surface incident shortwave radiation. Except for South Pole in 1993, the temporal correlations of downwelling shortwave exceed 0.9 at all three locations in both years. It is interesting that the

correlation at Neumayer where the SWDOWN variability is larger is comparable to that at both Dome C and South Pole with smaller variability. The biases show an excess in SWDOWN at all three locations and in both years.

In spite of difficulties in objectively assessing cloud forecast, higher model total cloud fraction is found to correspond to observations of overcast skies most of the time. Thus the model correctly identifies cloudy episodes. However there is a deficit in the model LWD (Table 2). Scatter plots (not shown) of model versus observed downwelling longwave radiation (LWD) confirm the deficit and show larger differences for higher LWD values (typically associated with *cloudy skies*). The occurrence of excess SWDOWN and LWD deficit together support the hypothesis of inadequate model cloudiness.

3.3 Upper-air variables

Seasonal temperature statistics for 2007 are presented in Figure 4 for six representative upper air stations. Variations in upper level variables between different model versions are small compared to those at the surface. The model forecasts the broad characteristics of the profile accurately, even capturing the large annual temperature range above 200 hPa (~60 K) which is nearly three times that near the surface. Away from the surface Polar WRF predicts vertical temperature profiles with high skill both in summer and winter except at Marambio. A general cold DJF bias occurs near the bottom of the profile in all versions and is consistent with the surface temperature bias discussed earlier. The RMSE values indicate that winter temperatures are more variable especially below 500 hPa but in summer a greater variability occurs near the tropopause. Correlations between forecasts and observed geopotential heights are generally high and remain above 0.9 in both seasons. In all three versions, geopotential height biases are smaller near the bottom but increase with height to at least three times as large at 200 hPa as they are at 700 hPa. Statistics for the total wind speed show higher winter correlations and marked height dependence in both seasons. Relative humidity statistics show the lowest skill of all the variables with the highest summer and winter correlations of 0.65 and 0.74 respectively below 700 hPa.

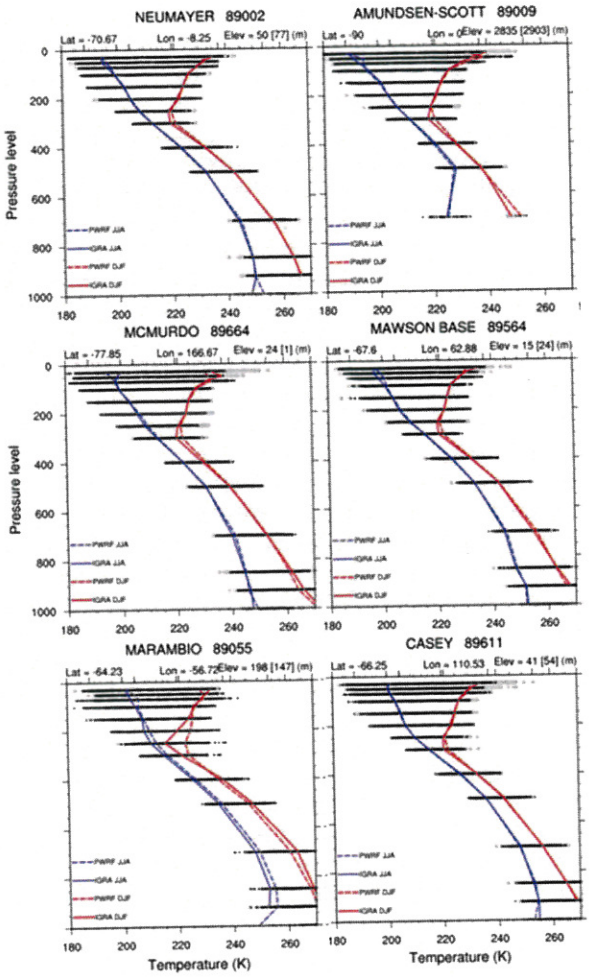

Fig. 4: Vertical temperature profiles for six Antarctic stations; black and gray dots are forecasts and observed temperatures respectively; blue curves are averages for the winter months (Jun-Jul-Aug) while the red curves represent summer (Jan-Feb and Dec) temperatures. Observed temperatures are continuous curves while forecasts are represented by dashed curves.

3.4 Sensitivity experiments

The magnitude of the responses of Polar WRF321 when driven by the GFS-FNL is comparable for different radiation and PBL physics schemes and the temperature biases remain negative (cold) in summer and positive (warm) in July in agreement with the earlier full year experiments. Wind speed statistics show that all three Polar WRF321 experiments have stronger than observed wind speeds in both January and July. Although not shown here, the most striking feature from an analysis of Polar WRF331 run with ERA-Interim instead of GFS-FNL is a drastic

reduction in both the summer and winter temperature biases which are not attributable to a cancellation of model errors. A possible summer explanation is that the GFS-FNL analysis initializes Polar WRF to a state that is too cold for the model to recover within a 48-hour period.

Scatter plots shown in Figure 5 enable an evaluation of model sensitivity in areas without observed data in the Southern Ocean and over Antarctica. The left panels show the impact of analysis (ERA-Interim versus GFS-FNL) while the right panels depict model sensitivity to the radiation physics (CAM versus RRTMG). More locations are warmer in the ERA-Interim run than in the GFS-FNL run for temperatures below 270 K. In both cases the temperature differences become smaller for temperatures above 274 K (right side of the vertical blue line). The surface pressure scatter plot (Figure 5b) shows larger surface differences near 1000 hPa (*over the ocean primarily*) which can occur due to differences in the locations of synoptic systems. Smaller differences corresponding to lower pressures are found primarily over elevated parts of Antarctica. Weaker winds (less than 5 ms^{-1}) are overpredicted in both cases (Fig.5c). The bottom panel shows that the GFS-FNL run forecasts more surface downwelling radiation than the ERA-Interim for values less than 400 Wm^{-2}. Switching the radiation physics to CAM reduces this bias but only has a modest impact for shortwave radiation exceeding 600 Wm^{-2}.

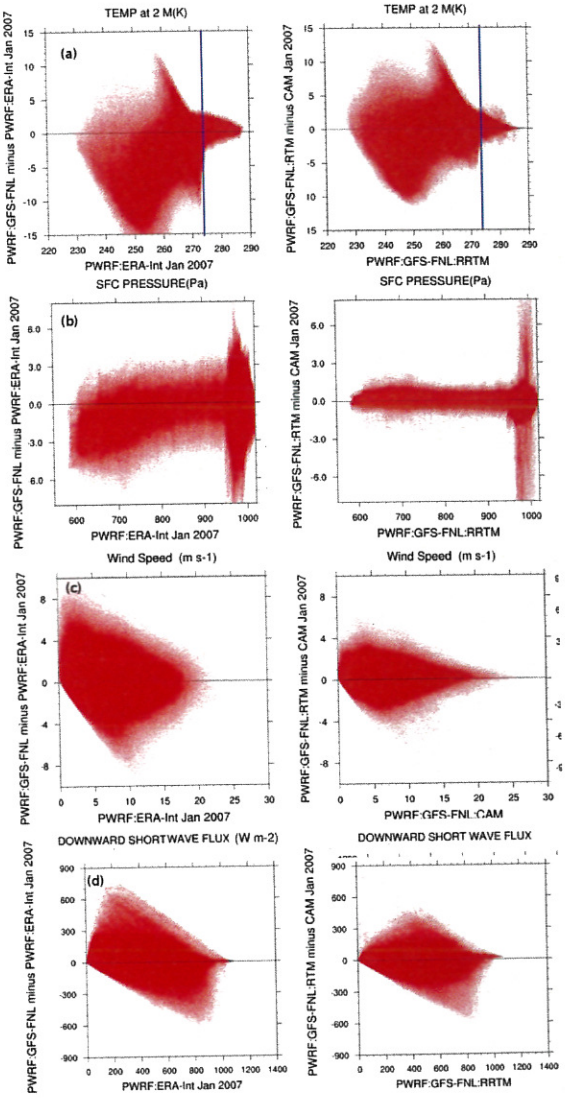

Fig. 5: January 2007 scatter plots of Polar WRF 3.2.1 differences (GFS-FNL minus ERA-Interim runs; left panel) and GFS-FNL with RRTM minus GFS-FNL with CAM WRF (right panel). The scatter plots show the range of differences found at Polar WRF grid points between two sensitivity experiments for (a) 2m temperature (b) surface pressure (c) wind speed and (d) downwelling surface shortwave radiation

4 Discussion

Summer surface temperatures increase by 1.4 K and 2.9 K respectively at Neumayer and South Pole when the downwelling longwave radiation is increased in the Stefan Boltzmann relationship by amounts comparable to the deficits in Table 2 for a scenario where all other fluxes are fixed; this increase nearly compensates for all the model cold summer temperature bias. Therefore a deficit in the downwelling longwave radiation, most likely due to inadequate cloud representation, is responsible for the cold summer bias. The excess in downwelling shortwave does not play a substantial role as 80% is reflected back due to the high surface albedo and the model skies lacking adequate cloud cover.

Stronger than observed wind speed appears to be a common problem for stable boundary layers with the all PBL schemes used here as well as the Yonsei PBL [*Clifford Mass* personal communication, 2011]. The sensible heat flux along the coast can be substantially larger than on the plateau due to mechanically induced mixing.

5 Conclusions

The results show that recent versions of Polar WRF have skill that is comparable to a recent Arctic simulation [*Wilson et al.,* 2011] and marginally better than an earlier Antarctic simulation using Polar MM5 [*Guo et al.,* 2003]. The model skill varies seasonally reflecting the different

roles played by local and synoptic scale systems at different times of the year. The model shows a cold surface temperature bias in the summer months but a warm bias during winter months when insolation plays a negligible role in heating the surface. No nudging was done in this study although it has been suggested [*Cassano et al.,* 2011] that spectral nudging near the model top can improve the performance of Polar WRF. The statistics presented therefore provide a pure forecast benchmark of the skill of Polar WRF in Antarctic simulations. Comparisons of the statistics from different years, physics schemes and analysis show that the model skill is affected more by the analysis used than by the parameterization physics or year to year differences in the atmospheric circulation. Thus improving the network of verification observations and quality of Antarctic analysis must remain a top priority for further development of numerical modeling in Antarctica.

6 Acknowledgments

This work was funded by NASA grant NNX08AN57G, NSF-ANT 113571, and NSF/OPP 0838967. The authors appreciate the support of the Antarctic Meteorological Research Center for the providing the AWS data (Matthew Lazzara and Elena Willmot, NSF grant number ANT-0838834). Aaron Wilson provided highly appreciated and valuable discussions from his insight from working with Polar WRF in the Arctic.

References

Bromwich, D. H., K. M. Hines, and L.-S. Bai, 2009: Development and testing of Polar WRF: 2. Arctic Ocean, *J. Geophys. Res.,* **114**, D08122, doi:10.1029/2008JD010300.

Bromwich, D. H., J. J. Cassano, T. Klein, G. Heinemann, K. M. Hines, K. Steffen, and J. E. Box, 2001: Mesoscale modeling of katabatic winds over Greenland with the Polar MM5, *Mon. Wea. Rev.,* **129**, 2290-2309.

Cassano J. J, M. E. Higgins and M. W. Seefeldt, 2011: Performance of the Weather Research and Forecasting (WRF) Model for month-long Pan-Arctic Simulations, *Mon. Wea. Rev., 139,* 3469-3488, doi: 10.1175/MWR-D-10-05065.1.

Comiso, J. 1999, updated, 2007: *Bootstrap sea ice concentrations from NIMBUS-7 SMMR and DMSP SSM/I*, [2007]. Boulder, Colorado USA: National Snow and Ice Data Center. Digital media.

Dee, D. P., S. M. Uppala, A. J. Simmons, P. Berrisford, P. Poli, S. Kobayashi, U. Andrae, M. A. Balmaseda, G. Balsamo, P. Bauer, P. Bechtold, A. C. M. Beljaars, L. van de Berg, J. Bidlot, N. Bormann, C. Delsol, R. Dragani, M. Fuentes, A. J. Geer, L. Haimberger, S. B. Healy, H. Hersbach, E. V. Hólm, L. Isaksen, P. Kållberg, M. Köhler, M. Matricardi, A. P. McNally, B. M. Monge-Sanz, J.-J. Morcrette, B.-K. Park, C. Peubey, P. de Rosnay, C. Tavolato, J.-N. Thépaut, F. Vitart, 2011: The ERA-Interim reanalysis: configuration and performance of the data assimilation system, *Q. J. R. Meteorol. Soc.,* **137***(656)*, 553–597, DOI: 10.1002/qj.828.

Durre, I., R. S. Vose, and D. B. Wuertz, 2006: Overview of the Integrated Global Radiosonde Archive. *J. Clim.,* **19**, 53-68, doi: 10.1175/JCLI3594.1.

Dutton, E. G, 2008: Basic and other measurements of radiation at station South Pole (2007-05), *Climate Monitoring & Diagnostics Laboratory, Boulder*, doi:10.1594/PANGAEA.706267.

EPICA community members, 2004: Eight glacial cycles from an Antarctic ice core, *Nature, 429,* 623–628, doi:10.1038/nature02599.

Gemmill, W., B. Katz and X. Li (2007), Daily Real-Time Global Sea Surface Temperature - High Resolution Analysis at NOAA/NCEP. NOAA / NWS / NCEP / MMAB Office Note Nr. 260, 39 pp. NOAA, Silver Spring, Md.

Guo, Z., D. H. Bromwich, and J. J. Cassano, 2003: Evaluation of Polar MM5 simulations of Antarctic atmospheric circulation, *Mon. Wea. Rev., 131*, 384-411, doi:10.1175/1520-0493 (2003)131<0384:EOPMSO>2.0.CO;2.

Hines, K. M., and D. H. Bromwich, 2008: Development and Testing of Polar WRF. Part I. Greenland Ice Sheet Meteorology, *Mon. Wea. Rev.,* **136**, 1971-1989, doi: 10.1175/2007MWR 2112.1.

Hines, K. M., D. H. Bromwich, L.-S. Bai, M. Barlage, and A. G. Slater, 2011: Development and testing of Polar WRF. Part III. Arctic land, *J. Climate,* **24**, 26-48, doi: 10.1175/2010JCLI3460.1.

IAATO, 2010:, Antarctic Tourism fact sheet http://iaato.org/tourism-statistics.

König-Langlo, G., 2011:, Basic and other measurements of radiation at Neumayer Station (2007-03), *Alfred Wegener Institute for Polar and Marine Research, Bremerhaven*, doi:10.1594/PANGAEA.759355.

Liu, H., K. Jezek, B. Li, and Z. Zhao, 2001: *Radarsat Antarctic Mapping Project digital elevation model version 2.* Boulder, CO: National Snow and Ice Data Center. Digital media.

National Research Council, 2011: Future Science Opportunities in Antarctica and the Southern Ocean,http://www.scribd.com/doc/64382324/Future-Science-Opportunities-in-Antarctica-and-the-Southern-Ocean#archive.

Ohmura A. and Coauthors, 1998: Baseline Surface Radiation Network (BSRN/WRMC), a new precision radiometry for climate research. *Bull. Amer. Meteor. Soc.*, **79**, 2115 - 2136.

Powers, J., K. W. Manning, D. H. Bromwich, J. J. Cassano, and A. M. Cayette, 2012: A decade of Antarctic science support through AMPS. *Bull. Amer. Meteor. Soc.*, accepted.

Reynolds, R.W., T. M. Smith, C. Liu, D. B. Chelton, K. S. Casey and M. G. Schlax, 2007: Daily high-resolution blended analyses for sea surface temperature, *J. Clim.,* **20**, 5473-5496 , doi:10.1175/2007 JCLI1824.1.

Skamarock, W. C., J. B. Klemp, J. Dudhia, D. O. Gill, D. M. Barker, X-Yu Huang, W. Wang, and J. G. Powers, 2009: A Description of the Advanced Research WRF Version 3, *NCAR Tech. Note NCAR/TN–475+STR*, 113 pp.

Velicogna, I., 2009:, Increasing rates of ice mass loss from the Greenland and Antarctic ice sheets revealed by GRACE, *Geophys. Res. Lett., 36*, L19503, doi:10.1029/2009GL040222.

Vitale, V., 2009: Basic measurements of radiation at Concordia Station (2006-02). *Institute of Atmospheric Sciences and Climate of the Italian National Research Council, Bologna,* doi:10.1594/PANGAEA.711756.

Wilson, A. B., D. H. Bromwich, K. M. Hines, 2011: Evaluation of Polar WRF forecasts on the Arctic System Reanalysis domain. Part I. Surface and upper air analysis. *J. Geophys. Res.,* **116**, D11112, doi: 10.1029/2010JD015013.

Wilson, A. B., D. H. Bromwich, and K. M. Hines, 2012: Evaluation of Polar WRF forecasts on the Arctic System Reanalysis domain. 2. Atmospheric hydrologic cycle. *J. Geophys. Res.*, **17**, D04107, doi:10.1029/2011JD016765

Yamanouchi, T., 2010: Basic and other measurements of radiation at station Syowa (2007-04). *National Institute of Polar Research, Tokyo*, doi:10.1594/PANGAEA.740932.

Abstract

An ensemble-based four-dimensional variational (En4DVar) algorithm proposed in the first part of the En4DVar series uses a flow-dependent background error covariance constructed by ensemble forecasts and performs 4D-Var optimization based on incremental approach and preconditioning algorithm. In the second part, we conducted Observing System Simulation Experiments (OSSE) using Advanced Research WRF (ARW) for En4DVar, and the results were promising.

The current study extends the En4DVar to assimilate real observations for a cyclone that happened in the Antarctic and the Southern Ocean on 2-5 October 2007. We performed an intercomparison of four different WRF-variational approaches for the case, including three-dimensional variational data assimilation (3DVar), first guess at the appropriate time (FGAT), ensemble-based three-dimensional variational (En3DVar) and four-dimensional (En4DVar) data assimilations. It was found that all data assimilation approaches could produce a positive impact in this case study. Applying the flow-dependent background error covariance (En3DVar and En4DVar) yields forecast skills superior to those obtained with the homogeneous and isotropic background error covariance (3DVar and FGAT).

In addition, we carried both FGAT and En4DVar three-day cycling experiments and 72-hour forecast respectively. The results show En4DVar get a better performance in the cyclone prediction.

BAS Antarctic Peninsula Automatic Weather Station Update 2011/12

Steven Colwell
British Antarctic Survey

The British Antarctic Survey services 5 AWS on the Antarctic Peninsula and Bladrick AWS half way between Halley and the South Pole see below.

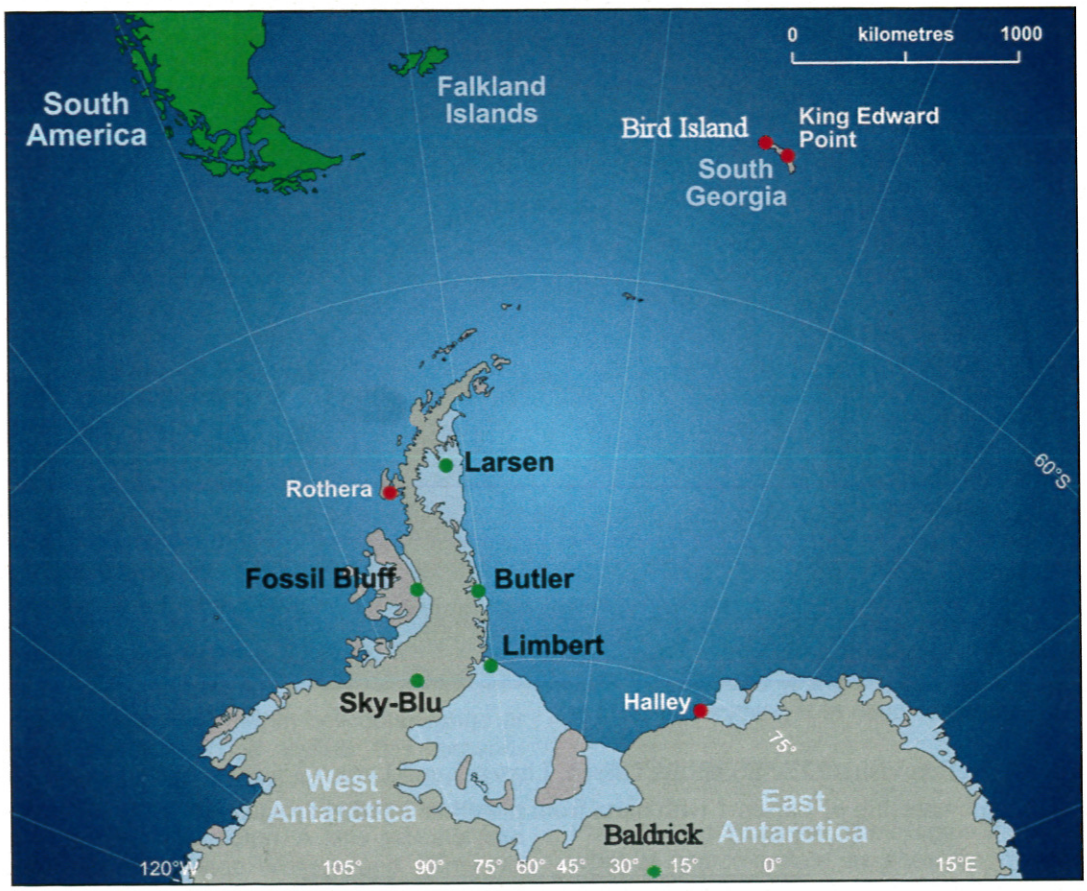

All station except Baldrick AWS were visited this year and the batteries were replaced at Larsen, Sky Blu and Limbert.

The wind sensor at Butler Island had moved during the winter but was still aligned with true south.

9602 Iridium SBD modems were installed at Larsen, Butler, Limbert and Sky Blu that are transmitting data back every 3 hours.

All the AWS are currently working well but there are some issues with the weekly iridium downloads from Butler, Sky Blu and Limbert

The AWS that was installed on the Fletcher Promontory at 77°53S, 082°35W last season was removed on the 4th December 2011 and relocated to the Jurassic site at 74° 19S, 073° 03W on the 11th January 2012. This AWS will be run for one year at this site and then removed once a drilling campaign has been carried out at the site during the 2012/13 season.

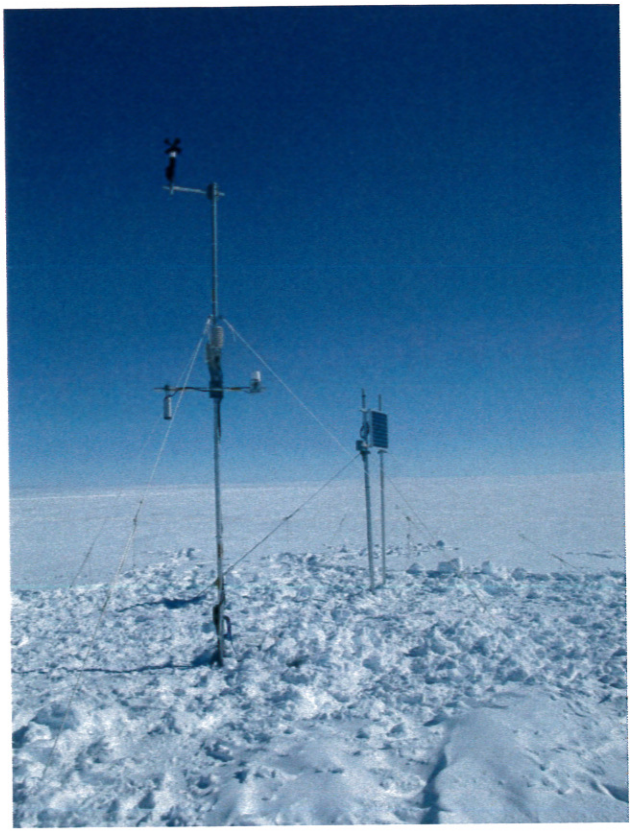

Konrad Steffen visited 3 AWS on the Larsen, Larsen 2 and Larsen 3 were removed and BAS has taken ownership of Larsen 1 with parts from the other 2 acting as spares

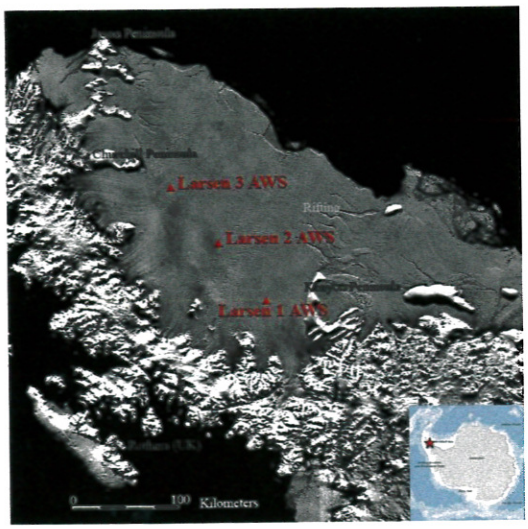

ANTARCTIC AUTOMATIC WEATHER STATION 2012-2013 FIELD SEASON PLANS

Matthew A. Lazzara[*,1] Jonathan E. Thom[1,2], Lee J. Welhouse[1], Linda M. Keller[2], David E. Mikolajczyk[1], and George A. Weidner[2]
[1]Antarctic Meteorological Research Center, Space Science and Engineering Center
[2]Department of Atmospheric and Oceanic Sciences
University of Wisconsin-Madison
Madison, Wisconsin

John J. Cassano[3]
[3]Department of Atmospheric and Oceanic Sciences
University of Colorado-Boulder
Boulder, Colorado

http://amrc.ssec.wisc.edu/

1. OVERVIEW

With an emphasis on maintenance, and some AWS removals, the 2012-2013 Antarctic Automatic Weather Station (AWS) field season will focus efforts in West Antarctica, Ross Ice Shelf, Ross Island region, and the Adelie Coast. No plans are expected for AWS work in the Antarctic Peninsula, East Antarctica or North Victoria Land. If collaborating science groups do visit AWS in the Pine Island Glacier Bay region, arrangements may be made to have recorded compact flash cards recovered from the stations, and new cards deployed. As always, these plans are subject to change depending on the health of the AWS network through the winter season.

2. ROSS ISLAND REGION

Many of the local AWS within helicopter range of McMurdo Station will be visited this season. Efforts will focus on continuing to convert AWS sites over to using the AWS Freewave network that is in place in the region. A new repeater site has been requested atop White Island. This will allow for Lorne AWS, Ferrell AWS, Linda AWS and Windless Bight AWS to be converted to using the Freewave network. Plans include the removal of the older AWS at Ferrell site – keeping the newer system installed. Visits in the region will be combined with the tropospheric ozone project, especially in the recovery efforts of recorded data compact flash cards. Additional visits are expected for repairs in the region including:

- Cape Bird AWS to replace the power system
- Linda AWS to raise the station and convert Freewave telemetry - if White Island repeater is installed
- Lorne AWS to convert to Freewave telemetry – if White Island repeater is installed
- Laurie II AWS to raise the station
- Willie Field AWS to conduct an inspection of station and replace the datalogger
- Windless Bight, raise the station and convert to freewave telemetry
- Pegasus North, station inspection and convert to freewave telemetery

Like Ferrell AWS site, Marble Point hosts two AWS systems, and we plan the possible removal the original AWS installation. Minna Bluff AWS is due for a maintenance inspection. This is a high wind location and yearly inspections are important to insure everything is in good condition.

3. ROSS ICE SHELF

Plans for the Ross Ice Shelf region include repair work at approximately six sites. An overdue site and servicing visit to Margaret AWS is scheduled, as the site has not been visited in over 5 years since it was first installed. Alexander (Tall Tower!) AWS is due for an inspection of the station and the tower. Vito AWS needs to have a failing sensor repaired. Both Elaine AWS and Emilia AWS need to have an update to the data logging programs, with Emilia AWS needing to be raised. Lettau AWS needs to be brought back on-line with a new electronics enclosure to be re-installed (Lettau failed because of a faulty Argos transmitter).

* Corresponding Author: Matthew A. Lazzara
Antarctic Meteorological Research Center, Space Science and Engineering Center, University of Wisconsin-Madison
Email: mattl@ssec.wisc.edu

4. WEST ANTARCTICA

Plans for West Antarctica call for the removal of Brianna AWS, if the site can be safely reached. Erin AWS is also being considered for either repair or removal. Janet AWS will be visited for inspection, as will Kominko-Slade (WAIS) AWS. Siple Dome AWS is in need of a raise, and possibly moved closer to the field camp.

5. ADELIE COAST

Plans for the Adelie Coast call for new AWS to be reinstalled at Port Martin and Cape Denison to continue the climate record at these sites. Working with our partners at Institut Polaire Francais – Paul Emile Victor (IPEV), we will have a complete replacement for Port Martin. Plans in parallel will have a new system for Cape Denison, working with Mawson's Hut Historical Foundation. Thanks for the efforts of our collaborators as they make these AWS and their observations possible.

6. LONG TERM PLANS

In the long term, plans include both new AWS sites and the removal of some sites. Removal of Kominko-Slade (WAIS) AWS is likely, as our commitment is to keeping Byrd AWS operating, relatively close to the WAIS site. Removal of 1 to 2 AWS in the Southern Ross Ice Shelf is also planned, with the completion of the Ross Ice Shelf wind studies. New sites in far West Antarctica are also planned to capture observations in an unobserved portion of the region.

7. ACKNOWLEDGEMENTS

This material is based upon work supported by the National Science Foundation under grant #ANT-0944018.

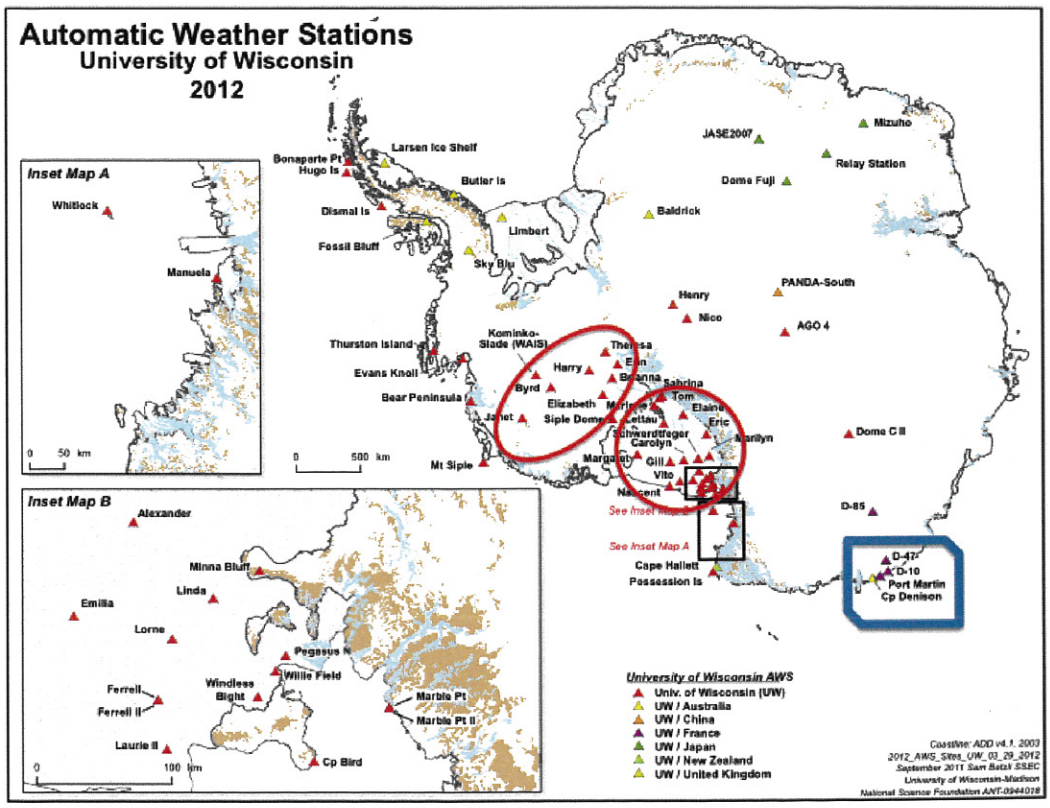

Figure 1. Regions targeted for AWS field work in the 2012-2013 field season. As of this publication, efforts are still under discussion and planning final arrangements are underway. Areas outlined in red are planned areas to work on the network by the team members, and the region in blue will be jointly accomplished with team members and international collaborators.

METEOROLOGICAL OBSERVATIONS AT ABOA, ANTARCTICA. DURING AUSTRAL SUMMER 2010-2011

Priit Tisler[1*], Rostislav Kouznetsov[1, 2], Timo Palo[1, 3], Timo Vihma[1], Tiina Kilpeläinen[1, 4]

[1] *Finnish Meteorological Institute, Helsinki, Finland*
[2] *A.M. Obukhov Institute of Atmospheric Physics, Moscow, Russia*
[3] *University of Tartu, Tartu, Estonia*
[4] *University of Helsinki, Helsinki, Finland*

1. INTRODUCTION

An extensive campaign consisting of a number of different meteorological observations was carried out during austral summer, December 2010 – January 2011, in western Dronning Maud Land. The campaign was a part of the Finnish Meteorological Institute research project - Antarctic Meteorology and its Interaction with the Cryosphere and the Ocean. Field work was performed by a team of three scientists: Priit Tisler, Rostislav Kouznetsov and Timo Palo.

2. OBJECTIVES

The expedition was a continuation for the three previous expeditions in 2006-2010, which have yielded results on atmospheric boundary layer processes (Tastula and Vihma, 2011), gravity waves generated by a nunatak (Valkonen et al., 2010), and snow structure and thermodynamics (Vihma et al., 2011). The measurements and objectives were essentially similar those of the previous seasons. In addition, however, number of new instruments (sodar, tethersonde, UAV) was applied in order to study vertical distribution of atmospheric boundary layer up to 2 km. The objectives of the expedition were:

(a) to measure radiative fluxes over the snow and ice to study the surface albedo and factors controlling its variations in diurnal and seasonal scale as well as spatially
(a) to measure the properties of snow to better understand the snow thermodynamics during the summer melt period and to study the impact of snow properties on the surface albedo
(b) to simultaneously measure the turbulent surface fluxes of heat and momentum and the near-surface profiles of wind speed and air temperature
(c) to study the snow and ice surface energy balance.
(d) to gather data on wind speed and direction, air temperature and surface fluxes to better understand the effect of nunataks on meso- and microscale weather features.
(e) to carry out simultaneous measurements with UAV, sodar and tethersonde to gather data of wind and temperature distribution in order to compare different methods/instruments and to gather data of vertical profiles up to 2 km.

* *Corresponding author address*: Priit Tisler, Finnish Meteorological Institute, P.O. BOX 503, FI-00101 Helsinki, Finland; e-mail: Priit.Tisler@fmi.fi

3. MEASUREMENTS

3.1 *Research station and measuring sites*

The Finnish Antarctic research station Aboa (73°03'S, 13°25'W) was built in Queen Maud Land, Antarctica, in 1988 - 89. Aboa is located 130 km from the shore, on the nunatak Basen in the Vestfjella Mountains. Aboa is occupied only during the Antarctic summer. At that time of the year the conditions are most suitable for research activity, air temperature typically ranging from 0 to -15°C.
The instruments were deployed on four different locations. Site I was located down on the snow-covered glacier, 3.3 km from Aboa (Fig. 1).

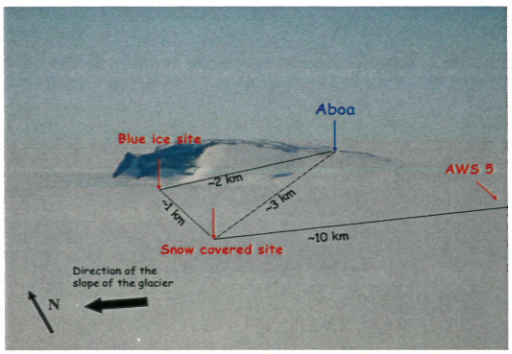

Figure 1. Measurement sites

Site II was located on the blue ice region, 2.4 km from Aboa and 1.5 km from Site I. Site III was located close to AWS5 10km away from the station.

Site IV, where the Kipp&Zone radiation station was later deployed was situated near the Aboa station.

3.2 *Radiation measurements*

Radiative fluxes were measured at site I, II, III and IV. Warm weather caused severe melting in the blue-ice area which made stabilization of the Kipp & Zone station challenging (Fig. 2). Problems were also created by melting of the ice beneath the station. The following fluxes were measured: incoming solar radiation, solar radiation reflected from the snow/ice surface, downward longwave radiation emitted by the atmosphere and clouds, and upward longwave radiation emitted by the snow/ice surface. The data were recorded at 1-minute intervals and transmitted by VHF radios to computers at Aboa living container. The instruments were leveled at the time of the deployment and the leveling was checked regularly. Adjustments were needed mostly at Site II. Both radiation stations had ventilators to prevent frost formation at the domes and to keep the dome temperatures more homogeneous. Power supply for the instruments and VHF radios was organized by batteries, which were charged at the station and changed usually every three days. Eppley radiation sensors use also solar panel and thus had not any need to recharge the batteries.

Figure 2. Kipp & Zonen radiation sensors at the blue ice site.

3.3 *Cloud cover*

Observations on the cloud cover were recorded automatically every 5 min by a camera equipped with fish-eye lenses. The camera was installed at the roof of the weather container.

3.4 *Snow measurements*

Vertical profiles of snow temperature were measured at depths of 0, 2.5, 5, 10, 15, 20, 25, 30, 40, 50 and 90 cm. The measurements were done with Ebro TFX 410 temperature sensor. Vertical profiles of snow density were measured typically at the depths of 1, 5, 10, 20, 30, 40 and 50 cm.

Snow grain photos were made at AWS5 measurement site (10km SE from Basen) when snow pits were done. 2 meters snow cave covered with a white plate was used to keep instruments cooled down and hide measurements from direct sun. Still sometimes there was too high air temperature to make correct photographs. Photographs were taken from snow grains at 4 different depth levels: surface; 5cm; 10cm; 20cm.

The snow temperature was monitored at the Snow site and at AWS5 by means of autonomous temperature loggers (I-buttons, Dallas DS1922L). The loggers were attached to wooden poles to be placed at depths of 2, 5, 10, 25 and 50 cm. Due to quite intensive and uneven melting and evaporation of the snow, the natural location of the snow surface can hardly be specified with accuracy more than 10 cm. To reduce the melting around the I-buttons, the poles were placed to have I-buttons at their southern side. To keep the snow surface more even and ensure the absence of air pockets around the I-buttons, the snow was eventually pressed around the poles.

3.5 *Turbulence and profile measurements*

The Metek USA-1 sonic anemometer was deployed on Site I. Three orthogonal wind components and air temperature with a sampling rate of 20 Hz were measured. The instantaneous data were collected by PC at Aboa via RF link. 12V power supply was used for the system.

The Aanderaa weather mast was located at Site I. The mast was equipped with cup anemometers and thermal sensors at 0.5, 1,2, 2,4, 4.7 and 10 meters, and a wind direction sensor at 10 meters. The data were collected with standard Aanderaa data storage units DSU2990.

The Campbell weather mast (Fig. 3) was equipped with Campbell 107-type temperature probes at 5 levels, 2D Gill WindSonic anemometers at 5 levels, Kipp&Zonnen CNR4 radiation budget probe, Campbell SR50A surface height sensor, Vaisala HMP45AC temperature and humidity probe and two Campbell CSAT3 3D sonic anemometers. The data were acquired, preprocessed and stored by means of Campbell CR3000 datalogger and can be downloaded using proprietary Campbell software via VHF radio link. The data logger performs averaging of the measured parameters as well as online computation of turbulence statistics. The initial setup was found to have numerous problems that lead to severe losses/corruptions of the data. The problems originate from both malfunctions of hardware and numerous hardware/software design mistakes (for example Gill WindSonic anemometers were found to stop responding sporadically). The batteries of the mast (same power source also for sodar) were equipped by 4 solar panels and wind generator (power consumption was however rather

high due additional PC organized parallel to datalogger).

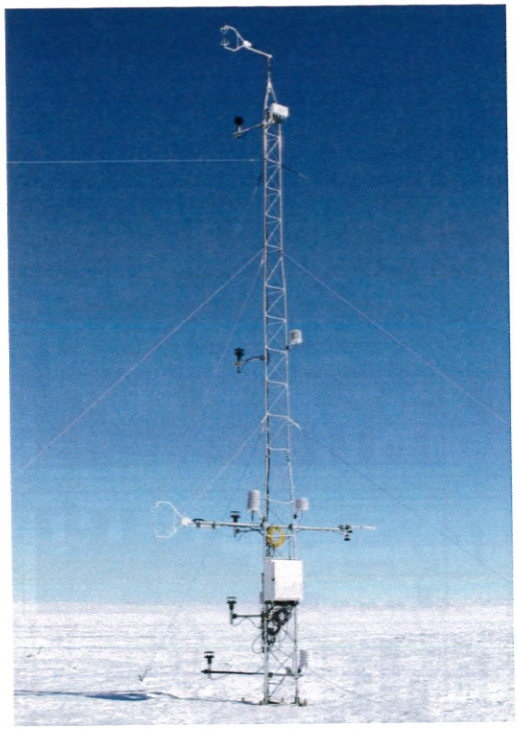

Figure 3. Campbell mast (10m) at AWS5 site.

3.6 *Tethersonde measurements*

Vaisala DigiCORA Tethersonde sounding system with maximum range of 2000 meters was used to carry out ABL soundings at AWS5 measurement site in Aboa (Fig. 4). Simultaneously three sondes were used on line in about 10-15 meters vertical interval. The descent and ascent of tethersondes was carried out by helium filled 7 m^3 balloon and electrical winch with 2000 m of tetherline. The tethered balloon was launched only under winds less than 10 ms^{-1}, which is the main limitation of the system. Altogether were made 12 series of measurements, consisting of 66 individual soundings. The maximum range of the profiles altitude was limited by the tetherline length as well by the occurrence of low-level jets. All series of measurements were carried out during evening or nighttime.

3.7 *Sodar*

At AWS5 site a 3-component Doppler acoustical sounder (sodar) LATAN-3m developed at the Obukhov Institute of Atmospheric Physics, Moscow, was deployed. The sodar was operated with 3120-cm dish antennae at sounding frequencies 1600-2200 Hz. The operating mode with frequency-coded sounding pulse was 6 x 100 ms pulses and the parallel operation of the antennae with pulse repetition rate of 10 s. Each sounding cycle was processed separately. The raw echo-signals are stored as well. The height range was set to 20-800 m with 20 m vertical resolution. The antennas were mounted on wooden sticks drilled into the hard snow surface. The acoustic shield needed to protect the antennae from wind and noise and to suppress the side lobes, was made of snow blocks.

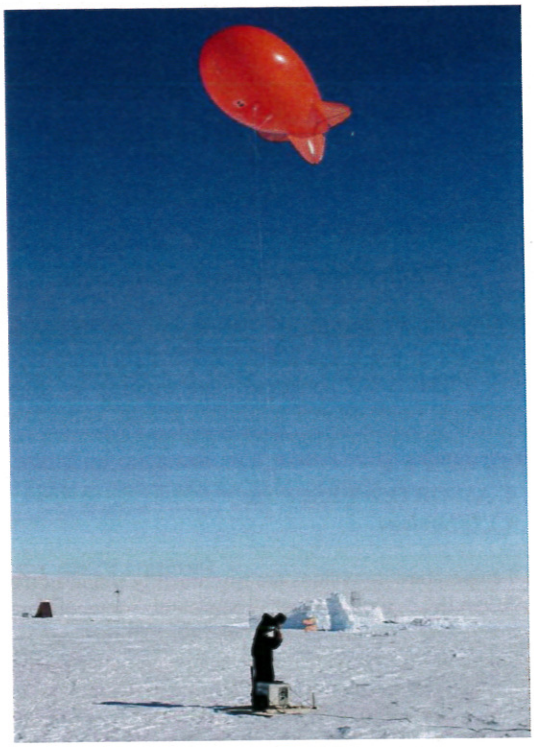

Figure 4. Tethersonde sounding system.

Figure 5. The sodar antennas in a shield.

3.8 *UAV flights*

The UAV was operated nearby AWS5 site. Successful flights were 26. The height of vertical profiles varies, maximum reached height was appr. 2000 m. The most typical flight pattern of one flight

Figure 6. Preparations before a UAV flight.

(determined temporally by the UAV battery) consists of one 1 km profile + 2-4 0.5 km profiles. All flights were performed late evening or after midnight (with desired conditions as light wind, low solar height angle, clear sky or few clouds).

4. ASSORTED RESULTS

4.1 *Inversions*

Temperature inversions are prominently found in the Antarctic, with most persistent temperature inversions occurring in winter. Unfortunately, temperature inversions are usually associated with the largest errors in near-surface variables in numerical weather prediction models. In order to study the characteristics (and factors controlling inversion properties) of the low-level tropospheric temperature inversions all soundings of the tethersonde system launched during the campaign were analyzed. The ascents and descents were considered separately which yielded 132 single vertical profiles of temperature. In addition, the temperature profiles were completed with a surface temperature which was calculated from the measured incoming longwave radiation. From each temperature profile, temperature inversions were identified and analyzed manually. Temperature inversions were identified as layers with a temperature increase with altitude of at least 0.3°C. This definition filtered out the weakest inversions. The temperature inversion depth TID is defined as the difference between the inversion base height, where the temperature starts to increase with altitude, and the top height, where the temperature starts to decrease. The temperature inversion strength TIS, in turn, is the difference between the temperature at the base height and the temperature at the inversion top height. Histogram of inversion statistics, based on the time of inversion occurrence, is given in Figure 7. From all analyzed profiles, surface-based inversions were rather common, observed in more than 60% of occasions. Comparing to the whole dataset, the surface-based inversions were the strongest, with the lowest inversion base temperature.

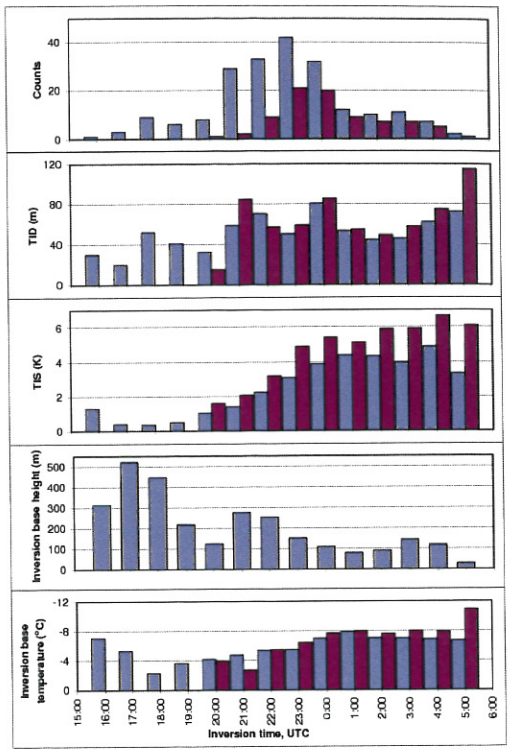

Figure 7. Mean values of temperature inversion characteristics plotted for the time of inversion occurrence. Blue bars refer to the whole dataset of observed inversion (205 cases) and purple bars consider only surface-based inversions (82 cases).

4.2 *Atmospheric profiling with UAV SUMO*

The Small Unmanned Meteorological Observer (SUMO) has been developed as a mobile and cost-efficient platform for atmospheric measurements in the lower troposphere. It is based on a light-weighted commercially available model airplane (FunJet by Multiplex) and provides temperature, humidity and wind profiles to maximum height of 3 km above surface. It has a Paparazzi autopilot system that allows the operator to define complex autonomous missions while in flight to perform any task or adapt to any scenario. The field campaign in Aboa was the first occasion for FMI researchers to test the SUMO.

To solve the UAV wind speed V, the optimization problem was solved minimizing the following sum:

$$\sum_i \left(V_{ai} - \left| \vec{V}_{gi} - \vec{V} \right| \right)^2$$

where V_g is the UAV ground speed from GPS data and V_a is air speed from Pitot tube, installed on the UAV.

Preliminary results of two case studies where profiles from tethered balloon system and sodar are compared with SUMO profiles are given in Figures 8 and 9. Wind speed and direction profiles, considered in Figure 8, were observed at January 3, 2011. The UAV flight took place at 22:42-23:03 UTC, the tethersonde sounding at 22:21-23.24 UTC and the sodar profiles are from 22:40-23:00 UTC (5 min averages). Note that tethersonde wind speed is given here as raw data, descent and ascent measurements are not averaged.

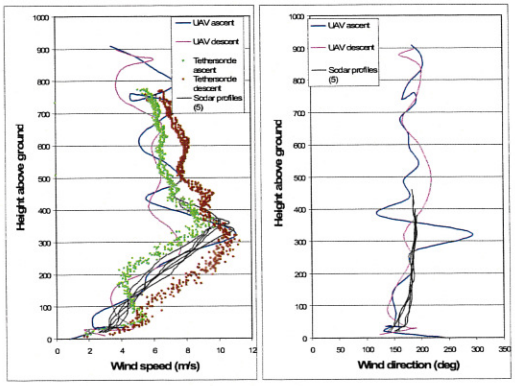

Figure 8. Comparison of vertical profiles of wind speed and direction at January 3, 2011.

The comparison of temperature and humidity vertical profiles is given in Figure 9. The measurements were performed at January, 15, 2011. The UAV flight took place at 21:27-21:54 UTC and tethersonde sounding was carried out at 21:00-22:14 UTC. The UAV measured temperature is in general slightly higher. Another distinctive feature of the temperature profile is a wavelike behavior during descent. This is obviously due the solar radiation error on temperature sensor, when UAV is slowly descending and follows the circling/helical flight pattern. The humidity profiles indicate the time lag of humidity sensor. This is clearly observed both during at the descent and ascent. At the first case, the UAV ascent is simply too fast for humidity sensor to observe fine scale details. During the descent the vertical displacement is observed, referring again to the sensor response time deficiency.

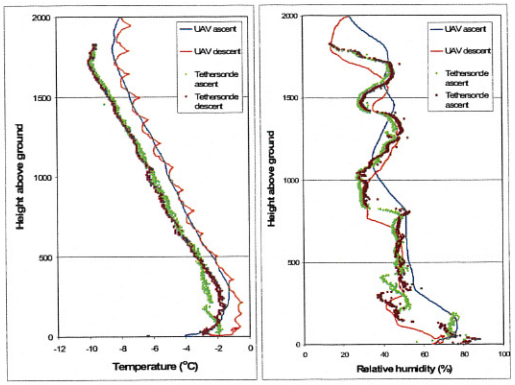

Figure 9. Comparison of vertical profiles of temperature and relative humidity at January 15, 2011.

In summary the UAV SUMO proved as relatively easy-to-hand "recoverable radiosonde" for boundary layer research, even under polar conditions. However, there is still a great potential for improvements. Firstly, the implementation of faster temperature and humidity sensors is desirable. Secondly, for reliable wind estimation accurate UAV attitude and Pitot tube values are required. Thirdly, the integration of IMU cards (combination of gyro and accelerometers) on the board of SUMO would be important step toward fully autonomous flights in clouds and under low clouds.

5. CONCLUSIONS

The expedition was carried out without any major problems and data sets gathered allow good possibilities for the studies listed in Section 2. In addition, modeling studies on snow thermodynamics and mesoscale meteorology can be done to support the data analyses. The data can be utilized also in detailed case studies.

REFERENCES

Tastula, E.-M., and T. Vihma (2011). WRF model experiments on the Antarctic atmosphere in winter. *Mon. Wea. Rev.*, 139, 1279-1291.

Valkonen, T., T. Vihma, S. Kirkwood, and M. M. Johansson (2010). Fine-scale model simulation of gravity waves generated by Basen nunatak in Antarctica. *Tellus*, 62A, 319–332.

Vihma, T., O.-P. Mattila, R. Pirazzini, and M. M. Johansson. (2011). Spatial and temporal variability in summer snow pack in Dronning Maud Land, Antarctica. *The Cryosphere.*, 5, 187–201.

Two summer seasons at Union Glacier: 2010-2011/2011-2012

-Antarctic Logistics and Expeditions
-After more than 20 years at Patriot Hills, ANI/ALE moved to Union Glacier in 2009-2010
-Camp set up/operations/activities
-Weather at UG
-Weather Forecasting at UG
-Weather Observing at UG
-New AWS WX11 at Sky Train Ice Rise

The British Antarctic Survey's new Halley VI station

The first station at Halley was established by the Royal Society in 1956 and was used to conduct research into meteorology, glaciology, seismology, radio astronomy, and geospace science for the International Geophysical Year (IGY). After the IGY ended the station was handed over to the British Antarctic Survey who have maintained a permanent presence ever since, while continuing to conduct many of the original studies uninterrupted.

There have been five Halley stations during its history, details of these stations can be found at: http://www.antarctica.ac.uk/living_and_working/research_stations/halley/halleyvi/?page_id=11

Halley is built on the Brunt Ice Shelf, a floating area of ice that is flowing off the Antarctic Plateau some 50km south of the station's current location. As the ice flows off the mainland the buildings move with it - each year the station drifts north-west by around half a kilometre. As the ice shelf is pushed further and further from the coast it is put under increasing strain by the motion of the tides until eventually a large section breaks off to form an iceberg.

During the 50 years that Halley has been on the Brunt Ice Shelf, several major calving events have been observed. Each new station has been built further inland to compensate, but Halley V's greater success has lead to it drifting further than any of the previous stations. BAS glaciologists studying the ice shelf's motion have forecast that the next significant calving event could occur south of the location of Halley V. Although these events typically take several years to break off completely, BAS made the decision to relocate further inland well before any event is likely to occur.

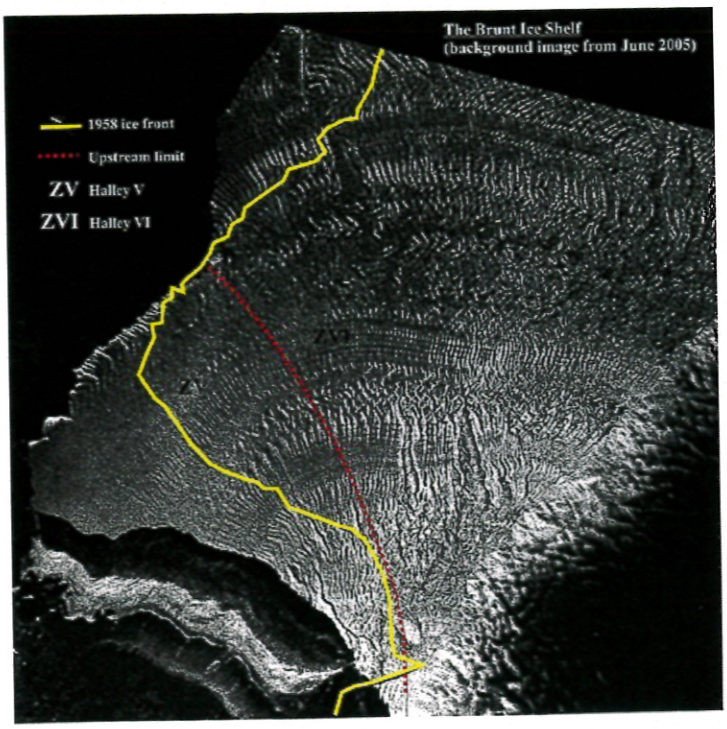

Opposite is a satellite image of the Brunt Ice Shelf taken in 2005. The yellow line indicates the location of the edge of the shelf shortly after the first Halley station was constructed. The red dashed line marks the furthest back that the ice shelf is likely to break back to if a carving event does occur.

The design of Halley VI combines the benefits of the jackable and ski-based buildings currently in use at Halley V. The station is made up of individual modules, which are connected together by short, flexible corridors. The modules are kept above the snow surface using hydraulic legs mounted on skis. As well as keeping the buildings above the rising snow level the new design will allows the station to be periodically relocated across distances of many kilometres. If the station must be moved the individual modules are designed to be separated, towed across the ice shelf by bulldozer, then reconnected again at the new site. This makes it possible for the station to remain a safe distance from the edge of the ice shelf.

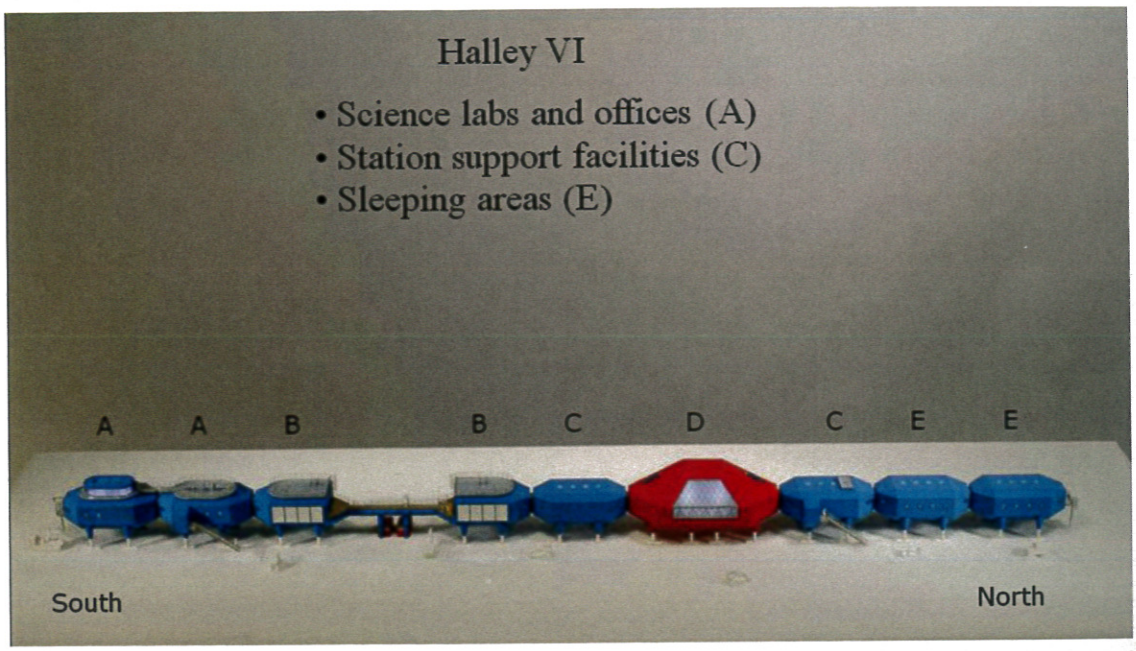

The building were finished in the last 2011/12 season with only minor works needed next season a picture of the finished station can be seen below.

New meteorological equipment was also installed this last season with the installation of a JAWS (Just Another Weather Station) system which is based around a Campbell CR1000 logger and has a Druck pressure sensor, temperature is obtained via a PRT in an aspirated radiation shield and humidity is obtained from a Vaisala HMP 45 probe also in an aspirated radiation shield.

There are two wind sensors, a Vaisala WS 425 sonic anemometer is the primary source of the wind data but there is also an RM young aerovane as a backup.

A CNR4 solar radiation sensor is attached to the system that can measure incoming and outgoing long and shortwave radiation.

Sunshine is recorded using a CSD1 sunshine detector.

There are daily radiosonde launches using a Vaisala MW31 ground station, RS92 radiosondes and 350gram balloons

A picture of a balloon launch from the balloon container with the meteorology mast in the background can be seen below.

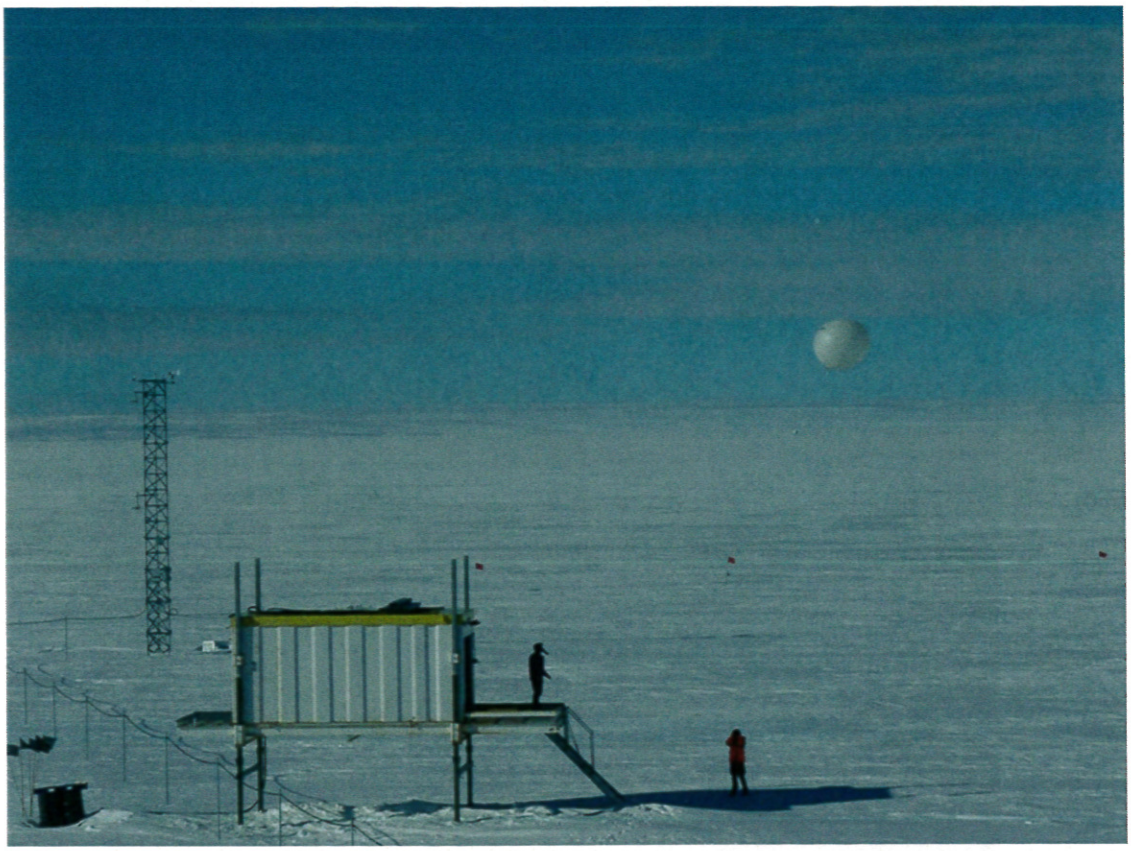

Inside the observation deck on the top of one of the science modules is located a Dobson spectrophotometer for making ozone measurements.

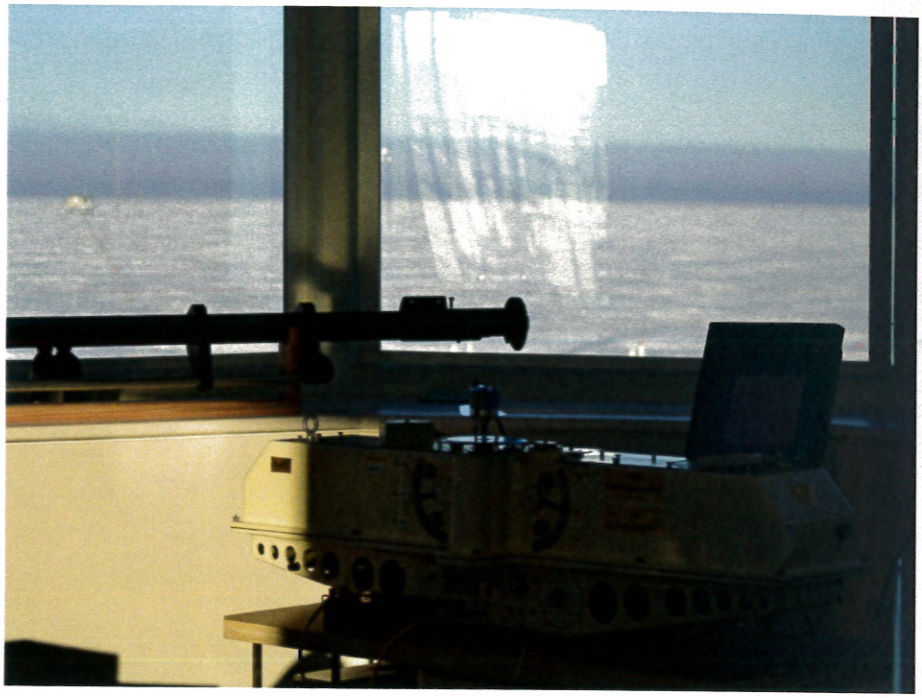

Atmosphere aerosol is measured using a Prede POM-01 sun photometer and cloud height is measured using a Vaisala CT25K Ceilometer. These instruments are located on the roof deck of the science module as shown below.

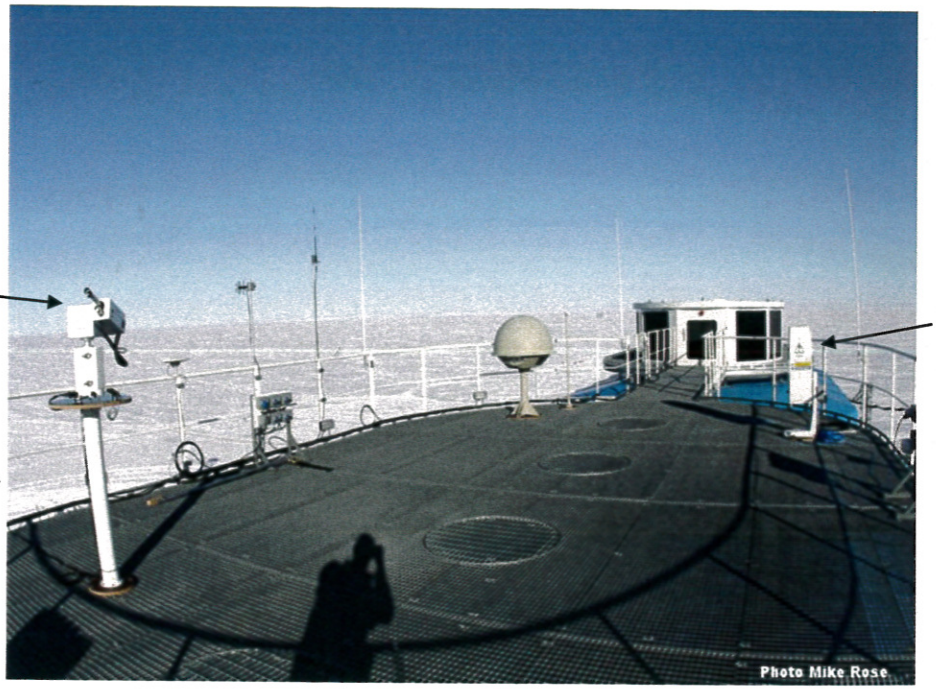

Observing the Antarctic Atmosphere with Small Unmanned Meteorological Observers (SUMO)

John J. Cassano
Cooperative Institute for Research in Environmental Sciences
and Department of Atmospheric and Oceanic Science
University of Colorado
Boulder, CO
john.cassano@colorado.edu

Unmanned aerial vehicles (UAVs) can provide detailed information about the three-dimensional structure of the atmosphere. Analysis of the detailed three-dimensional structure of the atmosphere allows us to better understand the physical processes acting to shape the dynamic and thermodynamic evolution of the atmosphere. In addition, data such as this can be used to evaluate high-resolution numerical weather prediction model output.

Previous UAV observations of the atmosphere were made using relatively large (3 m wingspan, 15 kg weight) Aerosonde UAVs to study air-sea coupling over the Terra Bay polynya in September 2009. The Aerosonde UAVs are costly (~$50,000 each) and logistically difficult to operate - requiring a team of 4 UAV operators and a groomed runway for take-off and landing.

In January 2012 the use of a small UAV known as the Small Unmanned Meteorological Observer (SUMO) was demonstrated in the vicinity of McMurdo Station. The SUMO UAV has an 80 cm wingspan and a take-off weight of 580 g. As used in January 2012 the SUMO UAV was equipped to measure temperature, humidity, pressure, and wind. Examples of the various boundary layer structures observed during 4 flight days in January 2012 will be shown, including a deep convective boundary layer and a strong surface-based inversion. Issues with the meteorological sensors will be reviewed as well as requirements for gaining clearance to operate the UAVs in the relatively crowded United States Antarctic Program airspace during the austral summer.

Augmentation of the Ross Island Region AWS network with New Autonomous Sensors for Measuring Atmospheric Composition in Antarctica.

L.E. Kalnajs
Laboratory for Atmospheric and Space Physics (LASP) University of Colorado, Boulder, USA

Antarctica is the most sparsely instrumented area of the Earth for the in situ observation of atmospheric composition and chemistry. The lack of instrumentation is largely attributable to the scarcity of suitable locations for instrumentation (year round research stations) and the high logistical overhead involved with operating monitoring instrumentations at the available locations. We have addressed these limitations by augmenting a sub set of Automatic Weather Stations in the Ross Island region with purpose built instrumentation for measuring ozone concentrations.

The Automatic Weather Station (AWS) network provides the greatest number of potential measurement locations through out Antarctica, with a high density of stations in some coastal areas, which are of particular interest for studies of tropospheric chemistry. In these coastal locations, ozone plays an important role in the overall chemical cycles in the as the dominant oxidizer. While tropospheric ozone exhibits a predictable seasonal variation, there are also poorly understood anomalies (ozone depletion events) at polar sunrise.

We have designed, built and installed a network of reliable, low- power ozone sensors, co-located with existing Automatic Weather Stations (AWS) in the Ross Island region that will produce a multi-season data set of surface level ozone observations. This network approach to ozone monitoring has important advantages over a single station both for establishing a record of surface level ozone distributions and for the study of specific phenomena such as ozone depletion events. The combination of the AWS and ozone sensor networks provides significantly more information than obtainable from any single measurement. The network approach provides information about the true chemical rate of ozone depletion, and the sources of ozone depleting species. This information can be obtained by observing ozone depletion from a single air mass as it passes over multiple stations. Additionally, meteorology is thought to play a significant role in the onset of surface level ozone depletion events through multiple mechanisms and the tight integration of ozone measurements and meteorological data from the AWS will give insight into the interplay of meteorology and chemistry on the formation of ozone depleted air masses. For example, boundary layer stability can magnify the intensity of the observed ozone depletion by increasing the residence time of an air mass in the boundary layer, and minimizing the in-fill of ozone rich air from the free troposphere. High boundary layer stability is a common occurrence in the Ross Island area where the network has been established. Surface level winds also play an important role in the formation of aerosol particles from snow and ice surfaces, and there is strong evidence to suggest that windblown snow and sea salt is an important source of the halogens that are thought to catalyze surface level ozone depletion. Finally, many of the ozone depletion events that have been observed at existing sites are not the product of local chemistry, but are driven by the transport of ozone depleted air from other areas. The availability of high-resolution local meteorological measurements from the AWS network in combination with numerical models (eg AMPS, HYSPLIT) allows for improved trajectory analysis to determine the source locations for ozone depleted air masses.

Furthermore, the remote locations of the AWS sites and the use of renewable non-polluting energy sources, provide ozone observations that are free of anthropogenic influence and hence more representative of the broader distribution in the region. This data set is invaluable for studying the natural background processes that control

tropospheric ozone, without the influence of transported pollution and local pollution sources that have muddied the interpretation of other polar ozone measurements. The addition of robust, low-cost and low-power ozone sensors to the Ross Island-region AWS network capitalizes on this existing and proven system, and expands the type of scientific questions related to high latitude tropospheric ozone that can be addressed.

Initial data from the network have shown a high level of agreement between stations and with the historical record from the NOAA monitoring station at Arrival Heights. Data is being returned to Boulder in near real-time via the AWS radio modem network as well as by Iridium satellite data. This data is quality controlled and archived on servers at the University of Colorado and will be available to the community on an operational basis after calibrations and data verification has been performed during a field visit this Austral spring.

In addition to the specific results presented here, the sensor-network presents a new paradigm for measurements in the Antarctic. The feasibility of remote, near-real time Antarctic measurement systems has been demonstrated by the AWS systems, but this project is the first to develop and deploy chemical sensors in the harsh conditions of the Antarctic. The success of this endeavor will pave the way for future design and deployment of more and varied chemical sensors to study the remote high latitude environment.

Funding for this research was provided by the NSF Office of Polar Programs (Award Number 1043266).

POWER, DATA TELEMETRY, AND IDEAS FOR ADDITIONAL SENSORS ON AUTOMATIC WEATHER STATIONS

Jonathan E. Thom*[,1], Lee J. Welhouse[1], and Matthew A. Lazzara[1]
[1]Antarctic Meteorological Research Center, Space Science and Engineering Center
University of Wisconsin-Madison
Madison, Wisconsin

http://amrc.ssec.wisc.edu/

1. OVERVIEW

The Automatic Weather Station (AWS) project expanded its scope in the past year with the development and deployment of large power systems to co-locate an ozone experiment at our AWS locations. The collaboration with the ozone experiment also provided additional motivation (besides cost savings) to begin transitioning our stations in the McMurdo area from Argos to 900 MHz radio data telemetry. The power system development will help with future deployment of new equipment that will help improve our measurements and expand what measurements are made at our sites.

2. Power Sytems

In collaboration with Laboratory for Atmospheric and Space Physics at the University of Colorado, the automatic weather station project developed a power system to run an ozone-sampling site at three locations in the McMurdo area. The fourth site is powered by a UNAVCO power system. The systems are deployed at Minna Bluff, Marble Point, Cape Bird and Lorne AWS sites. The systems provide approximately 5 watts of continuous power. They use a combination of solar and wind to charge a large battery bank. The design of the AWS project's system was based on a conglomeration of the PASSCAL and UNAVCO power systems.

3. Freewave

Local McMurdo area stations are gradually being shifted to a Freewave 900 MHz radio telemetry. Figure 1 shows current and future stations that will transmit data via 900 MHz radios. The stations currently on the radio network are Minna Bluff, Willie Field, Marble Point and Cape Bird. The data are relayed to the Internet through a base station located in Building 70 on T-site.

During the 2012-13 field season, Pegasus North will be converted to 900 MHz radio, and a repeater site will be installed to allow 900 MHz radio access to Linda, Lorne, Ferrell II and Windless Bight. The targeted location for a repeater is on White Island. The conversion to 900 MHz radio data telemetry has allowed us to collocate and provide radio connectivity to more than one system at our AWS locations. The radio selected has multiple ports for data transmission. Currently, the ozone data is using the 900 MHz radio network to collect data from Minna Bluff, Marble Point and Cape Bird.

4. Radiation Shields

Measuring the surface air temperature in theory is easy, but in practice, is extremely difficult. In regions of Antarctica where there are low winds and high solar incident radiation, using different thermometer radiation shields can greatly impact air temperature measurement. Winter measurements may also be affected by radiation shield selection. An aspirated radiation shield has been deployed at South Pole station for testing. The aspirated shield that was tested drew six watts. Issues related to aspirated shield use are power, and in a stable surface layer, what temperature is being measured. Options for different sensors and shields to achieve temperature measurements that are not contaminated by radiation issues are being researched. The development of an in-house power system will help with the deployment of some type of aspirated radiation shield.

* Corresponding Author: Jonathan Thom,
Antarctic Meteorological Research Center, Space Science and Engineering Center,
University of Wisconsin-Madison
Email: jthom@ssec.wisc.edu

5. New Sensors

Some possible new sensors that are being considered include an infrared thermometer for measuring the snow surface temperature and an upgrade to the silicon pyranometer. An infrared thermometer could potentially provide a useful observation for validating satellite remotely sensed temperature observations. The pyranometer being considered uses a thermopile and glass dome in contrast to the silicone sensor. The use of the dome may help prevent snow accumulation on the surface compared to the silicon pyranometer. The deployment of new sensors will allow the AWS project to add more value to our sites and will provide measurements that may be leveraged for other studies.

6. Conclusions

The power systems and Freewave Radio network will be assessed each field season to make improvements to the systems. The collocation of the ozone-monitoring site at our AWS has proven to be beneficial. Some new sensors will be tested in the coming season deployments, but most of the new sensor and shield additions will be fielded during the next grant.

7. ACKNOWLEDGEMENTS

This material is based upon work supported by the National Science Foundation under grant #ANT-0944018.

Figure 1: Map of Ross Island area weather stations that will be converted to Freewave radio data telemetry.

ANTARCTIC AUTOMATIC WEATHER STATION TEMPERATURE MEASUREMENTS
HOW GOOD ARE THEY?

George A. Weidner[2], Jonathan E. Thom[*1,2], Lee J. Welhouse[1], Matthew A. Lazzara [1],Linda M. Keller[2], David E. Mikolajczyk[1],
and George A. Weidner[2]
[1]Antarctic Meteorological Research Center, Space Science and Engineering Center
[2]Department of Atmospheric and Oceanic Sciences
University of Wisconsin-Madison
Madison, Wisconsin

http://amrc.ssec.wisc.edu/

1. OVERVIEW

Automatic Weather Stations (AWS) developed originally at Stanford University in the 1970's and since 1980 developed , deployed and maintained by the University of Wisconsin's AWS (now under the Antarctic Meteorological Research Center) program, have recorded air temperature and pressure along with wind data for over 30 years a few Antarctic sites. Some sites (e.g. Byrd Surface Camp) provide extensions of observations taken by station personnel prior to AWS deployment. As the data record has lengthened, investigators are using the data (particularly temperature), in studies that seek to determine if any climatic trends are observed in the records. We present a status report on how one should view the accuracy of the temperature measurements from the AWS.

2. AWS2B calibrations and measurements

The original Stanford AWS temperature circuit consisted of a modified bridge that had two bridge resisters - a one-percent precision resister and the Weed platinum resistance thermometer (PRT) in a two wire configuration. In the modified bridge both of these were referenced to system ground. The calibration point for the AWS was chosen to be 0.0 ^{o}C. A 1000 ohm (at 0.0 ^{o}C) PRT was selected as the temperature sensor. In order to set the PRT to 0C for a particular AWS, a 0.05% resister was substituted for the PRT and the AWS temperature output was observed. There was a nominal +/- 2.0 C offset observed. The output was set to 0C by setting an offset value in the AWS onboard software that compensated for the variation of the resistors in the bridge from their stated values. Since the measurements were from the ratio of two values temperature variations were minimized. After the calibration offset was programmed into the AWS software, other temperature values were simulated down to -75C. Typical "errors" from the PRT calibration table were less than 1.0 C.

The recent AWS based on Campbell Scientific's (CSI) CR1000 data loggers have used CSI's standard temperature sensor (model 43347 RTD) in a full four-wire bridge configuration.

3. AWS temperature shields

The AWS2B temperature shields on the sensor booms deployed by Stanford varied in composition, but were basically a three plate shield mounted on the original six foot boom. Temperature "errors" were observed in light winds and some of the mounts were not thermally isolated from the boom. The sensor boom was redesigned in 1983 and the temperature sensor shield consisted of a three inch diameter tube that was six inches in length. The inside was painted with flat black paint and the outside had Mylar reflective tape applied to it. The shield was naturally vented by a one inch space between the top of the shield and the bottom of the sensor boom. Examination of the temperature data has indicated a warm bias in light winds.

Recent AWS based on Campbell Scientific's CR1000 data loggers have use the 10 plate Young shield.

4. Shield comparisons at South Pole

From February to June of 2011 a test facility was set up at the South Pole to compare the temperature measurements of the Weed PRT with AWS2B shield, the CSI RTD with naturally

• Corresponding Author: Matthew A. Lazzara
Antarctic Meteorological Research Center, Space Science and Engineering Center, University of Wisconsin-Madison
Email: mattl@ssec.wisc.edu

ventilated shield and a CSI RTD with a ventilated shield that was powered for two minutes out of a ten minute measurement periods. Shortwave radiation and wind speed were also measured.

5. Preliminary results for AWS2B calibrations

As the AWS2B units are replaced with the new CR1000 based units, the returned AWS are again calibrated to determine if the calibration point at 0C is still valid and at simulated temperatures down to -75C. Results of these tests for a few AWS2B units show that some of the early AWS boards fabricated at Stanford had an incorrect resistor in the analog-to-digital circuit that created a nominally linear temperature offset as a function of temperature. Later AWS2B fabricated at Wisconsin did not exhibit this behavior and calibrations were within nominal specifications at 0C.

6. Preliminary results for South Pole shield comparison

The power to the South Pole test facility went below minimum requirements in early June 2011. Comparisons of the three temperature systems from February to June, indicated that at about four meters per second for wind speed, the CSI Gill naturally ventilated RTD and Weed with AWS2B shield were within calibrated margins of error (with only a slightly higher bias for the Weed in stronger solar radiation). We did not have the ventilated shield on long enough to bring the CSI RTD temperature sensor into equilibrium with the environment. The important observation here was that if the power is NOT on for the ventilated shield, the temperature error is typically 4 to 5 C.

7. ACKNOWLEDGEMENTS

This material is based upon work supported by the National Science Foundation under grant #ANT-0944018.

INVESTIGATING A UNIQUE SUMMERTIME PRECIPITATION EVENT IN THE MCMURDO DRY VALLEYS (MDV), ANTARCTICA

T. Dallafior, M. Katurji, I. Soltanzadeh, P. Zawar-Reza*
Centre for Atmospheric Research, University of Canterbury, Christchurch, New Zealand

1 INTRODUCTION

The McMurdo Dry Valleys (MDV) are the largest ice-free region in Antarctica (Doran et al., 2002). With average annual temperatures as low as -18°C (Doran et al., 2002) and average precipitation amounts between 3 and 50mm water equivalent (Fountain et al., 2010), the region classifies as a cold desert. Microorganisms, mosses, and lichen relying on liquid water populate this meager environment (Cary et al., 2010; Zeglin et al., 2009; Lee et al., 2011). The hydrology in the MDV is highly variable with liquid water only available during the summer months when surface soil temperatures are near freezing, and meltwater from glaciers reaches the MDV through ephemeral streams (Gooseff et al., 2011). Other liquid water sources comprise deposition of water vapor from the atmosphere (Levy et al., 2012), and precipitation / blowing snow with subsequent melting.

Coastal precipitation in Antarctica is linked to poleward moving air masses being blocked by the coastline and subsequent topographic lifting (Bromwich, 1988). The amount of snow received in the MDV was found to decrease with increasing distance from the coast (Fountain et al., 2010). Even though mid-latitude cyclone frequencies are lower during summertime, the Ross Sea region shows frequent mesoscale cyclone generation (Carrasco et al., 2003). Moreover, backward trajectory analyses suggest both, mesoscale and synoptic-scale cyclones as important moisture sources on the west coast of the Ross Sea (Sinclair et al., 2010). Interstingly, a site closer to the MDV (adjacent to the open Ross Sea) received most of its precipitation during midsummer and was always linked to synoptic-scale low-pressure systems (Markle et al., 2012).

*Corresponding author address: Peyman Zawar-Reza, Department of Geography, University of Canterbury, Private Bag 4800, Christchurch, New Zealand, peyman.zawar-reza@canterbury.ac.nz

Only little research so far has focused on the amount of liquid water in the MDV originating from precipitation and snow blow. In summertime, snow falling in the MDV was expected to be blown away by the winds or simply sublimate into the atmosphere rather than melt (Stichbury et al., 2011; Fountain et al., 2010; Gooseff et al., 2011). However, katabatic drainage is weaker and disrupted during summer months (Parish and Cassano, 2003; Parish et al., 1993). Futhermore, observations of snow fallen in Miers Valley, Antarctica, on the night between 18th and 19th January 2012 provide evidence for snow melt: Even though the snow was removed the following day within hours (see fig. 1), the top 2cm of the soil were clearly wet (see top soil profile in the corner of figure 1).

Figure 1: Miers Valley the day after snowfall (19th January 2012) at 12pm (left) and 1pm (right). Bottom left: Top soil profile (5cm) after snowfall with a clearly wet layer (about 1.5cm) below the snow. (Photos: Courtesy of Don Cowan)

To date, two studies derived high-resolution precipitation climatologies for the MDV region: Monaghan et al. (2005) modeled a precipitation distribution as derived from one year forecasts from the Antarctic Mesoscale Prediction System (AMPS) on a resolution of 3.3 km for the entire McMurdo region. Fountain et al. (2010) compared precipitation measurements using rain gauges with numerical output from

AMPS with a resolution of 2.2 km over a one year period. However, these resolutions are too low to capture the complexity of the MDV. Miers Valley, which is subject to the present study, is only 1.5 to 2.5 km wide (distance between the ridges of the valley sides) and would therefore barely cover two grid cells with such model resolutions.
Only one study derived a highly resolved spatial distribution of liquid water in the MDV. The calculation of a wetness index was mainly based on slope and the amount of water originating from upstream of a grid cell (Stichbury et al., 2011). Liquid water input from precipitation was taken into account using remote sensing data and probabilistic approaches to derive snow cover. However, atmospheric processes as well as surface energy balances were not considered.

In order to gain a better understanding of the nature of precipitation in the MDV, a case study of a precipitation event in Miers Valley (78°6'S 164°0'E) in the south of the MDV is presented. An exceptional amount of observational data documenting the event is available. These data are complemented with model output generated with the polar Weather Research and Forecasting model (Polar WRF, Skamarock et al., 2008; Hines and Bromwich, 2008; Bromwich et al., 2009; Hines et al., 2011) in order to account for the spatial heterogeneity of the area. Using high resolution modeling allows for an unprecedented level of detail to investigate the origin of precipitation in the MDV and investigate topographic as well as local dynamic effects more closely.

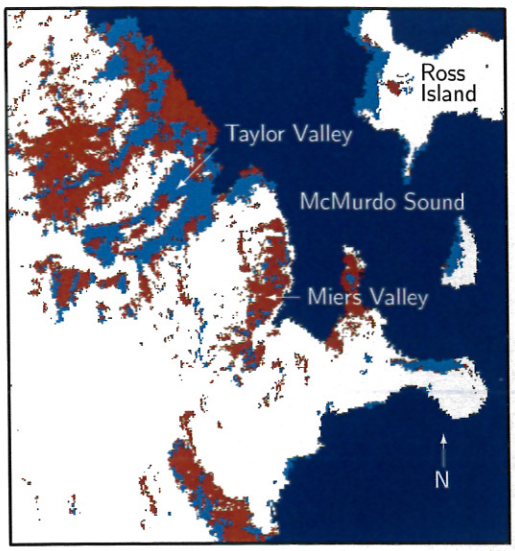

Figure 2: MODIS satellite image during snowfall in the northern MDV (18th January 2012, 5pm, GMT+13). Bright blue indicates cloud cover, white is snow-cover and brown corresponds to snow-free areas.

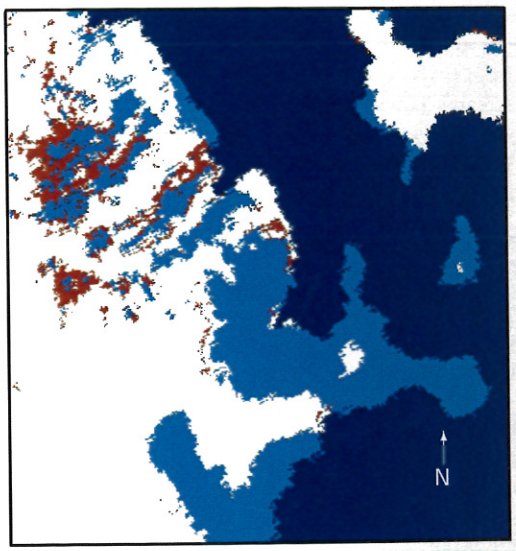

Figure 3: MODIS satellite image during snowfall in the Miers Valley region (19th January 2012, 3am, GMT+13).

2 METHODS

Polar WRF was run with four nested grids focussing on Miers Valley, which is situated in the Denton Hills in the south of the MDV (see figure 2). The region was modeled with four two-way nested modeling grids with horizontal spacings of 16 km, 4 km, 1 km, and 250 m respectively, and 38 terrain-following vertical levels with the lowest levels about 11 m apart. The first grid domain was forced by initial and boundary conditions from the National Centre for Environmental Prediction (NCEP) Final Analysis dataset (FNL, 1 degree resolution, 6-hourly). Microphysical processes were calculated with the WRF Single-Moment 6-class scheme. To account for the characteristics of the MDV, initial data for land-use categories, soil temperature and soil moisture were adapted to the study area as outlined in Steinhoff (2011) to better match observed characteristics of the MDV (Campbell et al., 1998; Thompson et al., 1971). Moreover, highly resolved topographic data (LIDAR, 4 m resolution) were incorporated for the region in and around Miers Valley (Courtesy of Gateway Antarctica, University of Canterbury, New Zealand).

The event was also monitored by a complete eddy covariance system to measure radiation, sensible, latent, and ground heat fluxes. This was necessary to derive the surface energy budget. Remote sensing was also employed via satellite derived images (MODIS) for cloud and snow cover for the large scale analysis of the event. Moreover, SODAR data provided vertical wind profiles of the boundary layer. Synoptic composites with Infrared pictures of the entire Antarctic continent are provided by the Antarctic Meteorological Research Center (AMRC), as well as sounding data from McMurdo Station.

3 RESULTS

3.1 Local Observations

The sensible and latent heat fluxes observed in Miers Valley are shown in figure 4. The gap in latent heat fluxes seen during the night of 18th / 19th January 2012 is caused by the moisture sensor freezing during snowfall. Sensible heat fluxes show a clear diurnal signal reaching peaks of up to 200 W m^{-2} both, before and after snowfall.
Latent heat fluxes are very close to zero the day before snowfall, showing hardly any diurnal signal, indicating very low soil moisture content. After snowfall, a peak of 50 W m^{-2} is reached on 19th January 2012, which quickly declines the following hours. Note however the weak diurnal signal persisting on the the second day after snowfall. This suggests that significant amounts of snow do melt and cuse increased top soil moisture content even a few days after snowfall. This could be relevant for the biosphere, which relies on water, sunlight and nutrients to thrive.

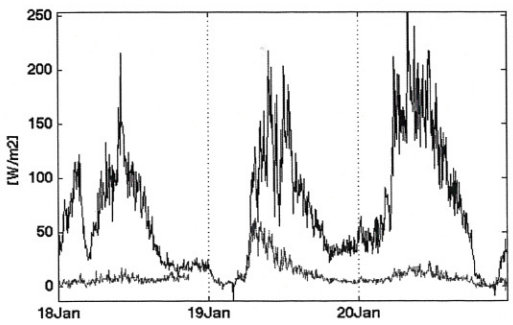

Figure 4: Five minute averages of sensible (black line) and latent (grey line) heat fluxes from observations in Miers Valley. The gap in latent heat flux data originates from the moisture sensor freezing up during snowfall.

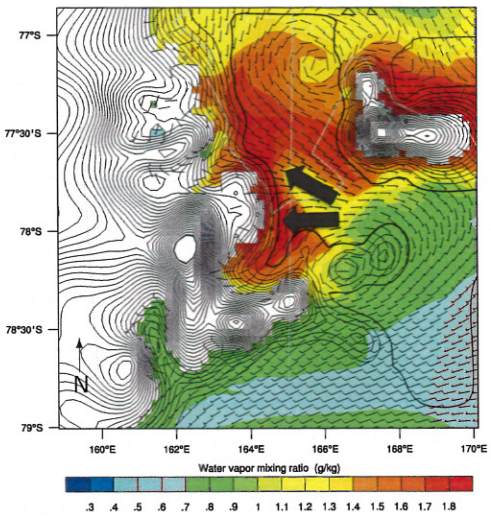

Figure 5: McMurdo Sound region at 900 hPa: Wind barbs and moisture content.

3.2 Large-scale Dynamics

As evident from MODIS satellite imagery (figures 2 and 3), there are major differences between the regions inside the MDV: While the northern part experienced cloud cover and snowfall on 18th January 2012 at 5pm local time, the Denton Hills (including Miers Valley) remained cloud-free. It is not until a few hours later that clouds extending over this area caused the observed snowfall in Miers Valley (figure 3, 19th January 2012 at 3am local time).

Synoptic surface observations (not shown here, Antarctic Meteorological Research Center, SSEC, UW-Madison) show a low-pressure system prevailing northeast of the Ross Sea region, directing moist air towards the McMurdo region. However, Ross Island prevents these air masses from directly impinging on the coastlines of the MDV area so that airflow is directed around the island before it reaches McMurdo Sound. For more detail about the synoptic situation, please refer to Zawa-Reza et al. (2012).

Polar WRF shows that moisture is concentrated in the lower levels of the troposphere and cloud cover evolves at levels as low as 900 hPa. Air masses entering McMurdo Sound from the east at this level are convergent due to topographic channeling between the Islands confining McMurdo Sound coast. Subsequent divergence (see figure 5) directs air masses towards the coastlines where topographic lifting desta-

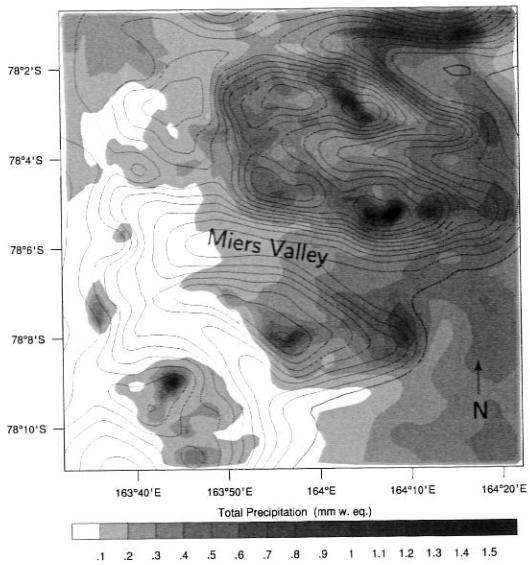

Figure 6: Total precipitation in mm water equivalent during the 19th January snowfall event in Miers Valley.

bilizes the air mass column, which fosters cloud formation. The shape of the coastline as well as the way air masses become modified by the topography of the islands decides, where this happens and therefore explains the different patterns seen in the satellite observations earlier (fig. 2 and 3).

3.3 Modeled Precipitation

In Polar WRF (250 m horizontal resolution grid), the time of modeled precipitation onset was in accordance with local observations. However, modeled precipitation amounts were about a factor of 5 lower than observed. As shown in figure 6, a clear gradient in total precipitation received is discernible along the valley with decreasing amounts further away from the coast. Moreover, the south facing valley side receives more snow than the north-facing side. Trajectory calculations show that coastal air masses going up Miers Valley are directed towards the south facing slope, which explains the cross-valley symmetry. This is mainly a consequence of the topography of the valley and its orientation in the south-east direction facing the incoming moist air. Moreover, local circulations resulting from differential heating of the slopes could result in deflection of air masses, which is an ongoing research objective in this work.

4 CONCLUSIONS AND OUTLOOK

The results presented here provide insight into a precipitation event in the MDV on an unprecendet level of detail. Results so far suggest that precipitation contributes more liquid water to the local biosphere than previously assumed.

Model results suggest a dominant role of topography in determining precipitation in the MDV. While previous studies attributed rain shadowing effects to the Transantarcis Mountains from a cliamtic perspective (e.g. Monaghan et al., 2005), our investigation stresses the importance of Ross Island in modifying northeasterly moist air masses reaching the region. We therefore reccommend properly resolving the McMurdo Sound wind divergence and covnergence zones in order to significantly improve weather and precipitation forecast in the region on short time scales.

Modeled precipitation patterns show an along-valley gradient in received precipitation amount as well as a cross-valley gradient. While the along-valley gradients is mainly related to the coastal origin of air masses, the cross-valley gradient can be related to local topographic and thermal circulation effects.

Future work will further investigate the effects of local circulations induced by surface energy fluxes and their impact on the airflow inside the valley. SODAR observations of the snowfall event will give insight into the vertical characteristics of the boundary layer in Miers Valley. The high-resolution model output will complement these in-situ observations and account for the spatial heterogeneity of the area.

Another objective of this work is to look into surface energy balances, which allow for an estimate of potential availability of meltwater from snowfall along and across the valley axis. A similar approach was employed in previous studies in Antarctica (e.g. Van den Broeke et al., 2004). This will be useful for research focussing on the ecological dynamics of the area as liquid water, along with light and nutrients, is an indispensable factor enabling life.

Acknowledgements

The authors appreciate the support of the New Zealand Terrestrial Antarctic Biocomplexity Survey (nzTABS), as well as Gateway Antarctica (University of Canterbury). Initial and boundary conditions

for the presented model results are from the Research Data Archive (RDA) which is maintained by the Computational and Information Systems Laboratory (CISL) at the National Center for Atmospheric Research (NCAR). NCAR is sponsored by the National Science Foundation (NSF). Furthermore, we like to thank the Automatic Weather Station Program and/or Antarctic Meteorological Research Center for the data set, data display, information, etc. A special thank-you also goes to Meike Kühnlein from Marburg University (Germany) for preparing the MODIS data for this analysis.

References

D.H. Bromwich. Snowfall in High Southern Latitudes. *Reviews of Geophysics*, 26(1):149–168, February 1988.

D.H. Bromwich, K.M. Hines, and L. Bai. Development and Testing of Polar Weather Research and Forecasting Model: 2. Arctic Ocean. *Journal of Geophysical Research*, 114, 2009.

I. Campbell, G. Claridge, D. Campbell, and M.R. Balks. *The Soil Environment of the McMurdo Dry Valleys, Antarctica*, volume 72, chapter Ecosystem Dynamics in a Polar Desert, the McMurdo Dry Valleys, Antarctica, pages 297–322. Antarctic Research Series, 1998.

J.F. Carrasco, D.H. Bromwich, and A.J. Monaghan. Distribution and Characteristics of Mesoscale Cyclones in the Antarctic: Ross Sea Eastward to the Wedell Sea. *Monthly Weather Review*, 131:289–301, 2003.

S.C. Cary, I.R. McDonald, J.E. Barrett, and D.A. Cowan. On the Rocks: The Microbiology of Antarctic Dry Valley Soils. *Nature Reviews: Microbiology*, 8:129–138, February 2010.

P.T. Doran, C.P. McKay, G.D. Clow, G.L. Dana, A.G. Fountain, T. Nylen, and W. B. Lyons. Valley Floor Climate Observations from the McMurdo Dry Valleys, Antarctica, 1986-2000. *Journal of Geophysical Research*, 107(D24), 2002.

A.G. Fountain, T.H. Nylen, A. Monaghan, H.J. Basagic, and D. Bromwich. Snow in the McMurdo Dry Valleys, Antarctica. *International Journal of Climatology*, 2010.

M.N. Gooseff, D.M. McKnight, P. Doran, A.G. Fountain, and W.B. Lyons. Hydrological Connectivity of the Landscape of the McMurdo Dry Valleys, Antarctica. *Geography Compass*, 9(5):666–681, 2011.

K.M. Hines and D.H. Bromwich. Development and Testing of Polar Weather Research and Forecasting (WRF) Model. Part I: Greenland Ice Sheet Meteorology. *Monthly Weather Review*, 136:1971, 2008.

K.M Hines, D. H. Bromwich, and L. Bai. Development and Testing of Polar WRF. Part III: Arctic Land. *Journal of Climate*, 24:26–48, 2011.

C.K. Lee, B.a. Barbier, E.M. Bottos, I.R. McDonald, and S. C. Cary. The Inter-Valley Soil Comparative Survey: The Ecology of Dry Valley Edaphic Microbial Communities. *The ISME Journal*, 6:1046–1057, December 2011.

J.S. Levy, A.G. Fountain, K.A. Welch, and W.B. Lyons. Hypersaline "Wet Patches" in Taylor Valley, Antarctica. *Geophysical Research Letters*, 39, March 2012.

B.R. Markle, N.A.N. Bertler, and K.E. Sinclair rand S.B. Sneed. Synoptic Variability in the Ross Sea Region, Antarctica, as Seen From Back-trajectory Modeling and Ice Core Analysis. *Journal of Geophysical Research*, 117(D02113), 2012.

A.J. Monaghan, D.H. Bromwich, J.G. Powers, and K.W. Manning. The Climate of the McMurdo, Antarctica, Region as Represented by One Year of Forecasts From the Antarctic Mesoscale Prediction System. *Journal of Climate*, 18:1174–1189, 2005.

T.R. Parish and J.J. Cassano. The Role of Katabatic Winds on the Antarctic Surface Wind Regime. *Monthly Weather Review*, 131: 317–333, 2003.

T.R. Parish, P. Pettre, and G. Wendler. A Numerical Study of the Diurnal Variation of the Adelie Land Katabatic Wind Regime. *Journal of Geophysical Research*, 98:12933–12947, 1993.

K.E. Sinclair, N.A.N. Bertler, and W.J. Trompetter. Synoptic Controls on Precipitation Pathways and Snow Delivery to High-accumulation Ice Core Sites in the Ross Sea Region, Antarctica. *Journal of Geophysical Research*, 115(D22112), 2010.

W.C. Skamarock, J.B. Klemp, J. Dudhia, D. O. Gill, D.M. Barker, M.G. Duda, X.-Y. Huang, W. Wang, and J. G. Powers. *A Description of the Advanced Research WRF Version 3*. NCAR Technical Notes - Mesoscale and Microscale Meteorology Division, National Center for Atmospheric Research, Boulder, Colorado, USA, June 2008.

I. Soltanzadeh, P. Zawa-Reza, M. Katurji, and T. Dallafior. Summertime Wind Regimes in Miers Valley, Other McMurdo Dry Valleys, Antarctica: High-resolution Numerical Simulation. In *7th Antarctic Meteorological Observation, Modeling, and Forecasting Workshop*, 2012.

D.F. Steinhoff. *Dynamics and Variability of Foehn Winds in the McMurdo Dry Valleys Antarctica*. PhD thesis, Ohio State University, 2011.

G. Stichbury, L. Brabyn, T. Green, and C. Cary. Spatial Modelling of Wetness for Antarctic Dry Valleys. *Polar Research*, 30, 2011.

D.C. Thompson, R. M. F. Craig, and A.M. Bromley. Climate and surface heat balance in an antarctic dry valley. *New Zealand Journal of Science*, 14:245–251, 1971.

M.R. Van den Broeke, C.H. Reijmer, and R.S.W. Van de Wal. A Study of the Surface Mass Balance in Dronning Maud Land, Antarctica, Using Automatic Weather Stations. *Journal of Glaciology*, 50(171): 565–582, 2004.

P. Zawa-Reza, I. Soltanzadeh, M. Katurji, and T. Dallafior. High-resolution Numerical Analysis of Up-valley Summer Flow in Miers Valley. In *7th Antarctic Meteorological Observation, Modeling, and Forecasting Workshop*, 2012.

L.H. Zeglin, R.L. Sinsabaugh, J.E. Barrett, M.N. Gooseff, and C.D. Takacs-Vesbach. Landscape Distribution of Microbial Activity in the McMurdo Dry Valleys: Linked Biotic Processes, Hydrology and Geochemistry in a Cold Desert Ecosystem. *Ecosystems*, 12:562–573, March 2009.

HIGH-RESOLUTION NUMERICAL ANALYSIS OF UP-VALLEY SUMMER FLOW IN MIERS VALLEY

Iman Soltanzadeh, Peyman Zawar-Reza*, Marwan Katurji, Tanja Dallafior
Centre for Atmospheric Research, University of Canterbury, Christchurch, New Zealand

1. INTRODUCTION

In response to shortwave interaction with the surface, summertime airflow patterns in McMurdo Dry Valleys (MDV) show bimodal behavior, either up-valley (easterly) or down-valley (westerly) (McKendry and Lewthwaite 1992; Doran et al. 2002). Observational evidence in Wright Valley indicates that up-valley easterly surges begin late morning and persist well into the evening when the flow reverses and the westerly down-valley winds become dominant. McKendry and Lewthwaite (1992) discovered that the role of static stability in the valleys was crucial in determining the diurnal evolution of boundary layer flow.

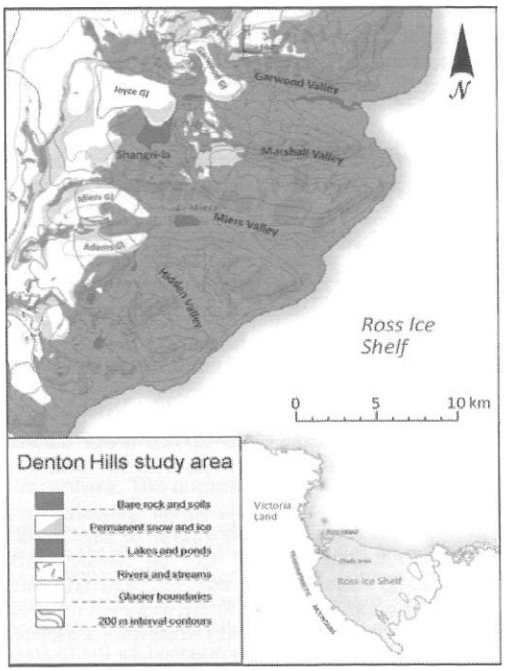

Figure 1. Garwood, Marshall, Miers and Hidden valleys, southern Victoria Land, Antarctica (after Stichbury et al. 2011).

Mechanisms that can produce up-valley wind regimes in the Dry Valleys have been proposed. These include regional intrusion of sea breeze currents originating from McMurdo Sound and Ross Sea area. A possible forcing for such thermally generated up-valley winds can be due to differential surface heating between the low albedo (snow/ice free) valley floors and the high-albedo glacier surfaces outside the valley system (McKendry and Lewthwaite 1990).

The main objective of the present work is to determine and further explain new and previously known physical mechanism(s) responsible for the development and spatial extent of up-valley winds in the Miers Valley during Antarctic summertime period of January 13-25, 2012. In the following sections we provide numerical evidence using an advanced polar optimized weather prediction code to elucidate the role of regional thermal differences during a synoptically stagnant condition in January 2012.

2. PHYISCAL SETTING

Miers Valley (78°6'S, 164°0'E) is one of the four east-west oriented ice-free valleys in the Denton Hill area of southern Victoria Land (Figure 1). This glacially excavated valley is 11 km in length, and is approximately 1.5-2.5 km wide; with an average elevation of 1300 m MSL. It contains two glaciers, Miers and Adams Glaciers, on its western flank, which feed into Lake Miers during the melt season. In the MDV, precipitation occurs exclusively as snow and the amount ranges from 3 to 50 mm/year (Fountain et al. 2010; Wall and Virginia, 1999). Air temperatures can climb to near freezing point during summer. Average wind speeds range between 2.5 and 5.3 m/s and wind directions are typically influenced by the orientation of individual valleys (Nylen et al. 2004).

3. SYNOPTIC FORCING AND VALLEY OBSERVATIONS

3.1 Synoptic scale conditions (13-25 January, 2012)

Figure 2 illustrates the mean sea-level pressure patterns and wind barbs at synoptic scale derived from the 1^{o} resolution National Centre for Environmental Prediction (NCEP) Final Analysis dataset (FNL). NCEP is used to nudge the coarsest grid of the WRF simulation at the boundaries and force compliance with the overall FNL field every six hours. We have only shown the field for the 13^{th} and 18^{th} of January; the pressure gradient over the Ross Ice Shelf is weak most of this time. On 13^{th}, a relatively weak low-pressure system is situated to the north of Ross Ice Shelf, forcing weak katabatic winds off the Transantarctic Mountains. By the 18th, a much developed low-pressure system has formed further

* *Corresponding author address:* Peyman Zawar-Reza, Centre for Atmospheric Research, University of Canterbury, Christchurch, New Zealand; e-mail: peyman.zawar-reza@canterbury.ac.nz

north, also with weak pressure gradients. Therefore for most of the period of interest, we are dealing with synoptic conditions that do not lead to strong katabatic events. This is a situation that would typically allow the formation of thermally generated winds at the mesoscale.

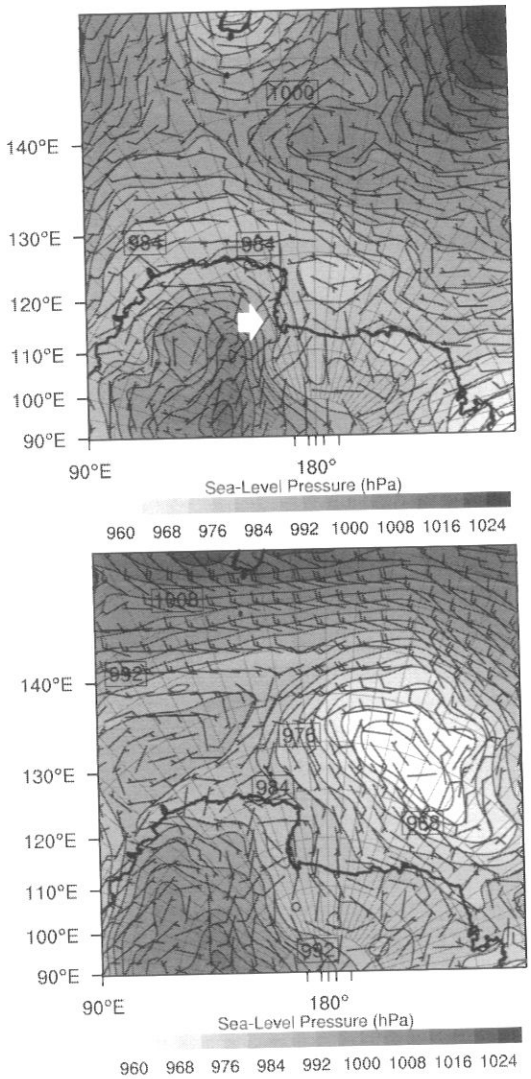

Figure 2. Sea level pressure and wind barbs for 1300 LST (0000 UTC) 13 January 2012 (top) and 1300 LST (0000 UTC) 18 January 2012 (bottom). White flash points the MDVs region.

The Miers Automatic Weather Station (AWS) (data not shown) indicate that for almost the entire period of study, January 2012, the boundary layer winds were persistently easterly (up-valley), this has also been corroborated by numerical modeling (to be presented in an accompanying paper). Modeling data from two selected days is shown in Figure 3. This period is characterized by persistent up-valley flow in Miers; yet, there is significant diurnal variation in wind speed. The fluctuation in wind velocity can be the result of diurnal heating/cooling cycles within the valley atmosphere and is investigated below.

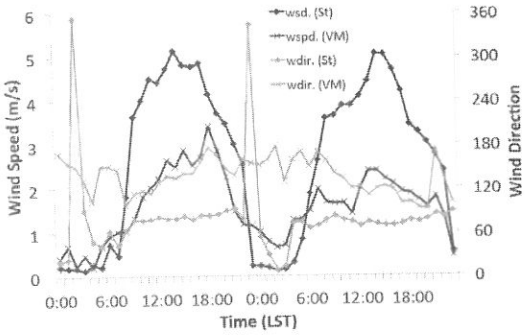

Figure 3. Surface wind speed and direction for the AWS location (78°06'S, 163°48'E) in Miers Valley (St) and the valley mouth (VM) 13 - 14 January 2012.

4. MODELING DETAILS

4.1 Model Description

Numerical simulations were performed using the 3rd version of Weather Research and Forecasting (WRF) (Skamarock et al. 2008). The WRF source code was modified according to changes posted by the Polar Meteorology Group at Byrd Polar Research Center (Hines and Bromwich (2008), Bromwich et al. (2009), Hines et al. (2010)). Modifications mainly deal with treatment of the land surface processes over ice/snow covered areas. Polar-WRF has been tested and evaluated mostly in the Arctic (Hines and Bromwich 2008; Wilson et al. 2012), fewer studies have been done on the performance of the model in Antarctica.

The slope and shadowing effects of the complex terrain in MDVs have important feedbacks in calculating surface fluxes (Dana et al. 1998) and consequently representing the correct thermal and dynamical terrain forcing. A LIDAR derived elevation data (4 m resolution) has been adapted for the highest resolution WRF grids, terrain height for the coarser grids use the 200 m RAMP digital elevation model (DEM) dataset (Liu et al. 2001). Land use dataset, which is used for the MDVs region is interpolated from a GeoTiff file of a LANDSAT 7 Satellite Image. Two new land use classes to represent surface characteristics of the Dry Valleys and blue-ice covered regions have been added to USGS land use table used in the model. Soil categorization for the Dry Valley region; "Loamy Sand" that comprises of 82% sand, 12% silt, and 6% clay has been chosen as the most realistic option to the observed soil (Northcott et al. 2009).

A two-way interactive grid nesting with 4 nests (16-, 4-, 1-km and 250-m horizontal resolution) has been employed in the simulations. The finest resolution domain covers entire Denton Hill area. Polar-WRF is initialized with the FNL dataset. The initial conditions of the soil model within the 1-km and 250-m grids were forced by in situ soil moisture and temperature. This is to ensure a more realistic initialization of simulated surface heat and moisture fluxes (Campbell et al. 1998, Thompson et al. 1971). All grids employ 10 out of the total 38 vertical half-sigma levels within the lowest 800 m to have a better boundary layer representation. The first half-sigma level is positioned 10 m above the valley floor.

5. RESULTS

5.1 Regional scale flow

Figure 4 shows the wind field simulated by 4 km and 16 km grids. In response to better resolved interaction with topography, there is significant complexity added to the NCEP fields. Two mesoscale cyclonic vortices are apparent north and south of the Ross Island (Figure 4 top). The convergence of the airstreams and mechanical effect of Ross Island cause a zone of stagnation over the Island, causing a weak easterly wind towards the MDV (see the arrow in bottom panel of Figure 4). This situation more or less persists for the entire period of study. In addition, a katabatic wind is evident on few days of the study period, flowing from Transantarctic Ranges near Byrd, and Darwin and Hatherton Glaciers (not shown). This flow interacts with Ross Island and enhances the easterlies by producing a clockwise vortex.

5.2 Local scale thermal contrasts

Although the sun does not set in January at this latitude, the variation in solar elevation and local shadowing due to steep valley sidewalls can still cause significant thermal variation in the valley atmosphere. The purpose of this section is to examine the horizontal temperature differences between the atmosphere of several points inside and outside of the Miers valley, so that we can discern the thermal contrasts that can lead to generation of local winds. As seen in Figure 3, the strength of the easterly inflow increases from 0600 LST onwards, till the next cooling cycle when the valley bottom is in shade.

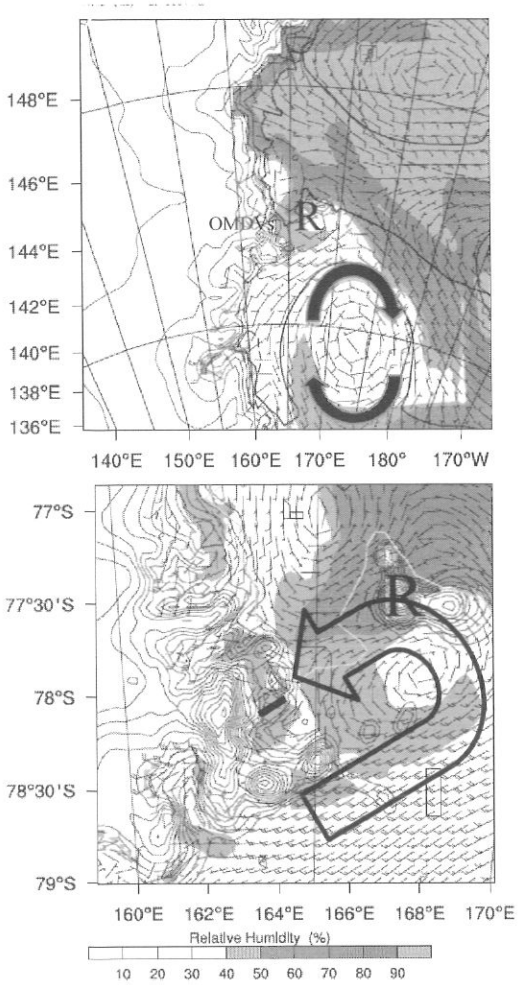

Figure 4. Topography (200 m contour interval), relative humidity (shaded) and wind barbs at 850-hPa on domain 2 (top) and domain 3 (bottom) for 0100 LST 16 January 2012. Thick line and "R" show the approximate position of Miers Valley and Ross Island correspondingly.

Time series of daily averaged potential temperature shows that with high solar elevation (0600 onwards), the valley atmosphere has a heat surplus in relation to Ross Island region (Figure 5 top). This should direct the local winds towards the valley and inside the valley, toward the sidewalls. From 2100 to 0600, the valley atmosphere is in deficit except for the valley sidewalls (not shown) which promote a shallow easterly; this has been supported by observations. The vertical advection terms for potential temperature indicate that the heating and cooling is pretty much restricted below the ridge tops and is in response the sensible heat flux from the surface.

Much of the early research in MDVs region illustrated the role of easterlies in controlling

temperature and its distribution along the valleys (Doran et al. 2002), yet our results show that at least for this episode, horizontal temperature advection in Miers Valley is very weak (Figure 5 bottom). There is also no diurnal signal in temperature advection above the ridge tops or over Ross Island region.

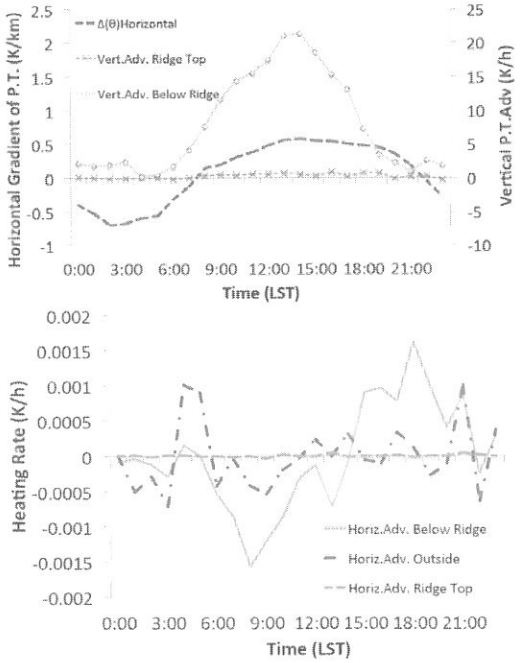

Figure 5. Time series of hourly averaged: horizontal potential temperature gradient between valley and the Ross Island region, and vertical heat advection within the valley atmosphere (Top); and horizontal advective components in potential temperature (bottom).

6. CONCLUSION

The results from this study show that the up-valley easterlies in Miers Valley have both local and regional scale thermal and dynamic forcings. At the regional scale the shallow pressure gradient over the Ross Ice Shelf; periodically enhanced by Ross Island deflected katabatic flows can produce a weak easterly flow outside of Miers Valley. This forcing is modulated by within valley heating and cooling cycles, and up-slope flows to promote a diurnal fluctuation in up-valley surges.

7. ACKNOWLEDGEMENT

Special thanks go to the New Zealand Terrestrial Antarctic Biocomplexity Survey (nzTABS) for supporting this research. The large-scale charts and initial/boundary condition data for the modeling exercise are from the Research Data Archive (RDA), which is maintained by the Computational and Information Systems Laboratory (CISL) at the National Center for Atmospheric Research (NCAR).

8. REFERENCES

Bromwich, D. H., K. M. Hines, and L. -S. Bai, 2009: Development and testing of Polar Weather Research and Forecasting model: 2. Arctic Ocean. *J. Geophys. Res.*, 114.

Campbell, I., G. Claridge, and D. Campbell, 1998: The soil environment of the McMurdo Dry Valleys, Antarctica. *Ecosystem Dynamics in a Polar Desert, the McMurdo Dry Valleys, Antarctica. Antarctic Research Series*, 72, 297-322.

Dana, G. L., R. A. Wharton Jr., and R. A. Dubayah, 1998: Solar radiation in the Mcmurdo Dry Valleys, Antarctica. *Ecosystem Dynamics in a Polar Desert: The McMurdo Dry Valleys, Antarctica*, AGU, 39-64.

Doran, P., C. McKay, G. Clow, and G. Dana, 2002: Valley floor climate observations from the McMurdo dry valleys, Antarctica, 1986–2000. *Journal of Geophysical*, 107, 1-12.

Hines, K. M., and D. H. Bromwich, 2008: Development and Testing of Polar Weather Research and Forecasting (WRF) Model. Part I: Greenland Ice Sheet Meteorology. *Monthly Weather Review*, 136, 1971-1989.

Hines, K. M., D. H. Bromwich, L.-S. Bai, M. Barlage, and A. G. Slater, 2010: Development and Testing of Polar WRF. Part III: Arctic Land. *Journal of Climate*, 24, 26-48.

Liu, H., K. Jezek, and B. Li, 2001: Radarsat antarctic mapping project digital elevation model version 2. Boulder, CO. National Snow and Ice Data Center (NSIDC).

McKendry, I., and E. W. D. Lewthwaite, 1990: The vertical structure of summertime local winds in the Wright Valley, Antarctica. *Boundary-Layer Meteorology*, 51, 321-342.

McKendry, I. G., and E. W. D. Lewthwaite, 1992: Summertime along-valley wind variations in the wright valley Antarctica. *International Journal of Climatology*, 12, 587-596.

Northcott, M. L., M. N. Gooseff, J. E. Barrett, L. H. Zeglin, C. D. Takacs-Vesbach, and J. Humphrey, 2009: Hydrologic characteristics of lake- and stream-side riparian wetted margins in the McMurdo Dry Valleys, Antarctica. *Hydrological Processes*, 23, 1255-1267.

Nylen, T. H., 2004: Climatology of katabatic winds in the McMurdo Dry Valleys, southern Victoria Land, Antarctica. *Journal of Geophysical Research*, 109, 1-9.

Skamarock, W., and Coauthors, 2008: A description of the Advanced Research WRF Version 3. *NCAR/TN-475+STR*.

Stichbury, G., L. Brabyn, T. A. Green, and C. Cary, 2011: Spatial modelling of wetness for the Antarctic Dry Valleys. *Polar Research*, 30.

Thompson, D. C., R. M. F. Craig, and A. M. Bromley, 1971: Climate and surface heat balance in an Antarctic Dry Valley. *New Zealand Journal of Science*, 14, 245-251.

Wall, D. H., and R. A. Virginia, 1999: Controls on soil biodiversity: insights from extreme environments. *Applied Soil Ecology*, 13, 137-150.

Wilson, A., and D. Bromwich, 2012: Evaluation of Polar WRF forecasts on the Arctic System Reanalysis Domain: 2. Atmospheric hydrologic cycle. *Journal of Geophysical Research*, 117.

CHARACTERIZING AND PREDICTING SURFACE MELT IN ANTARCTICA

David B. Reusch*
New Mexico Institute of Mining and Technology, Socorro, NM

Derrick J. Lampkin
The Pennsylvania State University, University Park, PA

David P. Schneider
National Center for Atmospheric Research, Boulder, CO

ABSTRACT

Combining satellite remote sensing with atmospheric modeling (i.e., Polar WRF), we will be attempting to diagnose the meteorological conditions associated with surface melting on the Antarctic ice sheet and its fringing ice shelves. With these results, we plan to predict whether the regional warming associated with anticipated anthropogenic global warming and related atmospheric circulation changes will lead to a future increase of melting.

Work in the first project year has focused on developing ERA Interim- and Polar WRF-based melt season climatologies and a case-study of the Dec/Jan 1991-92 melt event in West Antarctica.

1. INTRODUCTION

1.1 *Overview*

The presence of surface melting on ice sheets and ice shelves marks an important climatic and geophysical threshold in the cryosphere. Wetting of snow reduces albedo and encourages additional melt, meltwater runoff contributes to mass loss from ice sheets, and penetration of meltwater to the glacier bed can lubricate faster flow and contribute to ice-sheet mass loss.

This work is part of a three-year collaborative project with the following high-level objectives:

- Compare atmospheric model-based estimates of surface melt occurrence to satellite-based melt records to better understand this aspect of model skill for the Antarctic and to build confidence in our model-based predictions of the future.
- Diagnose the synoptic factors, present and future, controlling Antarctic surface melt through objective classifications and analysis of synoptic-scale meteorology (from global and dynamically downscaled datasets based on regional models) and sea ice conditions.
- Evaluate modern climates and surface melt estimates of CMIP5 general circulation models (GCMs) to identify best candidates for future prediction of surface melt occurrence.

We are currently focused on three main areas: evaluation and analysis of the Dec/Jan 1991/1992 melt event in West Antarctica, producing a 20-year Polar WRF record of melt season months (Nov-Feb), and developing ERA-Interim and Polar WRF-based climatologies. Once we have documented the utility and skill of our meteorological datasets in the development of diagnostic tools for identifying surface melt as observed by satellite and simulated by models, we will be looking at future changes.

2. DATA

2.1 *Satellite-based surface melt*

Our record of surface melt at 25-km spatial resolution was developed by C. Karmosky under the direction of Lampkin (Lampkin and Karmosky, in review). Karmosky used passive microwave data (NSIDC, 2008) and the cross-polarized gradient ratio (XPGR) algorithm (Abdalati and Steffen, 1995) to create a daily record of surface melt across Antarctica. This dataset is available daily for Nov-Dec-Jan-Feb, 1988-2008.

2.2 *Polar WRF boundary conditions*

The ERA-Interim archive is our main source of model boundary and initial conditions (Simmons et al., 2007). We also use the NASA Bootstrap daily sea ice dataset sea ice concentrations (Comiso, 1999). Sea-ice data were linearly interpolated to 6-hourly resolution during model preprocessing.

3. MODELING

3.1 *Overview*

The project is using v3.3.1 of the WRF modeling system (Skamarock et al., 2005), with the corresponding polar modifications developed by the Polar Meteorology Group at the Byrd Polar Research Center, Ohio State University (released Nov 2011). The modeling philosophy is to use 72-hour simulations to create 24 hours of spinup (discarded) and 48 hours of forecast data. The latter are concatenated into long-term time series. Simulations produce an outer and nested grids, 45 and 15 km, respectively, covering the entire Antarctic continent and surrounding oceans (Figure 1). Output files are saved every 6 hours for the outer grid and every 3 hours for the nested grid.

A modified version of Mark Seefeldt's wrfout_to_cf.ncl script is used to reduce the 15 km domain output to a manageable size. Modifications primarily concern switching to variable names matching the CMIP guidelines.

3.2 *Key options*

Physics, dynamics and numerous other settings** were guided by advice from Francis Otieno (BPRC)

and those used operationally by AMPS. Along with enabling `fractional_sea_ice`, key options are:

- `mp_physics` (microphysics) = WSM 5-class scheme
- `ra_lw_physics` (longwave radiation) = rrtmg scheme
- `ra_sw_physics` (shortwave radiation) = rrtmg scheme
- `sf_sfclay_physics` (surface-layer option) = Monin-Obukhov (Janjic Eta) scheme
- `sf_surface_physics` (land-surface option) = unified Noah land-surface model
- `bl_pbl_physics` (boundary-layer option) = Mellor-Yamada-Janjic (Eta) TKE scheme
- `cu_physics` (cumulus option) = Grell-Devenyi ensemble scheme

4. STATUS

4.1 *The Dec/Jan 1991-92 melt event*

Initial work focused on the three years centered on the 1991-9292 melt event in West Antarctica, i.e., Dec/Jan 1990-1991, Dec/Jan 1991-1992 and Dec/Jan 1992-1993. As documented in the XPGR-based record, this event developed in late December 1991 and persisted through mid-January 1992. Figure 2 shows the event near maximum extent. Preliminary SOM-based frequency analysis of both ERA-Interim and Polar WRF data for this period confirmed that for days during the melt event, warm T-2m anomaly patterns were most common. Likewise for days outside the melt event for cool T-2m anomaly patterns. As expected, the higher spatial resolution of the Polar WRF data did a better job with locating the temperature anomalies with respect to the observed melt location. Figure 3 provides single-day comparisons of ERA-Interim and Polar WRF T-2m during this study period.

It is interesting to note anecdotal on-the-ground evidence of this melt event: scientists doing a GPS-based ice-motion survey found their location poles melted out upon returning a few weeks after putting them out. Surface snow was also notably wet in a wide area of the Siple Coast.

4.2 *Climatologies*

To better assess the long-term meteorological environment, we are developing 30- and 20-year melt-season climatologies of ERA-Interim and Polar WRF data. The 30-year ERA-Interim climatology covers 1981-2010. ERA-Interim and Polar WRF 20-year climatologies cover the XPGR period 1988-2007.

Variables to be analyzed include temperature, pressure, winds and energy balance components, at and near the surface and at selected pressure levels (as appropriate).

5. FUTURE WORK

After we have developed a credible calibration of model data to observed melt for the recent period, we will be running new Polar WRF simulations driven by CMIP5 GCMs to assess future melt occurrence. We hope to explore two dimensions of future change: multiple emissions scenarios with one model and multiple models with one scenario. We expect to evaluate one future decade under this framework

ACKNOWLEDGEMENTS

This work supported by NSF grants ANT 10-43580 to D. B. Reusch and ANT 12-35231 to D. P. Schneider. We would like to acknowledge high-performance computing support provided by NCAR's Computational and Information Systems Laboratory (CISL). ERA-Interim data were provided by the Data Support Section of CISL. We thank the National Snow and Ice Data Center (NSIDC) for making available the sea-ice and passive microwave data used in this project. NCAR is sponsored by NSF. NSIDC is sponsored by NSF, NASA, NOAA, and other federal agencies.

REFERENCES

Abdalati, W. and K. Steffen, 1995: Passive microwave-derived snow melt regions on the Greenland ice sheet. *Geoph. Res. Letters*, **22,** 787-790.

Comiso, J. C., 1999: Bootstrap sea ice concentrations from NIMBUS-7 SMMR and DMSP SSM/I, National Snow and Ice Data Center, Boulder, Colorado USA. [Available online from http://nsidc.org/data/nsidc-0079.html.]

Lampkin, D. J. and C. Karmosky, in review: Estimation of Surface Melt Magnitude over Ross Ice Shelf, Antarctica using Satellite-Derived Estimates of Liquid Water Fraction. *Antarctic Science*.

NSIDC, 2008, cited 2009: DMSP SSM/I Pathfinder Daily EASE-Grid Brightness Temperatures. [Available online from http://nsidc.org/data/docs/daac/nsidc0032_ssmi_ease_tbs.gd.html.]

Simmons, A., S. Uppala, et al., 2007: ERA-Interim: New ECMWF reanalysis products from 1989 onwards. *Newsletter 110 - Winter 2006/2007*, 11.

Skamarock, W. C., J. B. Klemp, et al., 2005: A description of the advanced research WRF version 2, 88 pp.

* *Corresponding author address:* David B. Reusch, Department of Earth & Environmental Science, New Mexico Institute of Mining & Technology, Socorro, NM 87801; e-mail: dreusch@ees.nmt.edu

** Copies of parameter files available on request.

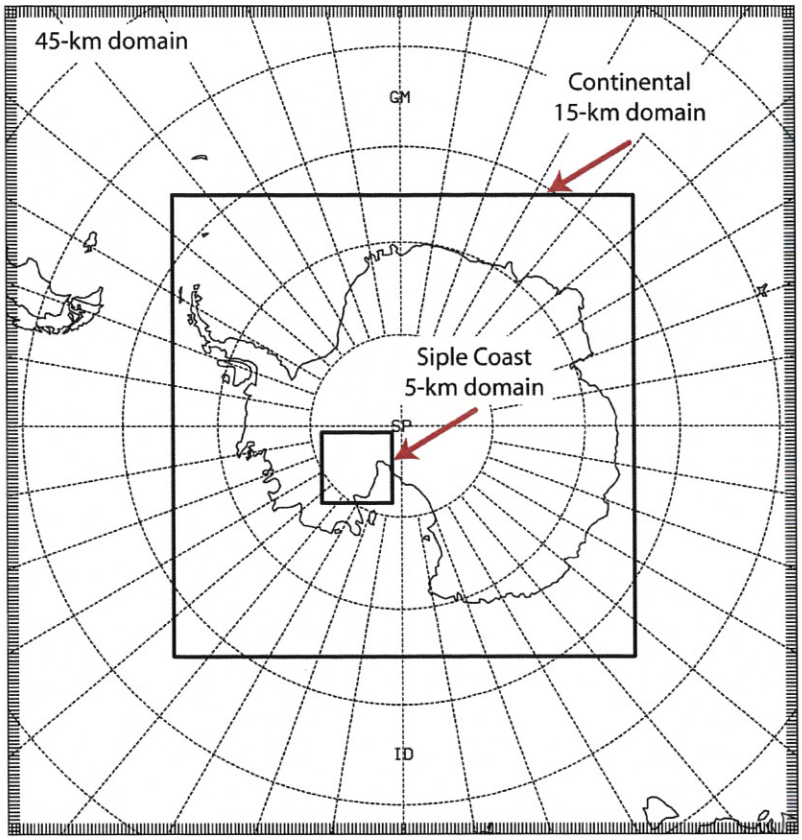

Figure 1. Project model domains tested (innermost domain only used in benchmarking). Outer grid is 210 x 220. Inner grid is 367 x 367.

Figure 2. XPGR-based surface melt (light red) for January 1, 1992.

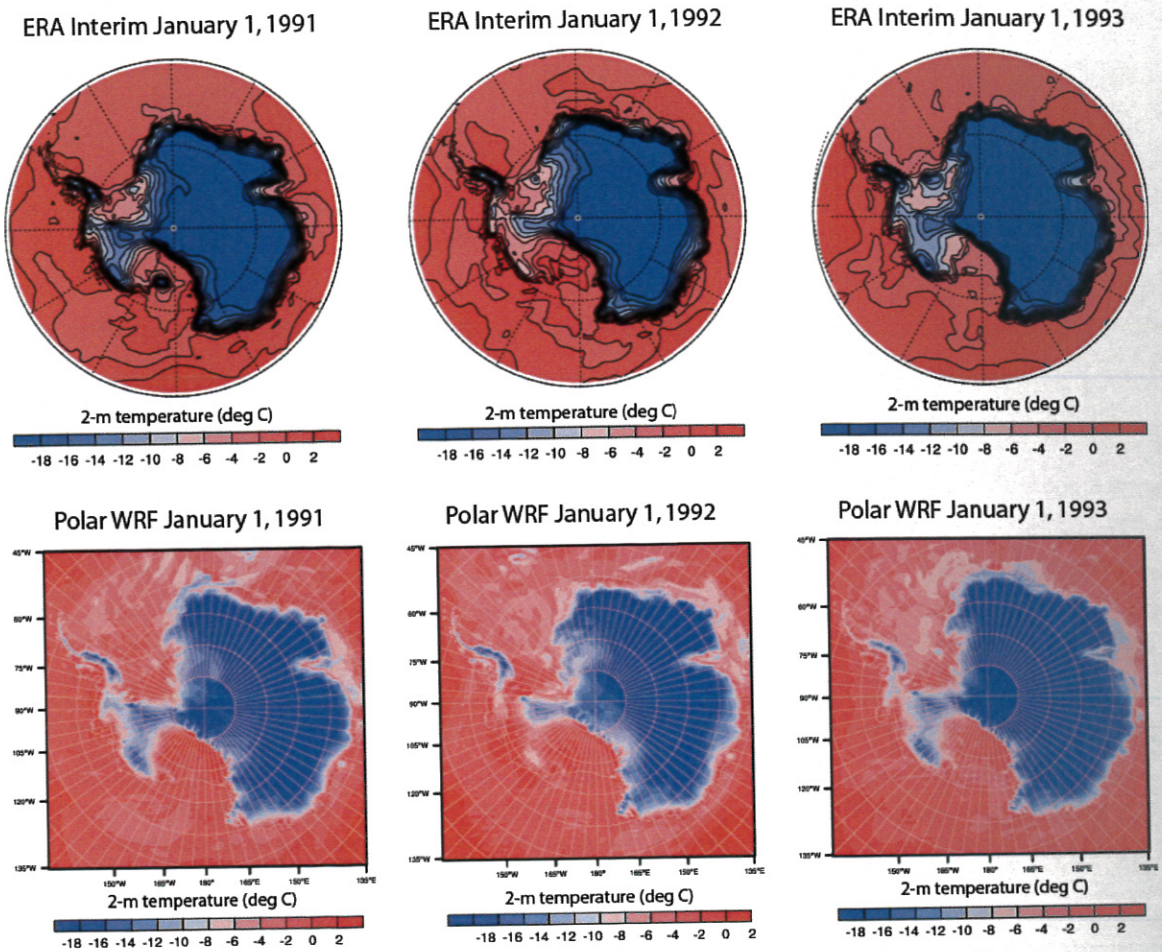

Figure 3. ERA-Interim (top) and Polar WRF (bottom) T-2m for January 1, 1991-1993, i.e., mid-melt season during the Dec/Jan 1990-1993 case study.

THE SYNOPTIC SETTINGS OF STRONG WIND EVENTS AT MCMURDO STATION

Jordan G. Powers
Mesoscale and Microscale Meteorology Division
NCAR Earth System Laboratory, National Center for Atmospheric Research
Boulder, Colorado, USA

1. INTRODUCTION

McMurdo Station is the main American base in Antarctica and serves as the gateway to Amundsen-Scott South Pole Station and the US's on-Ice field camps. Its summer population can reach 1100, and its winter population runs 130–200. Occasionally, McMurdo sees strong wind events that restrict or shut down activities and that can threaten lives and facilities. And, with McMurdo being the on-continent logistical center, these episodes can significantly affect United States Antarctic Program (USAP) operations. The current study analyzes strong wind events at McMurdo, which are here defined as bringing the station into weather "condition" (described below), implying sustained speeds of ≥48 kt (24.5 ms^{-1}). Both observations and AMPS (Antarctic Mesoscale Prediction System) (Powers et al. 2003, 2012) forecast model output are used for investigating a number of episodes at McMurdo. The goal is to elucidate the synoptic settings of these critical weather scenarios, ultimately to improve their forecasting and to understand their dynamics.

2. WIND EVENTS AND METHODOLOGY

The USAP has defined weather regimes around McMurdo for safety purposes and for the restriction of activities when necessary. "Condition 3" describes relatively benign weather that entails no special restrictions on activities. "Condition 2" reflects a degradation of weather and imposes restrictions on local travel. Condition 2 reflects expected wind speeds between 48–55 kts, or visibility of ¼ mi–100 ft (402–30 m), or wind chill temperatures of 75 °F– -100 °F (-60 – -73 C). "Condition 1" represents the worst conditions, with wind speeds greater than 55 kt, or wind chill temperatures colder than -100 °F (-73C), or visibility less than 100 ft (30 m) (USAP Participant Guide 2010–2012). For this study, a "strong" wind event is one that brings McMurdo or an adjacent site into Condition 2 or 1. Adjacent sites here are Ice Runway and observation sites in the McMurdo immediate vicinity (viz., Arrival Heights, T-Site, Crater Hill, Helo Pad). Nearby Scott Base or Williams Field are not included in this definition, however. All of the cases reviewed here put McMurdo Station itself into Condition 1.

Table 1 lists the six cases reviewed, and all of them are in transition seasons (i.e., spring, fall). Surface observations and satellite imagery are examined for determining the actual conditions. Table 1 presents the averages of the strongest winds seen in the observations for the McMurdo area, as well as the highest winds recorded in the area. For this, there are six reporting sites considered: McMurdo (NZCM), Ice Runway (NZIR), Arrival Heights, T-Site, Crater Hill, and Helo Pad. The dates of the three stronger events are highlighted in green.

Table 1 shows the approximate timings of the onset and peaks of the events. As the winds in all of these cases are out of the south, "onset" is defined as the time when the observations began to show 30 kt (15 ms^{-1}) winds from that direction. Apart from these cases, south is the direction from which McMurdo sees its highest winds.

Events Analyzed

- 15 May 2004
- 7 Nov 2007
- 8 Nov 2007
- 11–12 Apr 2009
- 18 Apr 2009
- 11–13 Nov 2009

The strongest event considered is that of May 15, 2004, which had winds of 100 kt and caused significant damage in the McMurdo area (Powers 2007). The episodes on 7 and 8 November 2007 were weaker, but still brought Condition 1 to McMurdo. The events of 11–12 April 2009 and 18 April 2009 were also strong, like May 2004, while the 11–13 Nov 2009 case were of similar amplitude to those of Nov 2007.

Figure 1 shows the main AMPS domains used for case analyses. For the 2004 and 2007 events, the WRF (Weather Research and Forecasting) (Skamarock et al. 2008) model grid spacings for the forecasts were 60-/20-/6.67-/2.22-km, while for the 2009 events they were 45-/15-/5-/1.67-km. Because the focus is on the synoptic scale, the output from the continent-wide 20-km/15-km grid (Fig. 1) is predominately used, although the other grids running in WRF for AMPS are also shown as frames within it in Fig. 1.

3. RESULTS

a. Surface characteristics

The defining characteristic of the high wind events studied is a deep low pressure area in the Ross Sea sector. For the cases studied, the WRF forecast output at the events' peaks portrays an average depth of 960 hPa. As described below, the synoptic-scale pressure gradient associated with the systems is fundamental to the flows that affect the McMurdo area.

The locations of the lows in the Ross Sea vary considerably during the high wind periods. Figure 2 locates the low centers at both the times of onset and peak wind of the events. These positions are approximate and, given the lack of surface observations across the Ross Sea, are based on identification through satellite imagery.

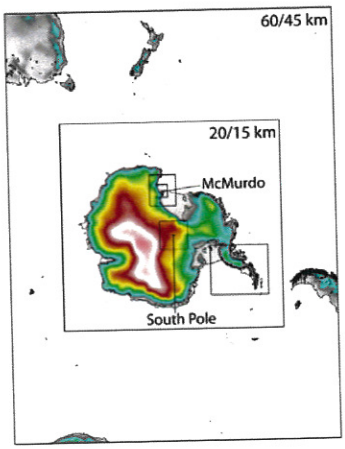

Fig. 1: AMPS WRF domains used in analyses. Outermost grid resolution: 60-km for 2004 and 2007 cases and 45-km for 2009 cases. Antarctic continent grid resolution: 20-km for 2004 and 2007 cases and 15-km for 2009 cases. Locations of McMurdo Station and South Pole marked. Grid outlines shown within 20-/15-km grids are of other AMPS WRF grids.

Only two of the studied cases featured lows that were near Ross Island during the periods of maximum winds, those of May 2004 and Nov 2009.[1] Thus, McMurdo wind events do not depend on close proximity of the low to Ross Island. It is seen, however, that in each case the trajectory of the low is toward McMurdo from event onset through peak.

Figure 3 compares the observed and forecast low tracks for the 11–12 April 2009 event. This case provides a more pronounced illustration of the tracking of these lows toward Ross Island. This system wound up transiting near Ross Island,

[1] The low for the 11–12 April 2009 event did approach Ross Island, but it did so on the 13th, after the strongest winds were observed. See Fig. 3 and discussion.

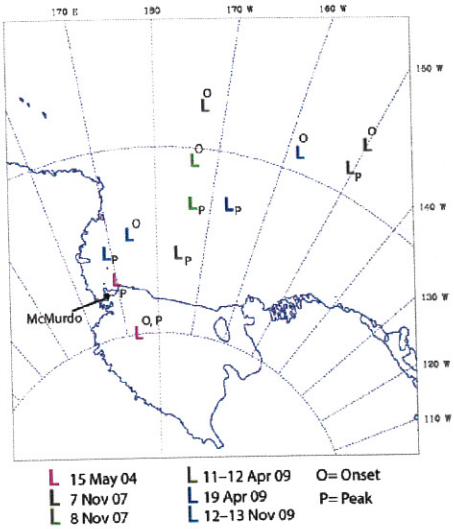

Fig. 2: Positions of surface low centers for McMurdo wind events. Event dates shown. Positions at onset (O) and peak (P) of episodes marked. The peak winds for the 2004 event spanned the whole episode, and are indicated at both low positions. Positions determined from analysis of satellite imagery.

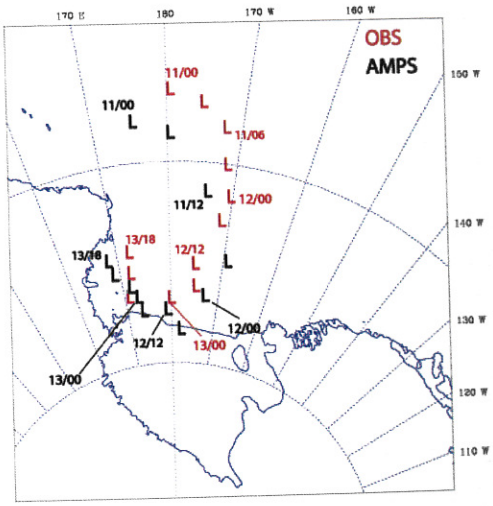

Fig. 3: Observed and AMPS forecast low tracks for the 11–12 April 2009 event. 6-hourly positions shown. Observed low positions from satellite imagery; modeled positions from AMPS WRF initialization of 0000 UTC 711 Apr 2009. Date/hr marked every 12 h.

although its closest approach to McMurdo was *after* the peak winds. While their positions are not time-synchronized, both the observed and modeled lows move southward through the central Ross Sea on the same trajectory. The modeled track does align with

that observed after 0000 UTC 13 Apr, and the system's southward movement to the edge of the Ross Ice Shelf followed by the northwestward curve into the western Ross Sea is captured.

The first-order forcing of the strong winds in the events is the synoptic pressure gradient that reflects the migratory lows juxtaposed with the East Antarctic high. As the pressure gradient force (PGF) is represented as

$$PGF = - 1/\rho \ \partial p/\partial x ,$$

the forcing on the large scale varies with the strengths of the low and high and the distance between the centers. To see this gradient and the component of the East Antarctic high, Fig. 4 presents the model sea level pressure fields for two cases at near peak time, examples of stronger (11–12 Apr 2009) and weaker (13 Nov 2009) episodes. For the April 2009 case (Fig. 4(a)) the AMPS forecast shows a 956 hPa low at the edge of the ice shelf just east of Ross Island, while the high is centered just east of the Transantarctic Mountains with a (derived) sea level pressure (SLP) of 1012 hPa. In contrast, the Nov 2009 case in Fig. 4(b) presents a weaker, 978 hPa low in the central Ross Sea, but a stronger, 1032 hPa high centered farther south, over the Antarctic Plateau. The modeled central SLP differences between the centers are 56 hPa for Apr 2009 and 54 hPa for Nov 2009, with the April SLP gradient tighter over the Ross Island region and Ross Ice Shelf (Fig. 4(a)).

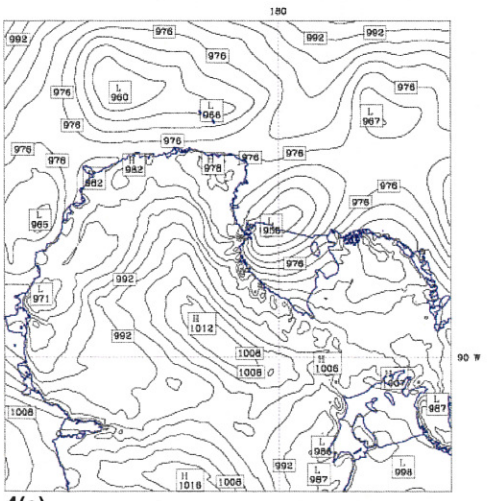

4(a)

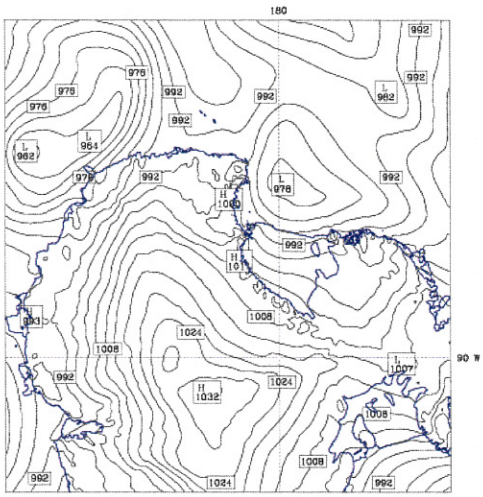

4(b)

Fig. 4: Sea level pressure fields from AMPS WRF forecasts for the 11–12 April 2009 and 12 Nov 2009 events. Contour interval= 4 hPa. (a) 1500 UTC 12 Apr 2009. Forecast hr 39 from initialization of 0000 UTC 11 Apr. (b) 0300 UTC 13 Nov 2009. Forecast hr 27 from initialization of 0000 UTC 12 Nov.

The flows experienced in the McMurdo area in high wind events are likely modulated by mesoscale effects. Thus, not investigated yet are the roles of the Transantarctic Mountains in directing barrier flow toward Ross Island and barrier flow dynamics on the mesoscale affecting the wind intensities at McMurdo. Likewise, possible topographical effects of the complex terrain in the McMurdo/Ross Island region have not yet been examined.

b. Upper-level characteristics

The upper-level settings for McMurdo wind events are characterized by troughs or closed low centers over the Ross Sea sector. Figure 5 illustrates the positions of the 300 hPa lows during the events. As can be seen, the upper-level centers are over the Ross Sea or eastern Victoria Land.

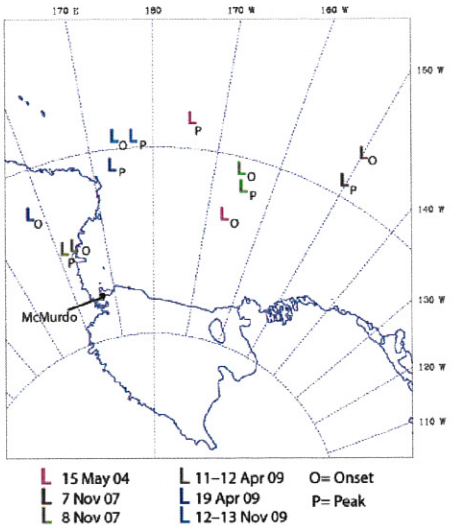

Fig. 5: Position of 300 hPa low centers for McMurdo wind events. Event dates marked. Positions for onset (O) and peak (P) marked. Low positions taken from AMPS WRF forecasts.

The upper-level (i.e., 300 hPa) flow picture generally presents a locally-maximized easterly flow over a zone from Marie Byrd Land to the Ross Ice Shelf, i.e., on the southern periphery of the low center aloft. The intensity of the flow varies across the cases, however: it is not uniformly strong. Figure 6(a) shows the pattern for the May 2004 event, which in the WRF simulation featured 300 hPa flows of 60+ ms^{-1} over Marie Byrd Land. In contrast, the 8 Nov 2007 event (Fig. 6(b)) only displayed a 25 ms^{-1} jet core over the Ross Ice Shelf. For the six cases, these examples span the range of forecast jet strength aloft at the times of the surface events, from strongest to weakest.

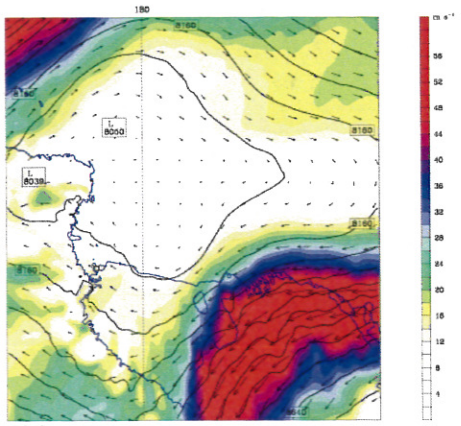

6(a)

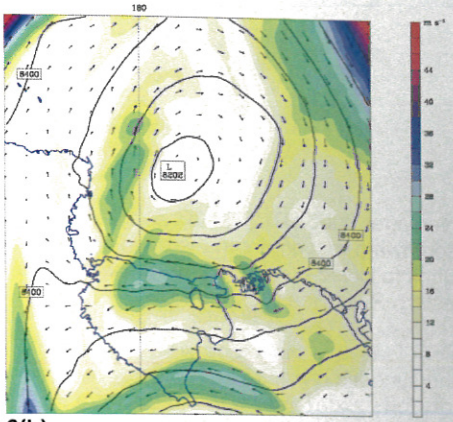

6(b)

Fig. 6: 300 hPa heights/winds for May 2004 and 8 Nov 2007 events. Analyses from AMPS WRF forecasts. Geopotential heights (m) solid, interval= 60m. Wind speeds shaded, scales to right. Wind vectors shown. (a) 2100 UTC 15 May 2004. (b) 2100 UTC 8 Nov 2007.

The presence of upper-level ridge axes appears to be an element in McMurdo wind episodes. Figure 7 shows the positions of 300 hPa ridge axes during the events based on the AMPS WRF output. While the analyzed ridges are not well-defined, the picture that emerges is of a ridge axis that is progressing across the Ross Ice Shelf or the Ross Island region. Usually the ridges move southward to southwestward across the ice shelf. The exception in the events considered is the weak ridge axis for the 2004 case (black line in Fig. 7), which translated northwestwardly over Ross Island.

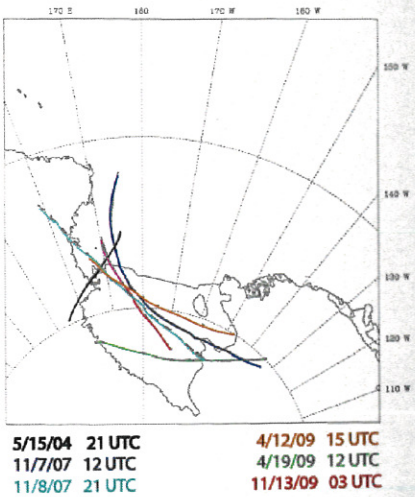

Fig. 7: Analyzed 300 hPa ridge axes from AMPS WRF forecasts. Event and time of analysis shown at bottom.

4. SUMMARY AND CONCLUSIONS

Strong wind events hitting McMurdo Station can disrupt schedules, shut down operations, damage facilities, or threaten lives. This study begins a review of the synoptic-scale conditions that characterize these events, which are defined here as episodes in which the station is brought into weather Condition 2 or 1. In all cases it is strong southerly flow which does this. Surface and satellite observations as well as AMPS WRF model output are used to analyze six selected cases.

It is found that the events all feature deep surface lows moving through the Ross Sea, with a range of positions relative to McMurdo seen. Model analyses show a mean central pressure of 960 hPa. The lows are progressing toward McMurdo during the episodes, but their locations may actually be distant (e.g., in the north-central or northeastern Ross Sea). It is found that it is not necessary that the lows be in the vicinity of Ross Island, although the strongest events studied did feature lows that wound up near it.

Analyses of upper-level (300 hPa) conditions typically find a closed low with a center in place over the Ross Sea or eastern Victoria Land. Jet cores are generally seen around the southern edge of the low aloft, with the strongest flow being easterly over Marie Byrd Land or the Ross Ice Shelf. Jet strengths vary, however: upper-level flows during the events are not always strong. Also seen aloft is the passage of ridge axes (albeit sometimes weak) across the ice shelf or the Ross Island region.

Not investigated here are the roles of mesoscale influences, such as the topography of the Ross Island area or possible barrier wind dynamics. In future work, these mesoscale elements can be examined as contributory to the synoptic conditions identified here.

REFERENCES

Powers, J.G., A.J. Monaghan, A.M. Cayette, D.H. Bromwich, Y.-H. Kuo, and K.W. Manning, 2003: Real-time mesoscale modeling over Antarctica: The Antarctic Mesoscale Prediction System (AMPS). *Bull Amer. Meteor. Soc.*, **84** 1533–1546.

Powers, J.G., K.W. Manning, D.H. Bromwich, J.J. Cassano, and A.M. Cayette, 2012: A decade of science support through AMPS. *Bull Amer. Meteor. Soc.*, **93** (in press).

Skamarock, W.C., J.B. Klemp, J. Dudhia, D.O. Gill, D.M. Barker, M.G. Duda, X.-Y. Huang, W. Wang, and J.G. Powers, 2008: A description of the Advanced Research WRF Version 3. NCAR Tech. Note, NCAR/TN-475+STR, 113 pp.

United States Antarctic Program Participant Guide, 2010–2012 Ed. Nat'l Science Foundation, NSF 10-162, 108 pp. [Available from Nat'l Science Foundation, 4201 Wilson Blvd., Arlington, VA 22230.]

Tab 1: McMurdo Wind Events Examined (Green: Stronger Events)

Date	Onset/Peak Winds	Max Winds MCM Area (kt)		
15 May 2004	1800 UTC	Max avg'd	**88**	Condition 1
	1800–0000 UTC 15–16 May	Max obsv'd:	100	Crater Hill
7 Nov 2007	0600 UTC	Max avg'd	**52**	Condition 1
	1200 UTC	Max obsv'd:	75	Crater Hill
8 Nov 2007	1500 UTC	Max avg'd	**44**	Condition 1
	2100 UTC	Max obsv'd:	62	Crater Hill
11–12 Apr 2009	0900–1200 UTC	Max avg'd	**75**	Condition 1
	1200–1500 UTC 12 May	Max obsv'd:	99	Crater Hill
19 Apr 2009	0300 UTC	Max avg'd	**73**	Condition 1
	0900–1200 UTC	Max obsv'd:	99	Crater Hill
12–13 Nov 2009	2100 UTC 12 Nov	Max avg'd	**47**	Condition 1
	0000–0300 UTC 13 Nov	Max obsv'd:	72	Crater Hill

Analysis of high winds over the Ross Ice Shelf, Antarctica: Barrier winds along the Transantarctic Mountains

M.A. Nigro[1,2], J.J. Cassano[1,2]
[1]*Cooperative Institute for Research in Environmental Sciences, Boulder, USA;* [2]*Department of Atmospheric and Oceanic Sciences University of Colorado, Boulder, USA*

The steep topography surrounding the Ross Ice Shelf (RIS), Antarctica greatly influences the wind patterns in the region of the RIS. The topography provides forcing for features such as katabatic winds, barrier winds and barrier wind corner jets. These features, combined with the synoptic forcing from polar lows that traverse the Ross Sea, create a region of strong, variable winds. This paper presents a wind climatology over the RIS using output from the Weather Research and Forecasting (WRF) model run within the Antarctic Mesoscale Prediction System (AMPS). The dataset has 15 km grid spacing and hence, is the first RIS wind climatology presented at this resolution. The wind climatology shows the Ross Ice Shelf airstream (RAS), a dominant stream of air flowing northward from the interior of the continent over the western to central RIS to the Ross Sea, is present over the RIS approximately 34% of the time. A subsequent climatology of only the RAS patterns over the RIS is presented. This climatology indicates the RAS varies in both its strength and position over the RIS. These variations exist because RAS patterns can be driven by a variety of forcing mechanisms. The RAS patterns with forcing mechanisms that result in barrier winds are analyzed in this paper.

Air-Sea Fluxes in Terra Nova Bay, Antarctica from In Situ Aircraft Measurements

Shelley L. Knuth and John J. Cassano
Department of Atmospheric and Oceanic Sciences/Cooperative Institute for Environmental Studies
University of Colorado

In September 2009, the first unmanned aerial vehicles (UAVs) were flown over Terra Nova Bay, Antarctica to collect information regarding air-sea interactions over a wintertime coastal polynya. The UAVs measured wind, temperature, pressure, and relative humidity in flights parallel to the downslope wind flow over the polynya, and in a series of vertical profiles at varying distances from the coast. During three flights on three different days, sufficient measurements were collected to calculate sensible heat, latent heat, and momentum fluxes over varying oceanic surface states, including frazil, pancake, and rafted ice, with background winds greater than 15 ms^{-1}. During the three flights, sensible heat fluxes upwards of 650 Wm^{-2} were estimated near the coast, with maximum latent heat fluxes near 120 Wm^{-2} just downwind of the coast. This presentation will summarize the methodology for calculating the fluxes from the UAV data, present the first ever in situ estimates of sensible and latent heat fluxes over Terra Nova Bay, and compare the UAV flux calculations to flux measurements taken during other field campaigns in other regions of the Antarctic, as well as to model estimates over Terra Nova Bay.

The Application of Automatic Weather Station (AWS) Observations and Antarctic Mesoscale Prediction System (AMPS) Data to the Analysis of Surface Level Ozone Observations in the Ross Island Region

Mark Seefeldt[1,2], Michael Tice[1], Allison Burg[1], Lars Kalnajs[3], Matthew Lazzara[4]

[1]Department of Engineering – Physics – Systems, Providence College, Providence, RI
[2]Cooperative Institute for Research in Environmental Sciences (CIRES), University of Colorado, Boulder, CO;
[3]Laboratory for Atmospheric and Space Physics (LASP), University of Colorado, Boulder, CO;
[4]Antarctic Meteorology Research Center (AMRC), University of Wisconsin-Madison, Madison, WI

During the 2011-12 field season a network of reliable, low power ozone sensors were deployed at existing automatic weather station (AWS) sites in the Ross Island region of Antarctica. The goal of the project is to provide a multi-season dataset of surface level ozone observations that are free of anthropogenic influence. The observations will be used to address high-latitude tropospheric ozone chemistry problems with an emphasis on the occurrence of ozone depletion events. A network of ten AWS sites covering the Ross Island region, with observations covering up to ten years, will be evaluated to establish an observationally based understanding of the region. Additionally, three years of output from the Antarctic Mesoscale Prediction System (AMPS) 1.67 km domain, covering the Ross Island region, will be studied to better identify the high-resolution features for the area. The combination of the AWS observations and the AMPS output provides a robust dataset analyzing the local features for the region. As the ozone observations are collected, with particular emphasis during the austral spring, the meteorology of the region will be analyzed to evaluate any meteorological connections and/or transport mechanisms associated with the ozone depletion events.

A study of winter static stability regimes in the Dry Valleys using pseudo-vertical profiles of temperature

Peyman Zawar-Reza*[,1], Marwan Katurji[1,2], Bob Noonan[1], Iman Soltanzadeh[1], Tanja Dallafior[1,3], Sharon Zhong[2]

[1]Centre for Atmospheric Research, University of Canterbury, Christchurch, New Zealand

[2]Department of Geography, Michigan State University, East Lansing, Michigan

[3]Institute for Atmospheric and Climate Science, ETH, Zurich, Switzerland

*peyman.zawar-reza@canterbury.ac.nz

1. Introduction

Surface climatology of the McMurdo Dry Valleys (MDV) has been studied relatively extensively in the past three decades. In winter, katabatic winds affect the climate of the MDV by increasing local air temperatures by as much as 30°C (Nylen et al. 2004). It has been estimated that an increase of 1% in frequency in strong katabatic events, can increase average winter temperatures by 1°C. The summer wind regimes can be quite different and are predominantly driven by the heating and cooling cycles of the surface in response to solar insolation during synoptically quiescent periods.

Due to logistical reasons and remoteness, little attention has been paid to the within the valley vertical structure of the boundary layer. A rare glimpse into the vertical stability of the valley atmosphere was provided by McKendry and Lewthwaite (1990; hereafter ML1990), but for the summertime field season only. ML1990 used a combination of airsondes, pilot balloons, and monostatic acoustic sounder to derive their Wright Valley vertical profiles. Subsequent studies that cited ML1990 did not build up on the papers knowledge base, so the state of knowledge has remained the same. ML1990 discuss the fact that down-valley strong katabatic winds (in summer) possess neutral stability extending to heights of 2000 to 4000 m, but they also measure periods when stable regimes decouple the surface layer air from aloft.

Although very informative, ML1990 studies stability for a few case studies and in summer, we hope to complement this work by extending the analysis into winter and at higher temporal resolution. There is no information available on the vertical extent of the (stable) boundary layer that can form during synoptically quiescent periods or the thickness of the katabatic intrusions into the valley system climatologically. Data on static stability of the atmosphere can guide not only surface based meteorological studies, but is a good source of validation for mesoscale modelling research.

To our knowledge, Whiteman et al. (2004) was the first study that pioneered the use of surface based temperature measurements to derive pseudovertical temperature profiles. They derived vertical stability by deploying a line of temperature dataloggers in a valley in Rocky Mountains. In that study, it was shown that pseudovertical temperature soundings at night approximated free air temperature soundings over the centre of the valley, thereby providing useful insight into night-time evolution of the boundary layer. Fast et al. (2005) applied the same reasoning to study nocturnal boundary layer over Phoenix, Arizona. Motivated by these studies, we apply the same methods towards the Dry Valleys atmosphere, initially for the Wright Valley. Therefore we present the first assessment of winter static stability in this valley using miniature temperature sensors called iButtons as described below.

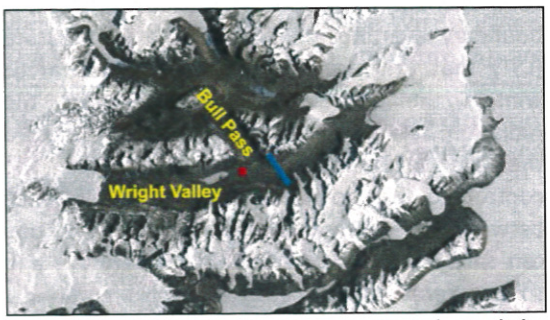

Figure 1 Map of McMurdo Dry Valleys; the red dot shows the location of the AWS while the blue line marks the line where the iButtons array was installed.

2. Data

Data used for this study is collected as part of the New Zealand Terrestrial and Biological Survey (nzTABS) research programme. The overall aim of nzTABS is to characterise biophysical drivers that determine spatial distribution of microbiota. Therefore standard climatological data alongside soil temperature, and remote sensing products (MODIS), is collected continuously; supplemented by data gathered during the summer field season.

Wind speed is obtained through a standard Automatic Weather Station (Campbell) installed near the Bull Pass Hut (unfortunately the wind vane was not operational for this period). Fourteen iButtons (model DS1921G) were positioned on a transect across the Wright Valley just east of Bull Pass (Figure 1; blue line). The transect was roughly aligned in a north-south direction and was located so that a range of elevations for both north and south facing aspects were sampled. The sensors were buried 2cm below the ground to ensure that they were not heated directly by short-wave radiation; however, as we have narrowed our analysis to winter, short-wave radiation is not an issue. To ensure the iButtons could be relocated and retrieved, the location of each device was recorded using a GPS and a bright orange stick was inserted in the ground. The sensors were retrieved the next field season and data downloaded and quality controlled. Since each sensor is logging soil temperature every two hours, a complete annual record is obtained this way at high temporal resolution.

Radiation and surface energy balance concepts dictate that heating/cooling cycles of the boundary layer are primarily driven by fluxes of energy from the surface (ignoring advective components). To a good approximation, in the boundary layer, it is the land surface temperature (LST) that drives air temperature. In Antarctic winter, the short-wave component of the radiation balance is obviously absent; therefore the top soil temperature should mostly be controlled by long-wave radiation balance between the soil and overlying air. That is, one can safely assume that the air temperature and soil temperature are in quasi-equilibrium.

Figure 2 shows a good correlation between air and shallow soil temperatures in winter. The air temperature is the primary driver of soil temperature in winter as the heat storage of soil gets depleted in time when the sun finally sets in Antarctic autumn. As figure 2 illustrates, there is a strong correlation between the air and soil temperatures in winter, lending credence for using the soil data as a proxy for air temperature.

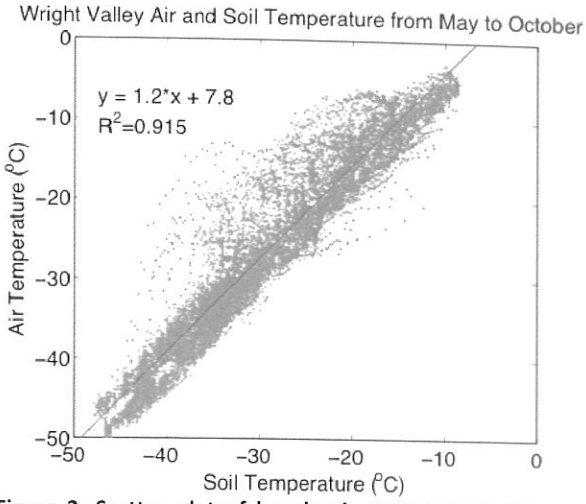

Figure 2: Scatter plot of hourly air temperature the 2cm soil temperature as measured by the AWS at Bull Pass (May to October 2011).

To establish a link with synoptic scale conditions, self-organizing maps (SOM) were constructed for the period of interest in winter. SOMs were recently used by Seefeldt and Cassano (2008) to study low-level jets over the Ross Island Sea (RIS) region. SOMs in this work are prepared by running Polar-WRF v3.3.1, initialized with National Centre for Environmental Protection (NCEP) reanalysis, and nudged every 6 hours. PWRF was setup with a simplified version of the AMPS configuration (http://www.mmm.ucar.edu/rt/amps/information/configuration/configuration.html), and ran two grids, with the inner most grid resolution of 15 km centred over the Ross Sea/Ice Shelf region. Pressure anomaly data was calculated from hourly simulation surface pressure data. Self Organising Maps analysis (SOM) was performed using SOM_PAK (http://www.cis.hut.fi/research/som-research/).

3. Results and discussion

Figure 3 illustrates the pseudovertical profiles of potential temperature alongside the corresponding daily average surface wind speed for the period of study.

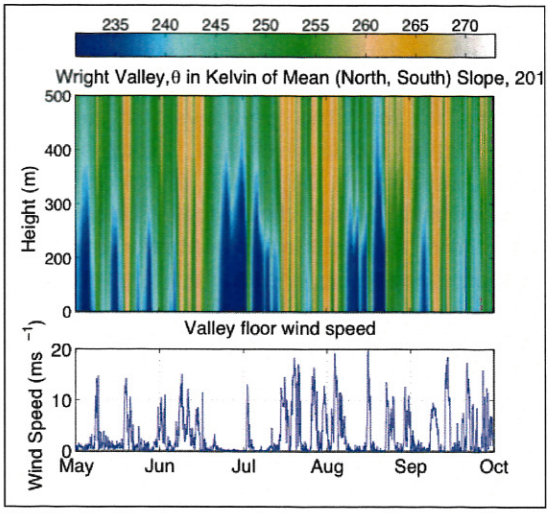

Figure 3: The top panel shows vertical profiles of potential temperature, the bottom wind speed time-series is for Wright Valley weather station.

It is immediately apparent that the pseudo profiles provide useful information about the vertical structure and static stability of the boundary layer. For example, the end of June beginning of July period is meteorologically very stagnant most of the time – wind speeds rarely go above 1 ms^{-1}. At the same time a 300m thick cold pool has settled in this portion of the valley. The top of the cold pool seems to oscillate; this is probably due to interaction with the overlying warm atmosphere. There is a brief period when wind speeds increase and go above 10 ms^{-1}, which leads to the immediate warming of the valley atmosphere; leading towards a more neutrally stratified regime. The katabatic flow in this case seems to be deeper than 500m.

Strong katabatic flows dominate the valley at the end of July and well into August; this results in a mostly neutral boundary layer that is approximately 25°K warmer than the stable cases. In this period, the cold pool is somewhat re-established as the wind speed drops, but never attains the strength of the previous prolonged stable period.

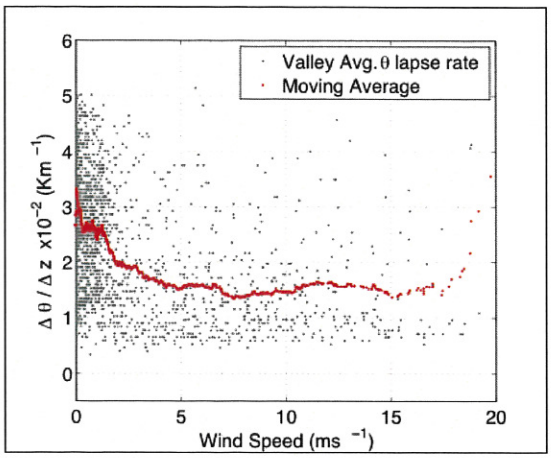

Figure 4: Scatter plot of vertical gradient of potential temperature against wind speed.

To establish a link between surface wind speed and static stability, average vertical gradient in potential temperature are calculated for the entire period of study (Figure 4). Positive values of gradient indicate an increase of potential temperature with height – the stable regime, while a tendency towards zero indicates neutral conditions. Clearly the high wind speeds tend to promote vertical mixing by being more turbulent enhancing neutral stability. Near-neutral stability exists predominantly for wind speeds above 5ms^{-1}.

Interestingly, average neutral conditions can also happen during stagnant periods. A closer examination of the data reveals that in certain situations most of the boundary layer can be neutral, either when the cold pool is forming (from below), or is eroding (from the top), as can happen when the katabatic starts or stops flowing into the area.

The SOM cohort is used to link the mean sea level pressure patterns over the Ross Ice Shelf with the mesoscale climate in the Wright Valley. The SOM nodes (sub-panels in Figure 5) are showing all possible pressure pattern configurations over RIS, these nodes are very similar to the ones described in Seefeldt and Cassano (2008).

Figure 5: Self-organising map for sea level pressure. Colour bar shows departure from the mean for each node.

The frequency of each node is computed for the periods of interest and is shown in Figure 6 alongside Wright Valley AWS data. When the June/July stable regime dominates the valley boundary layer, the SOM indicates higher frequency for the weak katabatic and light wind conditions. The July/August period is characterised by nodes showing strong katabatic forcing in the Ross Island Region, while the August/September period contains a mix of different types.

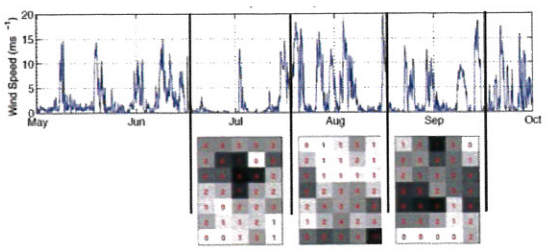

Figure 6: Time-series of wind speed in the Wright Valley and frequency of occurrence of nodes. White is for no occurrence and black is 10% occurrence. The node frequency matrix corresponds to respective panels in Figure 5.

4. Conclusion

We have derived winter static stability profiles in the Wright Valley using temperature sensors planted in soil. The pseudovertical potential temperature profile evolution throughout the valley atmosphere is tightly linked with the synoptic and surface climatology. Strong stable layers can form during synoptically quiescent periods decoupling the surface from upper atmosphere. The inversion depth can be quiet variable in time, but we are not able to explain this variation using just the temperature data alone, a ridge top weather station data is also needed. The katabatic intrusions into the valley boundary layer warm up the entire 500m thick layer by as much as 25°K.

5. Acknowldegments

The authors wish to thank Antarctic New Zealand for providing logistical support for this research. Data was kindly provided by the nzTABS programme.

6. References

Nylen, T. H., A. G. Fountain, and P. T. Doran (2004), Climatology of katabatic winds in the McMurdo dry valleys, southern Victoria Land, Antarctica, *Journal of Geophysical Research*, 109, D03114, doi:10.1029/2003JD003937.

Fast, J., Torcolini, J.C. and Redman, R. (2005) Pseudovertical Temperature Profiles and the Urban Heat Island Measured by a Temperature Datalogger Network in Phoenix, Arizona. *Journal of Applied Meteorology,* 44, 1-13.

McKendry I.G., Lewthwaite E.W.D. (1990) The vertical structure of summertime local winds in the Wright Valley, Antarctica. Boundary-Layer Meteorology 51: 321–342.

Seefeldt, M.W. and Cassano, J.J. (2008) An analysis of low-level jets in the Greater Ross Ice Shelf Region based on numerical simulations. *Monthly Weather Review* 136, 4188-4205.

Whiteman, C.D, B. Pospichal, S. Eisenbach, P. Weihs, C.B. Clements, R. Steinacker, E. Mursch-Radlgruber, and M. Dorninger (2004) Inversion breakup in small Rocky Mountain and Alpine basins. *Journal of Applied Meteorology*, 43, 1069–1082.

Synoptic control of the atmospheric meridional moisture transport into the Antarctic interior: a new approach.

Maria Tsukernik[1]
[1]*Brown University, Providence, RI*

The Antarctic ice sheet constitutes the largest reservoir of freshwater on earth, representing tens of meters of sea level rise if it was to melt completely. However, due to the remote location of the continent and the concomitant sparse data coverage, much remains unknown regarding the climate variability in Antarctica and the surrounding Southern Ocean. In particular, the distribution of Antarctic precipitation and associated long-term changes is one of the crucial and challenging parameters to measure.

In this study we evaluate the role of the moisture flux convergence associated with the mean circulation, planetary waves and synoptic scale systems, all of which are responsible for bringing precipitation into the Antarctic interior. We use the high resolution ERA-Interim data 1979-2010, which allows us to resolve synoptic and mesoscale storm – ultimately responsibly for the majority of atmospheric moisture transport. We find high interannual and regional variability in the meridional moisture flux, with no clear trend over the last 30 years. Further, the variability of the meridional moisture flux does not correlate with Southern Annular Mode or El Niño-Southern Oscillation indices, even in the Pacific sector, indicating that high frequency disturbances play the

We identify key regions that are significant for the meridional moisture transport: Amundsen Sea, Ross Sea and Indian Ocean (Figure 1). The Amundsen Sea sector, where the meridional moisture transport is the highest, reveals a statistically significant decrease in the moisture flux due to transient synoptic motion along the coastal zone. We suggest that the Amundsen Sea provides a window on the complex nature of atmospheric moisture transport in the high Southern latitudes. The Ross Sea region, unlike most of the other regions, reveals a tendency of the meridional moisture flux to increase over 1979-2010, alas the total MMF trend is not quite significant (Table 2). Both Amundsen and Ross Sea have been studied quite substantially from both the atmospheric circulation (Fogt et al., 2012) and cryospheric (Turner et al., 2009, Pezza et al., 2012) perspective. The importance of the Indian Ocean region acting as a "window" for synoptic systems to enter the East Antarctic continental interior is somewhat unexpected. Moreover, according to recent studies on moisture sources (Sodemann and Stohl, 2009) precipitation accumulated over this region can be traced back to the storm track activity in Southern Hemisphere midlatitudes. Hence we decided to investigate moisture pathways of accumulation events in the Indian Ocean region in greater detail. It is interesting to note that the meridional storm track (30°-50°S) activity in this region reveals a statistically significant decreasing trend over the 1979-2010 time period. In addition, this trend is not directly translated into the coastal (60°-75°S) transient eddy activity (Table 2) of this region, suggesting a rather complicated synoptic situation.

We perform detailed analysis of two cases from 2009 and 2010 accumulation events utilizing Polar Weather Research and Forecasting (WRF) model forced with ERA-Interim data as boundary conditions. According to the Automated Weather Station (AWS) observation 2009

and 2010 seasons revealed very different accumulation pattern (Gorodetskaya et al., 2012). The model is used to examine the effects of increased horizontal resolution and nesting on the moisture transport pathways and precipitation amounts. We also perform observational nudging experiment including measurements from the AWS (Gorodetskaya et al., 2012) into our simulation.

Region	Longitudes	Total MMF	Coastal TE	Storm track TE
Weddell Sea	60°W - 0° E	+0.6 (39%)	+0.6 (81%)	-0.5 (56%)
Indian Ocean	0°E - 90°E	-0.9 (89%)	+0.1 (50%)	**-1.0 (95%)**
Pacific Ocean	90°E - 160°E	-0.9 (92%)	-0.1(13%)	**-1.1(95%)**
Ross Sea	160°E - 140°W	+1.8(79%)	-0.6(74%)	+1.2(84%)
Amundsen Sea	140°W - 60°W	-1.7 (86%)	**-1.0 (96%)**	-0.7 (64%)

Table 1. Linear trends in kg m-1 s-1for 1979-2010 period for total meridional flux and transient eddy meridional flux for all 30°-90°S, storm track (30°-50°S) and coastal (60°-75°S) latitude bands. Significant values are in parenthesis, bold values represent statistically significant linear trends at 95% level.

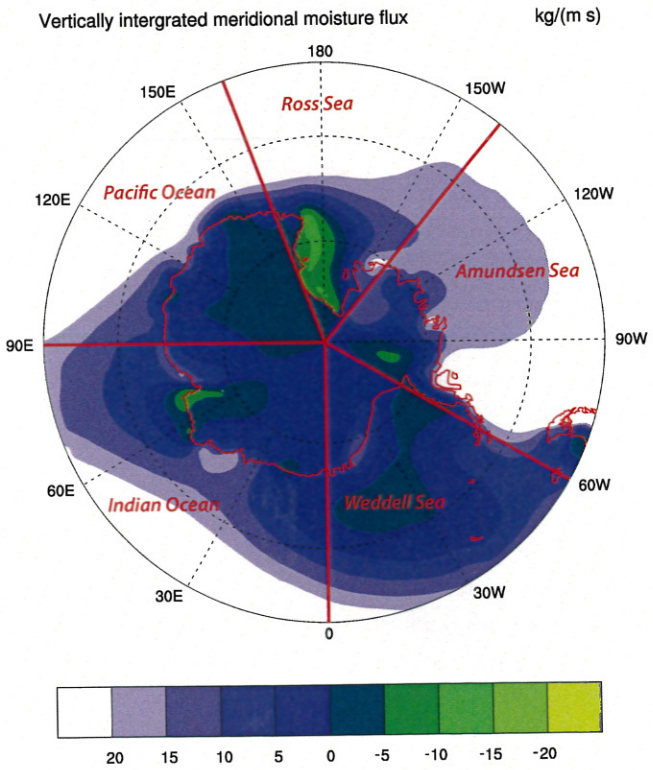

Figure 1. Vertically integrated total meridional moisture flux in kg m-1 s-1 from ERAI 1989-2009 with outlined and labeled regions. Colors indicate poleward (positive) and equatorward (negative) transport.

Fogt, R.L., A.J. Wovrosh, R.A. Langen, and I. Simmonds, 2012: The characteristic variability and connection to the underlying synoptic activity of the Amundsen-Bellingshausen Seas Low, Journal of Geophysical Research, 117, D07111, doi:10.1029/2011JD017337.

Gorodetskaya, I.V., N.P.M. Van Lipzig, M.R. Van den Broeke, W. Boot and C. H. Reijmer, 2012: Meteorological regimes and accumulation patterns at Utsteinen, Dronning Maud Land, East Antarctica: Analysis of two contrasting years. Journal of Geophysical Research, in review

Pezza, A.B., H.A. Rashid, and I. Simmonds, 2012: Climate links and recent extremes in Antarctic sea ice, high-latitude cyclones, Southern Annular Mode and ENSO, Climate Dynamics, 38, 57–73, doi:10.1007/s00382-011-1044-y

Sodemann, H. and A. Stohl, 2009: Asymmetries in the moisture origin of Antarctic precipitation. Geophysical Research Letters, 36, L22803, doi:10.1029/2009GL040242

Turner J., J.C. Comiso, G.J. Marshall, T.A. Lachlan-Cope, T. Bracegirdle, T. Maksym, M.P. Meredith, Z. Wang and A. Orr, 2009: Non-annular atmospheric circulation change induced by stratospheric ozone depletion and its role in the recent increase of Antarctic sea ice extent. Geophysical Research Letters 36, L08502

GCOS, SCAR and EC-PORS

The British Antarctic Survey is the GCOS (Global Climate Observing System) designated lead centre for Antarctica and this means that we monitor the observations that are sent from Antarctic stations and AWS. To do this some web based resources are produced which are listed below.

Latest Antarctic CLIMAT messages received at BAS

http://www.antarctica.ac.uk/met/READER/GCOS/climat.html

Percentage of SYNOPS for main synoptic hours received at BAS on the GTS

http://www.antarctica.ac.uk/met/READER/GCOS/PERCENTAGES/monthly_percentages.html

Plots of 6 hourly synoptic data received from the GTS

http://www.antarctica.ac.uk/met/READER/GCOS/PLOTS/main_index.html

Check of CLIMAT values against met data

http://www.antarctica.ac.uk/met/READER/COMPARISON/index1.html

AntON CLIMAT monitoring

http://www.antarctica.ac.uk/met/jds/met/AntON_CLM_2012.pdf

AntON SYNOP and TEMP monitoring

http://www.antarctica.ac.uk/met/jds/met/AntON_SYN_2012.pdf

Much of this work also links into the work carried out within the SCAR expert group on operational meteorology in Antarctica and also the ATT (Antarctic Task Team) part of EC-PORS (the WMO panel of experts on polar observations research and services).

Screen shots of the web pages will be shown and the links between the groups will be explained.

THE USE OF AMPS IN ICE CORE STUDIES – SOLVED AND UNSOLVED PROBLEMS

Elisabeth Schlosser[1], Jordan G. Powers[2], Michael G. Duda[2], Kevin W. Manning[2]*

[1]Institute of Meteorology and Geophysics, University of Innsbruck, Austria
[2] Earth System Laboratory, National Center of Atmospheric Research, Boulder, CO

1. INTRODUCTION

A thorough understanding of the climate of the past and thus of the climate system is necessary to assess the presently observed climate change and future climate changes. One of the most fascinating and successful methods in paleoclimatology is the study of ice cores from the large ice sheets of Greenland and Antarctica. In these cores, valuable information about the former climate and the composition of the past atmosphere is stored. One of the crucial ice core properties for climate studies is the stable oxygen (hydrogen) isotope ratio of the ice since it is used to derive paleotemperatures. However, for a correct interpretation of the stable isotope profiles from ice cores, the atmospheric processes that led to the precipitation found subsequently as ice in the cores, have to be fully understood. Changes in the general atmospheric circulation can change the origin and seasonality of precipitation, both strongly influencing the stable isotope ratios (Schlosser 1999, Schlosser et al. 2004, 2008). Thus an understanding of the precipitation regime is essential for any ice core study.

2. THE ANTARCTIC MESOSCALE PREDICTION SYSTEM

The Antarctic Mesoscale Prediction System (AMPS) (Bromwich et al. 2005; Powers et al. 2003) provides numerical forecasts for Antarctica, especially for the McMurdo Station region, to support flight operations and scientific activities of the United States Antarctic Program (USAP). These forecasts have been produced since 2000 and archived since 2001, and have also been used for scientific investigations. AMPS was developed by the National Center of Atmospheric Research (NCAR) and the Polar Meteorology Group of Byrd Polar Research Center (BPRC) of The Ohio State University. While AMPS currently employs the Weather Research and Forecasting (WRF) model (Skamarock et al. 2008), at the time of the investigations presented here AMPS used a polar-modified version of the MM5 (5th-Generation Pennsylvania State University/NCAR Mesoscale Model). This version was optimized for use over high latitudes and extensive ice sheets and the polar modifications include: i) representation of fractional sea ice coverage in grid cells; ii) accounting for sea ice with specified thermal properties; iii) modified properties of snow and ice; iv) use of latent heat of sublimation for calculation of latent heat flux over ice surfaces; and v) additional levels in the MM5's soil model for a better representation of heat transfer through ice sheets.

Figure 1 shows the different domains used in AMPS as well as the locations mentioned in this study. The AMPS setup at the time of the study had six grids, with horizontal spacings of 45 km, 15 km, 5 km (three grids), and 1.67 km. These grids had been of lower resolution at the time of the February 2003 event described later: 90 km, 30 km, 10 km, and 3.3 km, respectively. Thus, the latter spacings apply to the case study of February 2003 mentioned in section 4. For most investigations, data from the 30-km domain covering the continent were used.

*Corresponding Author address: Institute of Meteorology and Geophysics, University of Innsbruck, Innrain 52, A-6020 Innsbruck, Austria; e-mail: Elisabeth.Schlosser@uibk.ac.at

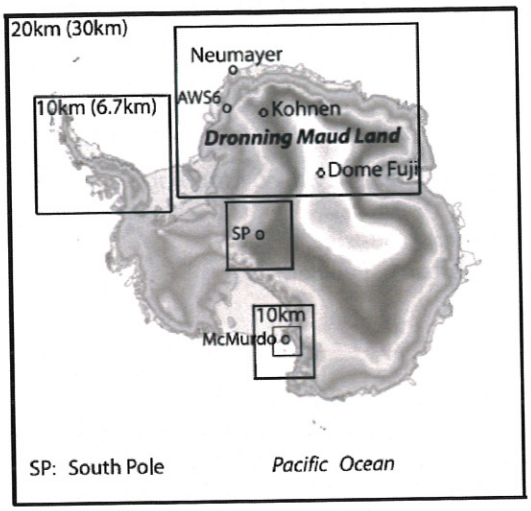

Fig. 1 *AMPS grids at the time of the study: outer frame: 30km domain (20km since September 2005). 10-/6.7km domains over Antarctic Peninsula, South Pole (SP), and western Ross Sea, 3.3-/2.2km domain over Ross Island. An outer domain of 90-/60-km(not shown) extended to New Zealand, Australia, South Africa, and South America. Gray shades refer to model topography. Locations mentioned in the text are also shown: Neumayer, AWS6, Kohnen Station, Dome Fuji.*

For representing physical processes in the atmosphere, the MM5 in AMPS was configured with a suite of schemes and parameterizations. For the case study the key schemes operating were as follows: The Reisner microphysics scheme (Reisner et al. 1998) was used for grid-scale cloud and precipitation processes, while the Grell cumulus parameterization (Grell et al. 1994) handled subgrid-scale convective cloud processes. Note that with respect to the cumulus parameterization, it is minimally active and produces minimal convective precipitation south of 60°S and over Antarctica due to the lack of tropospheric conditions sufficient for convective triggering (e.g., instability, moisture, convective available potential energy (CAPE)). The Eta PBL scheme (Janjic 1994) was used for boundary layer processes. AMPS has previously been analyzed in forecast performance reviews (e.g., Bromwich et al. 2005) and has been applied in climatological investigations (Monaghan et al. 2005; Schlosser et al. 2008) and weather event case studies (Bromwich et al. 2003; Powers 2007).

3. SPATIAL DISTRIBUTION OF PRECIPITATION/ACCUMULATION

The temporal and spatial distribution of precipitation in Dronning Maud Land was investigated using data from the Antarctic Mesoscale Prediction System (AMPS) (Powers et al 2003) archive (Schlosser et al 2008). Comparison to a just previously published mass balance map derived from glaciological data from Western DML (Rotschky et al 2007) showed good agreement between mass balance and mean annual precipitation. Precipitation is found to generally decrease from the coast to the inland plateau.

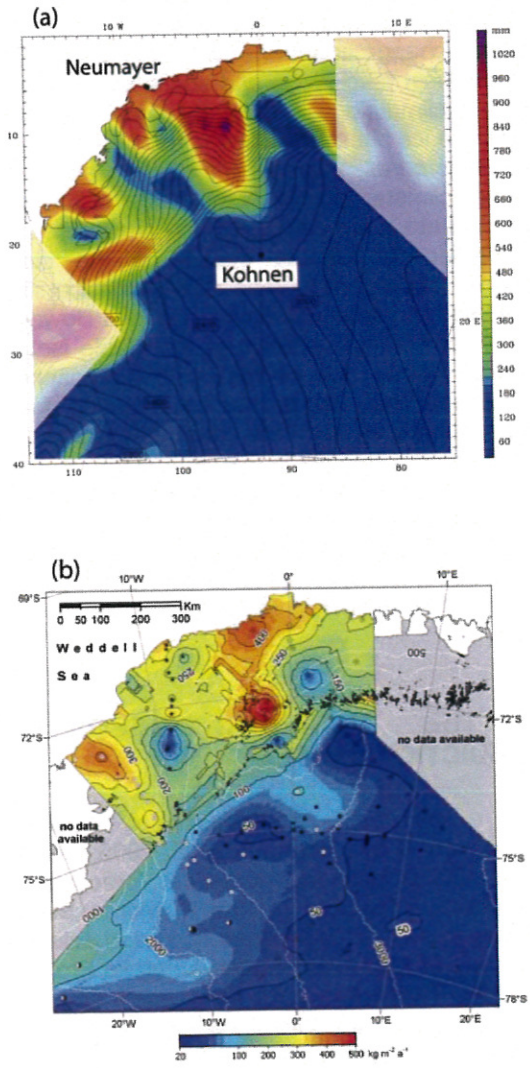

Fig. 2: *Comparison of AMPS precipitation with accumulation map from Rotschky et al (2007)*

Along the escarpment between the low-altitude coastal areas and the interior plateau, local minima and maxima in precipitation correspond to the leeward and windward sides of topographical ridges. Interannual variability of monthly sums of precipitation is fairly high due to the influence of cyclonic activity, which affects the interior of the continent more than previously thought and leads to several high precipitation events per year at the EPICA drilling site Kohnen.

4. TEMPORAL DISTRIBUTION OF PRECIPITATION/ACCUMULATION

It was shown that precipitation in Antarctica has a highly episodic component (see Fig. 3). Whereas on the majority of the days diamond dust prevails in the interior of the continent, the amount of precipitation is strongly influenced by synoptic-type precipitation that can bring up to 50% of the total annual accumulation, although it occurs only on a few days per year (for Kohnen Station: approximately eight events per year).

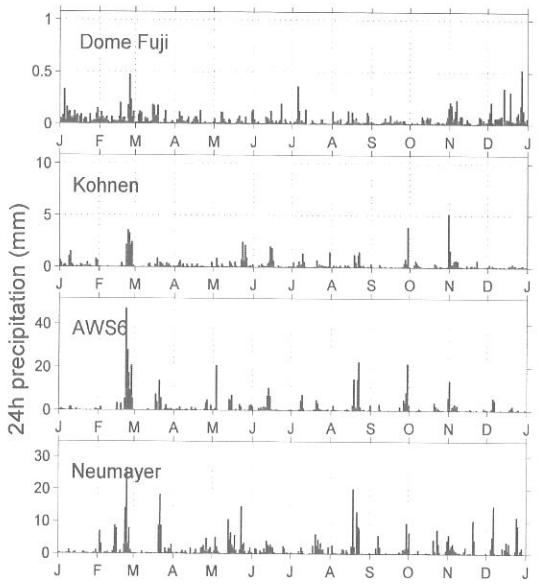

Fig. 3: *Daily precipitation sums for 2003 derived from AMPS for Neumayer (coast), AWS6 (escarpment), Kohnen and Dome Fuji (both inland)*

The clearly visible outstanding event in February 2003 was investigated in a case study (Schlosser et al 2010b).

5. PRECIPITATION MECHANISMS

The characteristics of these high-precipitation events were studied, again using AMPS data for the period 2001-2006 (Schlosser et al 2010a). This investigation includes a case study of an outstanding event in 2003 (Schlosser et al 2010b). Fifty-one cases of synoptic-type precipitation at Kohnen Station were studied in detail. Only for 20% of the investigated cases the responsible synoptic weather patterns were directly connected to frontal systems of cyclones. The majority of the events occurred in connection with anticyclones and corresponding amplified Rossby waves, which leads to advection of warm, moist air from relatively low latitudes. The question remains whether these events prefer certain seasons and whether this seasonality changed between glacials and interglacials. To answer this question remains a challenge. A solution can only be found by combining the efforts of the modeller and ice core communities.

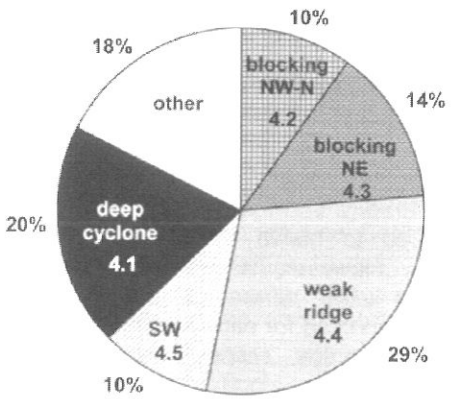

Fig. 4: *Frequency distribution of different synoptic patterns for high-precipitation events (Schlosser et al 2010a, numbers in the pie plot refer to sections in the original paper)*

6. INFLUENCE OF/ON SEA ICE

Furthermore the interactions between Antarctic sea ice and synoptic activity in the circumpolar trough were investigated (Schlosser et al 2011). For practical reasons we used ECMWF Interim Re-analysis data to assess the synoptic situations, however, for temporal variability of precipitation/accumulation the results of the precipitation study with AMPS were used. Sea ice data were provided by NSIDC from passive-microwave satellite measurements. Total Antarctic sea-ice extent does not show large interannual variations. However, large differences are observed on a regional/monthly scale, depending on prevailing wind and currents, and thus on the prevailing synoptic situations. The sea-ice edge is also a preferred region for cyclogenesis due to the strong meridional temperature gradient (high baroclinicity) in that area. The motivitation for this study was to gain a better understanding of the interaction between sea-ice extent and the general atmospheric flow, particularly the influence of warm-air intrusions into the interior of the Antarctic continent, since this influences precipitation seasonality and must be taken into account for a correct climatic interpretation of the cores. Two cases of extreme sea-ice concentration anomalies were studied in relation to the prevailing atmospheric conditions. It was shown, that both strong positive and strong negative anomalies can be related to warm biases in ice cores (indicated by stable-isotope ratios), especially in connection with the negative phase of the Southern Annular Mode.

7. MOISTURE TRANSPORT AT UPPER LEVELS

A linear relationship between air temperature and the oxygen stable isotope ratio is used to derive paleotemperature from ice cores. However, whereas the relationship is always linear, different slopes and y-intercepts are found/used for different regions of Greenland and Antarctica, respectively. Particularly, in Antarctica, the slope changes abruptly at an altitude of about 2000m (Masson-Delmotte et al 2008). Only vague explanations for this change exist so far, since the mechanisms of moisture transport to the interior of the continent and to the escarpment as well as the isotopic fractionation during this transport are not fully understood yet. A study with a mesoscale model (Polar WRF) combined with an isotope model should be done in order to find a better applicable temperature-stable isotope relationship for all altitudes involved.

8. MOISTURE TRANSPORT IN THE ESCARPMENT

Comparison of stable isotope ratios of coastal cores from the vicinity of Neumayer to cores drilled at intermediate altitudes (540-760m) in the hinterland of Neumayer Station have shown that the stable isotope ratios do not generally decrease up to an altitude of 650m meters (Fernandoy et al 2010). Only one core below 600m altitude showed clearly lower values compared to the Neumayer (35m) data. Several cores at altitudes larger than 600m had isotope ratios similar to Neumayer cores, which is contradictory to the theory. The isotope values found in these cores cannot be explained yet. A high-resolution study with Polar WRF might be able to shed some light onto the processes involved.

ACKNOWLEDGEMENTS

This study was financially supported by the Austrian Science Fund (FWF) (V31-N10). AMPS is supported by the US National Science Foundation, Office of Polar Programs and the University Corporation for Atmospheric Research (UCAR) and Lower Atmosphere Facilities Oversight Section.

REFERENCES

Bromwich, D.H., A.J. Monaghan, J. G. Powers, J. J. Cassano, H. Wei, Y.-H. Kuo, A. Pellegrini, 2003: Antarctic Mesoscale Prediction System (AMPS): a case study for the 2000-01 field season. *Mon. Weather Rev*. 131, 412-434.

Bromwich, D.H., A.J. Monaghan, K.W. Manning, J. G. Powers, 2005: Real-time forecasting for the Antarctic: an evaluation of the Antarctic Mesoscale Prediction system (AMPS). *Mon. Weather Rev*. 133, 597-603.

Fernandoy, F., H. Meyer, H. Oerter, F. Wilhelms, W. Graf, J. Schwander, 2010. Temporal and spatial variations of water stable isotope ratios and accumulation rates in the hinterland of Neumayer Station, East Antarctica. *J. Glaciol.* 56 (198), 673-687.

Grell, G.L., J. Dudhia, and D. R. Stauffer, 1994: A description of the 5th-generation Penn State/NCAR Mesoscale Model (MM5). *Tech. Note 398+STR*, 122pp, Natl. Cent. for Atmos. Res., Boulder, Colo.

Janjic, Z.I., 1994: The step-mountain eta coordinate model: Further development of the convection, viscous sublayer, and turbulent closure schemes. *Mon. Weather Rev.*, 122, 927-945.

Masson-Delmotte, V. and 27others, 2008: A Composition: Observations, Atmospheric Circulation, and Isotopic Modeling. *J. Climate*, 21, 3359-3387.

Monaghan, A.J., D.H. Bromwich, J.G. Powers, K.W. Manning, 2005: The climate of McMurdo, Antarctica, region, as represented by one year of forecasts from the Antarctic Mesoscale Prediction System. *J. Climate*, 18, 1174-1189.

Powers, J. G., A.J. Monaghan, A.M. Cayette, D. H. Bromwich, Y. Kuo, and K.W. Manning, 2003: Real-time mesoscale modelling over Antarctica. The Antarctic Mesoscale Prediction System. Bull. Am. Meteorol. Soc., 84, 1522-1545.

Powers, J.G., 2007: Numerical prediction of an Antarctic severe wind event with the Weather Research and Forecasting (WRF) model. Mon. Weather Rev., 135, 3134-4157.

Reisner, J. R., R. M. Rasmussen, and R. T. Bruintjes, 1998: Explicit forecasting of supercooled liquid water in winter storms using the MM5 mesoscale model. Q.J.R. Meteorological Soc., 124, 1957-1968.

Rotschky, G., P. Holmlund, E. Isaksson, R. Mulvaney, H. Oerter, M.R. Van den Broeke, and J.-G. Winther, 2007: A new surface accumulation map for western Dronning Maud Land, Antarctica, from interpolation of point measurements. *J. Glaciol.*, 53(182), 385-398.

Schlosser, E., 1999: Effects of seasonal variability of accumulation on yearly mean $\delta^{18}O$ values in Antarctic snow. *J. Glaciol.* , 45 (151), 463-468.

Schlosser, E., C.H. Reijmer, H. Oerter, W. Graf, 2004: The influence of precipitation origin on the $\delta^{18}O$-T relationship at Neumayer Station, Ekströmisen, Antarctica. *Ann. Glaciol.*, 39, 41-48.

Schlosser, E., Duda, M. G., Powers, J. G, Manning, K. H., 2008: The precipitation regime of Dronning Maud Land, Antarctica, derived from AMPS (Antarctic Mesoscale Prediction System) Archive Data. *J. Geophys. Res.*, 113. D24108, doi: 10.1029/2008JD009968.

Schlosser, E., K. W. Manning, J. G. Powers, M. G. Duda, G. Birnbaum, K. Fujita, 2010a: Characteristics of high-precipitation events in Dronning Maud Land, Antarctica. *J. Geophys. Res.,* 115, D14107, doi:10.1029/2009JD013410.

Schlosser, E., Powers, J. G., Duda, M. G., Manning, K. W., Reijmer, C.H., Van den Broeke, M., 2010b: An extreme precipitation event in Dronning Maud Land, Antarctica - a case study using AMPS (Antarctic Mesoscale Prediction System) archive data. *Polar Research,* doi:10.1111/j.1751-8369.2010.00164.x.

Schlosser, E., J. G. Powers, M. G. Duda, K. W. Manning, 2011: Interaction between Antarctic sea ice and synoptic activity in the circumpolar trough – implications for ice core interpretation, *Ann. Glaciol.* 52 (57), 9-17.

Skamarock, W.C., J.B. Klemp, J. Dudhia, D.O. Gill, D.M. Barker, M.G. Duda, X.-Y. Huang, W. Wang, J.G. Powers, 2008: A description of the Advanced Research WRF version 3. NCAR Technical Note 475. Boulder: National Center for Atmospheric Research.

THE ROLE OF ATMOSPHERIC RIVERS IN ACCUMULATION IN DRONNING MAUD LAND, EAST ANTARCTICA

I. V. Gorodetskaya[1*], N. P. M. van Lipzig[1], F. M. Ralph[2], G. A. Wick[2], M. Tsukernik[3], A. W. Delcloo[4], A. Mangold[4], and W. D. Neff

[1]Catholic University of Leuven, Belgium, [2]National Oceanic and Atmospheric Administration, USA, [3]Brown University, USA, [4]Royal Meteorological Institute of Belgium

1. INTRODUCTION

The poleward moisture transport in midlatitude regions is largely accomplished by the filamentary features of narrow enhanced water vapor bands, the so-called "atmospheric rivers" (Zhu and Newell 1998). The importance of atmospheric rivers for the coastal precipitation in middle latitudes is tremendous: in California they result in severe precipitation events causing floods (Ralph et al. 2006, Bao et al. 2006) and contribute up to 50% of the state's total annual precipitation (Dettinger et al. 2011), and in the South American Andes they are responsible for most of the heavy orographic precipitation, especially in winter (Viale et al. 2011). The role of atmospheric rivers in the Antarctic accumulation has not been yet investigated to the authors' knowledge.

The large part of the annual total snow accumulation over the Antarctic plateau has been attributed to several strong precipitation events, both over the ice sheet interior (Braaten 2000) and over the escarpment and coastal areas (Gorodetskaya et al. 2012a, Noone et al. 1999, Schlosser et al. 2010). One of the most affected regions by the episodic high accumulation events is Dronning Maud Land (DML) in the East Antarctica (Reijmer and Van den Broeke 2003, Schlosser et al. 2010), which is located in the meridional sector of the largest and most persistent moisture flux into the Antarctic ice sheet (Bengtsson et al. 2011) and is marked by a high density of extratropical cyclones nearby (Noone et al. 1999). Synoptic-scale extratropical cyclones are usually associated with large- and meso-scale frontal processes that can result in a narrow region of strong meridional water vapor flux (Ralph et al. 2004). This points to the high potential of atmospheric river contribution to DML moisture transport. Combined with the orographic precipitation effect due the ascent to the Antarctic plateau, atmospheric rivers might be responsible for high accumulation events especially in the escarpment area. The goal of this work is to detect atmospheric rivers reaching the Antarctic ice sheet and investigate their contribution to snow accumulation focusing on DML region.

*Corresponding author address: Irina Gorodetskaya Dept Earth and Env Sci, K. U. Leuven, Celestijnenlaan 200E, 3001 Heverlee, Belgium; email: Irina.Gorodetskaya@ees.kuleuven.be

2. DATA AND METHODS

The analysis is based on the European Centre for Medium-range Weather Forecasting (ECMWF) Interim (ERA-Interim) re-analysis data with 0.25°x0.25° horizontal resolution during 2009. We also use satellite integrated water vapor (IWV) composed images for Southern Hemisphere from the Special Sensor Microwave Imager (SMM/I) derived using Wentz algorithm (Sohn and Smith 2002) for qualitative analysis of atmospheric rivers.

Local snow accumulation data are available from the hourly measurements by the acoustic height meter installed as part of the Automatic Weather Station (AWS) near the Princess Elisabeth (PE) base located in Dronning Maud Land at the ascent to the East Antarctic plateau (72°S, 23°E, 1420 m asl). The AWS has been operating from 2 February 2009 through the present time. During 2009, there is a data gap from November 21 to December 31.

Backward trajectories are calculated using APTRA model available at ECMWF with a horizontal resolution of 1° and time resolution of 6h using ERA-Interim wind fields (Delcloo and De Backer 2008). It has been shown that the kinematic trajectories based on the 3D wind data from a numerical model or other dynamically consistent data set such as provided by ECMWF yields realistic results for five-day analysis (Fuelberg et al. 1996).

3. RESULTS

3.1 Atmospheric river detection

The daily total (meridional and zonal) moisture flux has been separated into the "river" and "broad" fluxes following the threshold established by Zhu and Newell (1998):

$$Q_r \geq Q_{mean} + 0.3(Q_{\max} - Q_{mean}), \qquad (1)$$

where Q_r denotes the "river" moisture flux, Q_{mean} is the zonal mean flux along a given latitude, Q_{max} indicates the magnitude of the maximum flux along a given latitude, and the constant 0.3 is related to the strength of the rivers (after a series of trials this constant established by Zhu and Newell (1998) was found also best suitable for the Antarctic cases). Figure 1 shows the map with river moisture fluxes defined by equation (1) during 19 May 2009, when a deep cyclone was positioned near the DML coast blocked on the east by a high-pressure ridge. This synoptic situation caused anomalously high accumulation at PE station located in the eastern part of DML (Gorodetskaya et al. 2012a).

In order to investigate the long-term moisture transport paths, backward trajectories have been built for several heights above surface and a range of locations around PE. Figure 2 shows the five-day trajectories initiated on 19 May 2009 00 UTC for 500 hPa level at 72°S, from 23°E (PE location) to 63°E (the most easterly extent of the atmospheric river reaching the Antarctic coast in the vicinity of PE on that day). The 500 hPa level represents precipitation height frequently observed at PE (as measured by precipitation radar, Gorodetskaya et al. 2012b). The figure demonstrates the tropical origins of the moisture flux along the atmospheric river arriving east of DML from the Indian Ocean. The origins of the air mass arriving to DML and particularly to PE also show contributions from South Africa, the Atlantic Ocean, and the Weddell Sea in association with the extratropical cyclone.

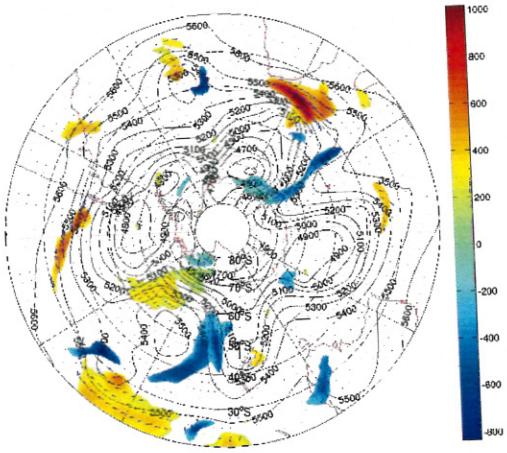

Figure 1. *Moisture flux (kg m^{-1} s^{-1}) by atmospheric rivers Q_r isolated from the broad flux using Eq. (1) (color and vectors) and 500 hPa geopotential height contours for 00 UTC 19 May 2009.*

The close correlation between the vertically integrated water vapor fluxes and IWV has allowed using IWV as a proxy for determining the positions and widths of the atmospheric rivers (Ralph et al. 2004). The method proposed by Ralph et al. (2004) detects atmospheric river cases as narrow (≤1000 km in width), elongated (≥2000 km in length) IWV bands with IWV values in the along- and cross-plume direction exceeding 2 cm. We modify the atmospheric river detection method developed for midlatitudes in order to apply it to cases influencing the Antarctic continent. Two important factors are taken into account: the decrease of the atmospheric moisture-holding capacity due to the strong decrease in the tropospheric temperature and the fact that an atmospheric river reaches the Antarctic coast.

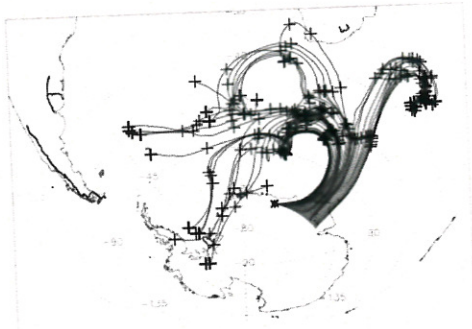

Figure 2. *Five-day back trajectories initiated at a range of locations at 72°S, from 23° to 63°E with one-degree step, at 500 hPa level, on 19 May 2009 00 UTC.*

Most of the meridional moisture transport to Antarctica is concentrated in the layer from 900 to 300 hPa as shown in figure 3 for 70°S and also by van Lipzig and Van den Broeke (2002) for the Antarctic grounding line. The tropospheric holding capacity for this layer is calculated as the integrated saturated water vapor:

$$IWV_{sat} = \int_{900}^{300hPa} q_{sat}(T)dp \qquad (2)$$

The annual mean temperature averaged for this layer and IWV_{sat} both show a strong decline from the equator to the pole with IWV_{sat} decreasing below 2 cm at around 40°S (Fig. 4). It should be also taken into account that warm poleward advection associated with atmospheric rivers can strongly increase IWV_{sat} allowing larger moisture influx into the Antarctic ice sheet compared to the annual mean values. Figure 5 shows a map of IWV_{sat} for the synoptic event during 19 May 2009 associated with atmospheric river moisture flux into DML (Fig. 1). A drop in IWV_{sat} below 2 cm occurs at the 50% sea ice concentration boundary (much further poleward than shown in Fig. 4), decreasing to 0.7 cm at 70°S (compared to 0.4 cm for the annual mean values shown in Fig. 4).

As atmospheric river events are associated with a strong warm and moist advection into DML and the values of IWV_{sat} at each latitude within the atmospheric river are significantly higher than their corresponding annual means, we calculate the IWV thresholds based on the IWV_{sat} for particular atmospheric river case on 19 May 2009 (Fig. 5). We use the 2 cm threshold established in previous studies for midlatitudes for the latitudes, where IWV_{sat}>2 cm (40°, 50° and 60°S) and use 0.5 cm at 70°S. The atmospheric river detection is limited DML region by choosing the events when maximum IWV along each of the above-mentioned latitudes within the meridional sector from 0 to 80°E was greater or equal to the

corresponding threshold. The choice of latitudes ensures the atmospheric river length of ≥2000 km.

3.2 Atmospheric river events at DML

Using the described above method, 18 atmospheric river events were identified within the 0-80°E sector in 2009. SSM/I IWV maps analysis showed that all except three atmospheric rivers were stretching from the Indian Ocean, mostly from the eastern coast of South Africa with a few rivers originating further east. In the three exceptional cases, the atmospheric rivers originated from the Atlantic Ocean.

The total net accumulation at PE during the days with atmospheric rivers comprised 92 mm w.e. or 40% of the total annual accumulation during 2009. The majority of this contribution comes from only three events with daily accumulation larger than 10 mm w.e.

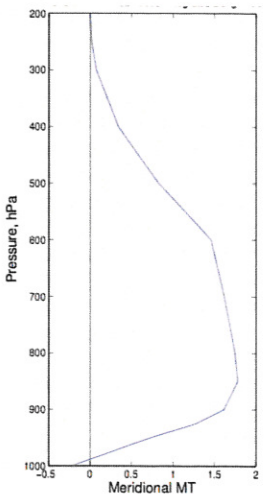

Figure 3. *a) Meridional moisture flux profile (kg m^{-1} s^{-1}) integrated along 70°S latitude (positive southward) as $-\oint qVdl$, averaged for 2009.*

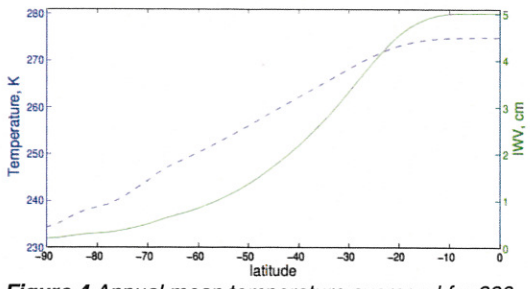

Figure 4 *Annual mean temperature averaged for 900-300 hPa tropospheric layer (blue dashed line) and integrated saturated water vapor calculated for the same vertical layer (Eq. 2) (green solid line). All values are calculated and averaged for 2009.*

4. CONCLUSIONS

The atmospheric rivers reaching the Antarctic ice sheet were detected using a modified method initially developed for midlatitudes. Integrated water vapor threshold established for middle latitudes (Ralph et al. 2004) was lowered from 2 cm to 0.5 cm at 70°S following the decrease in the tropospheric moisture holding capacity due to the tropospheric air temperature drop in the polar latitudes.

Using the new definition, 18 atmospheric river events have been identified during 2009 in the 0-80°E sector of the East Antarctica including the region of our interest Dronning Maud Land. Using the accumulation data from the automatic weather station installed at Princess Elisabeth station, in the escarpment area of eastern DML, we found that these atmospheric river events were responsible for 40% (92 mm w.e.) of the annual total accumulation at PE during 2009. Year 2009 has been characterized by high accumulation at PE location compared to 2010 (Gorodetskaya et al. 2012a). The large contribution of atmospheric rivers to accumulation within this sector means that the difference in the total yearly accumulation can be caused by the fact that just a few large storms and associated with them atmospheric rivers arrive or fail to arrive in Antarctica. The five-day backward trajectory analysis demonstrated the tropical origins of one of the atmospheric river cases reaching the Antarctic coast. This links Antarctic accumulation to tropical latitude moisture availability and dynamics. The current work is focused on refining the atmospheric river definition based on more case studies and extending the analysis to other years and regions.

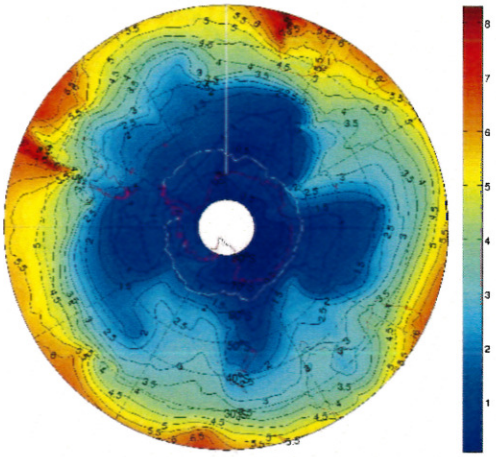

Figure 5. *Map of integrated saturated water vapor (cm, colors and contours) calculated using Eq. 2 for 19 May 2009. Grey line shows 50% sea ice concentration boundary on that day.*

References

Bao, J.-W., S. A. Michelson, P. J. Neiman, F. M. Ralph, and J. M. Wilczak (2006): Interpretation of Enhanced Integrated Water Vapor Bands Associated with Extratropical Cyclones: Their Formation and Connection to Tropical Moisture. Mon. Wea. Rev., 134, p. 1063-1080.

Bengtsson, L., Hodges, K. I., Koumoutsaris, S., Zahn, M. and Keenlyside, N. (2011), The changing atmospheric water cycle in Polar Regions in a warmer climate. Tellus A, 63: 907–920. doi:10.1111/j.1600-0870.2011.00534.x

Braaten, D. A. (2000), Direct measurements of episodic snow accumulation on the Antarctic polar plateau. J. Geophys. Res., 105 (D6), 10,119-10,128.

Delcloo, A. W., and H. De Backer (2008), Five day 3D back trajectory clusters and trends analysis of the Uccle ozone sounding time series in the lower troposphere (1969-2001). Atm. Env., 42, 4419-4432.

Dettinger, M. D., F. M. Ralph, T. Das, P. J. Neiman, and D. R. Cayan (2011), Atmospheric rivers, floods and the water resources of California. Water, 3, 445-478, doi:10.3390/w3020445.

Gorodetskaya, I. V., N. P. M. Van Lipzig, M. R. Van den Broeke, W. Boot, and C. H. Reijmer (2012a), Meteorological regimes and accumulation patterns at Utsteinen, Dronning Maud Land, East Antarctica: Analysis of two contrasting years. *J. Geophys. Res., in review.*

Gorodetskaya, I.V., N.P.M. van Lipzig, S. Kneifel, M. Maahn, S. Crewell, and M. R. Van den Broeke (2012b), Summer cloud and precipitation properties at Utsteinen, Dronning Maud Land, Antarctica, measured by ground-based remote sensing instruments. Abstract at the European Geoscience Union General Assembly 2012, Vienna, Austria, 22-27 April 2012.

Fuelberg, H. E., R. O. Loring Jr., M. V. Watson, M. C. Sinha, K. E. Pickering, A. M. Thompson, G. W. Sachse, D. R. Blake, and M. R. Schoeber (1996), TRACE A Trajectory intercomparison 2. Isentropic and kinematic methods, J. Geophys. Res., 101(D19), 23,927–23,939, doi:10.1029/95JD02122.

Noone, D., J. Turner, and R. Mulvaney (1999), Atmospheric signals and characteristics of accumulation in Dronning Maud Land, Antarctica, *J. Geophys. Res.,* 104(D16), 19191-19211, doi: 10.1029/1999JD900376.

Ralph, F. M., P. J. Neiman, and G. A. Wick (2004), Satellite and CALJET aircraft observations of atmospheric rivers over the Eastern North Pacific Ocean during the winter of 1997/98, *Mon. Wea. Rev.,* 132, 1721-1745.

Ralph, F. M., P. J. Neiman, G. A. Wick, S. I. Gutman, M. D. Dettinger, D. R. Cayan, and A. B. White (2006), Flooing on California's Russian River: Role of atmospheric rivers. Geophys. Res. Lett., 33, L13801, doi:10.1029/2006GL026689.

Reijmer, C. H. and M. R. Van den Broeke (2003), Temporal and spatial variability of the surface mass balance in Dronning Maud Land, Antarctica, as derived from Automatic Weather Stations, J. Glaciol., 49(167), 512-520, doi: 10.3189/172756503781830494.

Schlosser, E., K. W. Maning, J. G. Powers, M. G. Duda, G. Birnbaum, and K. Fujita (2010), Characteristics of high-precipitation events in Dronning Maud Land, Antarctica. J. Geophys. Res., 115, D14107, doi:10.1029/2009JD013410.

Sohn, B.-J., and E. A. Smith (2002), Explaining sources of discrepancy in SSM/I water vapor algorithms. J. Clim., 16(20), 3229-3255.

Van Lipzig, N. P. M., and M. R. Van den Broeke (2002), A model study on the relation between atmospheric boundary-layer dynamics and poleward atmospheric moisture transport in Antarctica. Tellus, 54(A), 497-511.

Viale, Maximiliano, Mario N. Nuñez (2011), Climatology of Winter Orographic Precipitation over the Subtropical Central Andes and Associated Synoptic and Regional Characteristics. J. Hydrometeor, 12, 481–507.

Zhu, Y., and R. E. Newell (1998), A proposed algorithm for moisture fluxes from atmospheric rivers. Mon. Wea. Rev., 126, 725-735.

INSIGHT INTO ANTARCTIC PRECIPITABLE WATER FROM AMPS FORECASTS AND NEW GROUND-BASED GPS MEASUREMENTS

Julien P. Nicolas[1]*, David H. Bromwich[1], and Ian D. Thomas[2]

[1]Polar Meteorology Group, Byrd Polar Research Center, and Atmospheric Sciences Program, Department of Geography, The Ohio State University, Columbus, Ohio, USA
[2]School of Civil Engineering and Geosciences, Newcastle University, Newcastle Upon Tyne, UK

1. Introduction

Cloud forecasting, especially in the lower atmospheric levels, represents one important research effort of the Antarctic Mesoscale Prediction System (AMPS) project (Nicolas and Bromwich 2011b). Indeed, during the Antarctic field season, inaccurate cloud forecasts can have significant impact on aircraft operations. The small number of radiosonde observations in Antarctica greatly limits the possibility for model verification and/or data assimilation of atmospheric moisture fields at these latitudes, especially in the interior of the ice sheet.

The possibility to derive total precipitable water (PW) from ground-based GPS measurements along with the extension of the Antarctic GPS network in recent years have provided important new perspectives to address the problem. Estimates of PW can be inferred from GPS data by using the delay experienced by the GPS signal as it traverses the Earth's atmosphere (this delay is partly a function of the atmospheric moisture content) (Bevis et al. 1992, 1994). Although this technique has been primarily developed and tested for mid-latitude regions, its applicability to the Antarctic region has been recently demonstrated (Thomas et al. 2011).

Since the last International Polar Year, a large number of GPS receivers have been installed in West Antarctica, particularly under the auspices of the Polar Earth Observing Network (POLENET) project (see Fig. 1 and http://www.polenet.org). This represents a potentially substantial improvement of the observing network in an area devoid of upper-air observations. It is also important as the West Antarctic sector largely controls the moisture advection to the McMurdo area in the western Ross Sea, because of persistent moisture convergence to Mary Byrd Land (Nicolas and Bromwich 2011a), and the local wind pattern over the Ross Ice Shelf (e.g., Ross Ice Shelf Air Stream).

The purpose of our study is therefore to explore the value of the PW retrievals from the recently extended GPS network and compare them with PW estimates from AMPS forecasts.

2. Data

Our investigation focuses on a 12-month period between January and December 2011, the period with the most complete GPS network in Antarctica.

* Corresponding author address: nicolas.7@osu.edu

GPS data for a total of 66 sites were obtained but only those with >50% of observations during our one-year study period (55 sites) were actually used in our analysis (Fig. 1). The GIPSY software package (JPL) is used to process the GPS data and estimate the zenith total delays (ZTD), which are related to the observed slant (path) delays between receiver and satellite pairs using the Vienna Mapping Functions 1. Two methods were employed to decompose the ZTD into its hydrostatic and wet components, and infer PW. For the sites equipped with meteorological sensors (POLENET network; Fig. 1, yellow stars), in-situ measurements of surface pressure and temperature were used. The mean tropospheric temperature (*Tm*) necessary to derive PW, is estimated as in Bevis et al. (1994). For the sites without such observations, estimates of the surface pressure and *Tm* were taken from the ECMWF operational analyses.

The AMPS PW data are from AMPS model grid 2 with a 15-km grid spacing. The AMPS forecasts are generated with the Polar WRF model, the polar-optimized version of the Weather Research and Forecasting model. As an operational model, the AMPS model is subject to frequent configuration changes. The

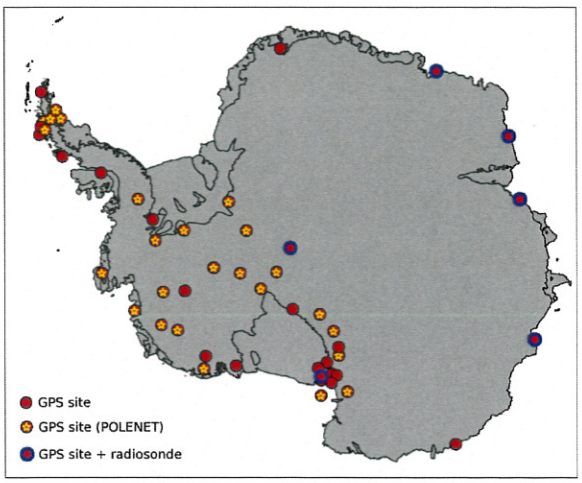

Fig. 1. *Locations of Antarctic GPS sites used in our study, i.e., sites with >50% of data during 2011. The yellow star symbol denotes the GPS sites that are part of the POLENET network and are equipped with meteorological sensors (pressure, temperature). The blue circles denote GPS sites collocated with radiosonde observations.*

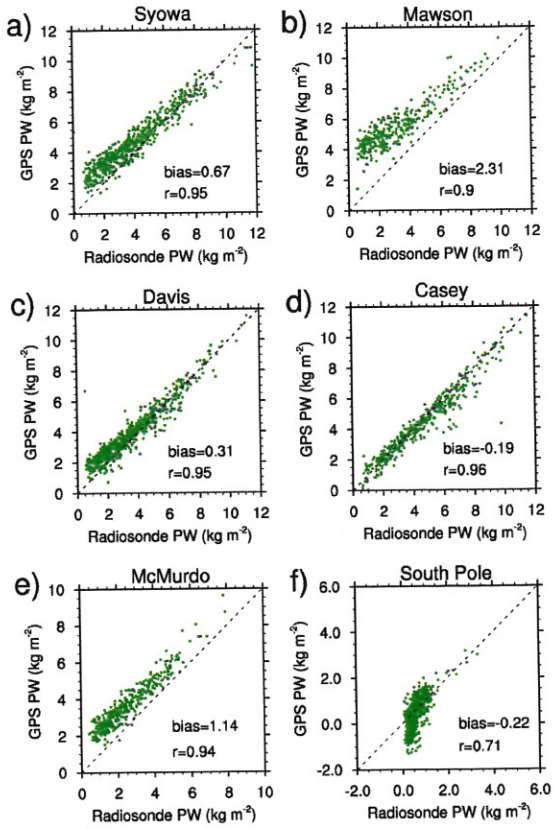

Fig. 2. *Scatter plots of GPS PW estimates versus radiosonde PW observations at six Antarctic stations (blue circles in Fig. 1). Each plot also displays the mean annual bias and correlation (r).*

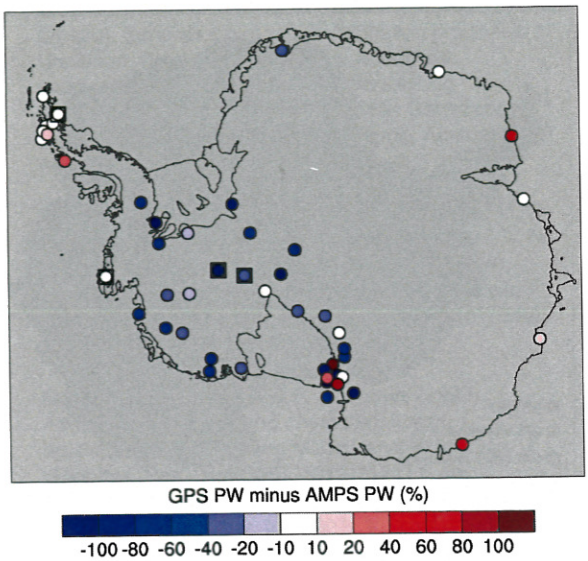

Fig. 3. *Differences in mean annual PW between GPS and AMPS (i.e., GPS PW minus AMPS PW). The differences are expressed in percentages of the AMPS estimates. The four black squares denote the sites whose PW time series are displayed in Fig. 4*

most notable changes during our focus period occurred in April 2011 with the model upgrade from WRF v.3.0.1.1 to WRF v.3.2.1 and the use of the RRTMG long-wave radiation scheme in place of the RRTM scheme. For our investigation, we use PW estimates from the first 24 hours of the daily model forecasts initialized at 00 UTC. Six-hourly time series are constructed by joining together the 0h- (analysis), 6h-, 12h, and 18h-forecasts.

Radiosonde observations were obtained from the Integrated Global Radiosonde Archive (IGRA) for six Antarctic stations collocated with a GPS receiver (Fig. 1, blue circles).

3. Results

Our investigation begins with a comparison of GPS PW estimates against radiosonde observations (Fig. 2). Similar comparison is presented in Thomas et al. (2011) for the year 2004, but changes in the processing of the GPS data argue here for a reevaluation of the GPS-based PW retrievals. At the five coastal sites (Fig. 2a-e), the GPS PW estimates are generally well correlated with the radiosondes but tend to overestimate PW. This wet bias in the GPS was surprisingly not present in the study by Thomas et al. (2011). It is, however, consistent with a possible dry bias of the radiosondes (e.g., Gettelman et al. 2006; Rowe et al. 2008). This issue remains highly dependent upon the radiosonde type used at each site during 2011, which is not known at this point and will therefore deserve further investigation. The comparison at South Pole reveals a different problem, with predominantly negative (non-physical) GPS PW values during the non-summer months, when PW falls below 0.5 kg m^{-2}. Better agreement between GPS and radiosonde is found in summer. Notably, a peak in PW at the end of 2011 is captured both by the radiosonde and the GPS.

Figure 3 compares the GPS-derived mean annual PW estimates with those from AMPS at all GPS sites (the figure shows GPS PW minus AMPS PW expressed as a percentage of AMPS PW). Note that, at this stage, it is still premature to interpret these results as 'biases' either in the GPS or in the model data. The darkest shade of blue denotes sites with GPS PW < 0, a problem similar to that found at South Pole in Fig. 2f. Coastal areas in East Antarctica and the Antarctic Peninsula are generally associated with small differences (within ±10%) or GPS PW estimates higher than those from the AMPS model. The western Ross Sea does not exhibit a coherent picture, which can be attributed in part to the complex topography of the region.

Although the negative GPS PW values suggest some issues likely related to the very dry atmosphere (see Fig. 4), the excessively low PW estimates at inland sites may also result (in part) from elevation differences between the GPS heights (above the geoid) and the 15km resolution model topography. Indeed, GPS receivers are generally installed on isolated rock outcrops or nunatacks that are likely not resolved by the model grid. Yet, we find that lower GPS PW estimates

compared to the model do not necessarily come from sites where the GPS elevation is higher than the model's (i.e., where the GPS 'senses' a smaller portion of the atmosphere than the model).

Figure 4 shows four examples of 6-hourly PW time series that were used to generate Fig. 3. The top two plots (Fig. 4a,b) pertain to coastal sites ('robi' in the northern Antarctic Peninsula, and 'thur' on Thurston Island) where the mean annual PW amounts from model and GPS agree well with each other (see Fig. 3). The PW time series confirm the remarkable agreement between model and GPS, both in term of magnitude and temporal variability (the temporal correlations, *r*, are respectively 0.93 at robi and 0.91 at Thurston). The agreement also persists throughout the year with no apparent seasonality. Of note is the fact that at robi, the initialization of the AMPS model benefits from the constraint of radiosonde observations in the northern Antarctic Peninsula (e.g., Rothera, Marambio). On the other hand, Thurston Island is located in the middle of a region devoid of surface and upper-air humidity observations. Yet, atmospheric moisture observations are not completely absent since SSM/I PW estimates over ice-free ocean are assimilated into the NCEP GFS model, which is used to initialize AMPS forecasts.

The two bottom plots in Fig. 4 show PW time series for two higher-elevated inland sites in central West Antarctica. The 'benn' site (Fig. 4c) reveals good overall agreement between GPS and AMPS (r = 0.88) despite the very low atmospheric moisture content (< 2 mm) and a 325-meter difference between GPS and model elevation. We note however a few episodes with negative GPS PW values (around DOY 100 and DOY 260). For the 'whtm' site (Fig. 4c), located on Mount Whitmore, the GPS PW time series reveal a more systematic occurrence of negative values and lower temporal correlation with AMPS (r=0.58). Figures 4c and 4d illustrate the fact that the issues detected in the GPS PW estimates may not be solely caused by very low moisture contents (AMPS suggests that PW is on average higher at whtm than at benn) or discrepancies between GPS and models elevations ($H_{gps} < H_{amps}$ at benn whereas $H_{gps} > H_{amps}$ at whtm).

4. Conclusions

Our analysis provides for the first time some insight into the moisture content of the Antarctic atmosphere from an extensive network of ground-based GPS measurements. The validation of the GPS-based PW estimates reveals good agreement with radiosoundings at coastal sites, although the comparison is complicated by potential biases present in radiosonde humidity observations. In the Antarctic interior, PW estimates from AMPS and GPS generally exhibit very similar temporal variability. However, for most of the inland sites, the GPS PW retrievals remain excessively low (often with PW < 0). Future work will be needed to address this issue.

In any case, even if GPS-based PW retrievals are only applicable in low-elevated coastal areas of Antarctica, they still represent a very valuable source of observations against which AMPS PW (and PW estimates from other models) can be evaluated.

With regards to our efforts to address the deficient cloud simulation in AMPS forecasts, the remarkable agreement between GPS PW and AMPS PW over Thurston Island suggests that the model realistically captures the amount and temporal variability of atmospheric moisture in this extremely data-sparse area, and points toward the model microphysics as the primary cause of the problematic forecasting of low-level cloud.

Acknowledgements

This research is funded in part by the National Science Foundation Office of Polar Programs via Grant ANT-1135171. The GPS data analysis is supported in part by the Natural Environment Research Council. Most of the work presented here was carried out during

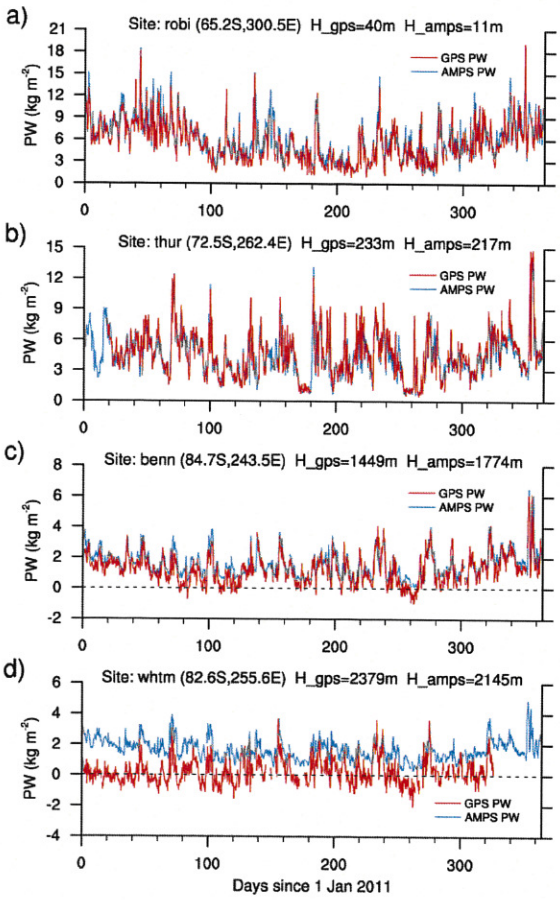

Fig. 4. *Six-hourly PW time series from the GPS (red) and AMPS (blue) data at four sites (robi, thur, benn, and whtm) shown in Fig. 3 (black squares). The header of each plot shows the name of the GPS site, its coordinates, and its height above the geoid (H_gps). H_amps represents the model surface elevation interpolated to the GPS site.*

the visit of Ian Thomas at the Byrd Polar Research Center in February-March 2012 thanks to financial support from Newcastle University. The authors acknowledge all GPS data providers, especially the POLENET program, the International GNSS Service, and the UNAVCO GPS Data Archive (http://facility.unavco.org/data/data.html).

References

Bevis, M., S. Businger, T. A. Herring, C. Rocken, R. A. Anthes, and R. H. Ware, 1992: GPS Meteorology Remote sensing of atmospheric water vapor using the Global Positioning System. *J. Geophys. Res.*, **97**, 15 787-15 801.

Bevis, M., S. Businger, S. Chiswell, T. A. Herring, R. A. Anthes, C. Rocken, and R. H. Ware, 1994: GPS Meteorology: Mapping zenith wet delays onto precipitable water. *J. Appl. Met.*, **33**, 379-386.

Gettelman, A., et al., 2006: Relative humidity over Antarctica from radiosondes, satellites, and a general circulation model. *J. Geophys. Res.*, **111**, D09S13, doi:10.1029/2005JD006636.

Nicolas, J. P, and D. H. Bromwich, 2011a: Climate of West Antarctica and influence of marine air intrusions. *J. Climate*, **24**, 49-67, doi: 10.1175/2010JCLI3522.1.

Nicolas, J. P., and D. H. Bromwich, 2011b: An evaluation of low-level clouds forecast by AMPS Polar WRF. Paper presented at the *6th Antarctic Meteorological Observations, Modeling, and Forecasting Workshop*, Australian Bureau of Meteorology, Hobart, Tasmania, 22-24 June.

Nicolas, J. P., D. H. Bromwich, and I. D. Thomas, 2010: Validating the moisture predictions of AMPS at McMurdo using ground-based GPS measurements of precipitable water. Paper presented at the *5th Antarctic Meteorological Observations, Modeling, and Forecasting Workshop*, Byrd Polar Research Center, Columbus, Ohio, 12-14 July.

Rowe, P. M., L. M. Miloshevich, D. D. Turner, and V. P. Walden, 2008: Dry Bias in Vaisala RS90 Radiosonde Humidity Profiles over Antarctica. *J. Atmos. Oceanic Technol.*, **25**, 1529-1541.

Thomas, I. D., M. A. King, P. J. Clarke, and N. T. Penna, 2011: Precipitable water vapor estimates from homogeneously reprocessed GPS data: An intertechnique comparison in Antarctica. *J. Geophys. Res.*, **116**, D04107, doi:10.1029/2010JD013889.

REGIONAL CLIMATE RESEARCH IN THE ANTARCTIC PENINSULA REGION AND SCHEME OF THE LONG-RANGE FORECAST OF MEAN MONTHLY AIR TEMPERATURE

V. Martazinova, V. Tymofeyev*
Ukrainian Research Hydrometeorological Institute Kiev Ukraine

1. INTRODUCTION.

It is known that a significant increase in the near-surface air temperatures (SAT) has been a characteristic feature of the recent climate at the stations of the Antarctic Peninsula (Marshall et al., 2006, Turner et al., 2005). Regional warming has already led to significant degradation of glaciers, decrease in sea-ice, change in ecosystems etc. Geographical area is characterized by a complex topography with special requirements for measurements at remote points at islands, glaciers, sea ice. Data of The NSF Automatic Weather Station network being assimilated into Antarctic Mesoscale Prediction System is also excellent tool to study local meteorology, however some parts of the Antarctic Peninsula (AP) is underrepresented (plateau glaciers, Palmer Land).

This complicates the modeling of weather conditions in mesoscale, especially local topoclimates, although successful simulations of regional weather conditions obtained in (van Liepzig et al. 2004).

This work discusses needs for future measurements from viewpoint of the regional climate change, and outlines basics of the seasonal forecast in the region of AP.

2. REGIONAL CLIMATE

Warming in this region including Larsen Ice Shelf region is attributed to change in the Southern Annular Mode (SAM) especially in summer (Marshall et al., 2006). In the terms of synoptic meteorology that means frequent cyclones resulted in stronger westerlies crossing the northern Antarctic Peninsula.

Trends in SAT by the data of regional stations show general multi-years growth especially at west coast points as Vernadsky or Rothera (Turner, 2005).

* *Corresponding author address:* V. Tymofeyev, Ukrainian Research Hydrometeorological Institute, Kiev 03028 Ukraine tvvlad@mail.ru

The long-term annual growth in SAT is also observed at stations located in different geographical conditions including Bellingshausen, Orcadas and Esperanza.

The warmest full five-year period at the stations of the Antarctic Peninsula - 1996-2000, and during the recent decade positive anomaly persists at Vernadsky (Fig. 1). However regional warming rate has been slowed down during the latest decade; some stations showed cooling in some seasons.

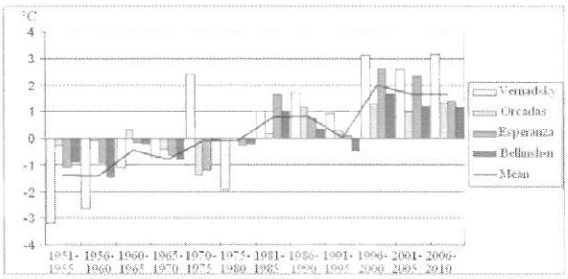

Fig. 1 Accumulated anomalies of mean annual air temperature (from 1961-1990), averaged over five years, at 4 stations of Antarctic Peninsula, and total mean, during 1951-2010.

Since this area is characterized by diverse topography, a comparison is made with data of Marambio and Rothera stations.

Like most stations in the region, the average monthly temperature in January at all stations is increasing, with above-freezing SAT at Vernadsky (from mid-1960s) and Rothera and below-freezing January at Marambio (Fig. 2). However by the end of the reporting period a transition through the freezing point at Marambio is seen.

So one can expect change in summer precipitation/ablation regime like it was at Vernadsky 2 decades ago, with a greater share of the liquid phase precipitation and thus greater ablation in summer.

There is also a decrease in the temperature contrast between the stations Vernadsky and Marambio: 2°C in 1971-1980 and 1°C in 2002-2007.

At a smaller scale, a comparison of Vernadsky air temperatures with the nearest coastal area at the peninsula showed a large temperature difference up to 8-10°C in winter, at elevated points difference is even greater. Monthly difference is estimated as 1-1.5°C, although no long-term time series exist. The Vernadsky station is located at small island as far as 8 km from the AP, and thus it represent rather marine conditions especially in summer.

The main question here is how precipitation/ablation changes in summer at the AP glaciers.

If we assume, that the average temperature at AP is at least 1° C colder over a period of ablation than at Ukrainian station Vernadsky, it can be argued that the period of ablation on Peninsula is much less prolonged, with a predominance of precipitation in solid phase, which means that there are conditions for a total accumulation at low-level glaciers.

However, this requires further investigation with regular measurements at the peninsula and the installation of automatic weather stations.

In addition, the development of local katabatic circulations like föhns resulted in additional warming and drying. Back in the 1950s field parties at stations George Yu and Hope Bay as well as in Adelaide Island, registered unusual increase in temperature, decreased humidity under certain wind directions (Meteorology, 1954).

Föhns are contributed to the monthly maxima of temperature, and when registered frequently they increase monthly mean temperature. So föhn winds is an additional factor in increasing the temperature at Vernadsky station. As they are formed when air flows intersect a mountain ridge in cyclones passing north of 65°S föhns are good indicator of regional circulation and climate change. The phenomenon is observed at both sides of the Antarctic Peninsula, depending on the trajectory of cyclones; Föhns at East side associated with the additional warming which led to calving of the marginal part of the Larsen Ice Shelf.

In the application to climate The following questions arise: have foehns became warmer in the modern era of global warming, and how they contribute to the state of marginal glaciers? In research of the regional climates it is important to know how thermodynamics around mountains has changed, has much moisture is ascended and is there a precipitation change on different elevations, and what is a role of the temperature inversion.

2. ATMOSPHERIC CIRCULATION: FINDING PERIODICITIES

Another aspect of our study is Atmospheric circulation and weather forecasts, including longer-range, up to seasonal. Early we carried out Classification of MSLP fields by classes of probability showing role of the atmospheric circulation in the multi-years' warming in AP region (Martazinova et al, 2007). We also showed circulation mechanism that led to the stabilization of the growth of surface air temperature at the stations of the Antarctic Peninsula in the recent decade.

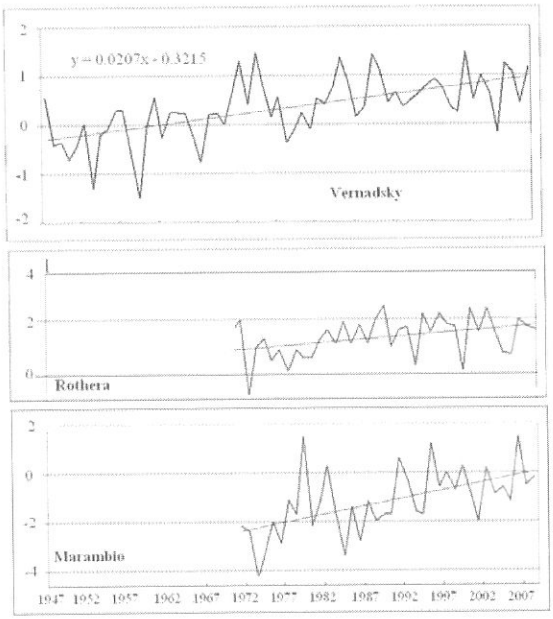

Fig. 2 The mean air temperature of ablation season at Vernadsky, 1947-2009, and January mean at Marambio and Rothera, 1971-2009

Finding periodicities is an important application to this research, and early we showed significant similarity of MSLP fields in comparison to the Northern Hemisphere (Martazinova, 2005).

In accordance with Fig. 3, it is four-vortex circulation system that predominates at the surface; climatic cyclones are located in the Indian Ocean sector of 90-120°W, 200-240 °W (Ross Sea), in the sector 280-330 °E (Bellingshausen Sea), and another low is seen at 10-30 ° E (Weddell Sea). Tracks of the circulation are visible and being outlined better or worse they suggest deepening or weakening of the

large-scale of synoptic formations as a result of eastward displacement where a diagram of the first half of 2008 is shown.

Quasi-2-monthly periodicity is detected via displacement of individual synoptic systems; they move at about 4 ° meridian during the day that is somewhat slower than in the Northern Hemisphere. According to (Carleton, 1981) such objects can be permanently occluded cyclones in the areas of regenerating cyclones.

Further we show how the periodicity on the atmospheric circulation can be detected by means of temporal stability of MSLP fields. Here statistical approach based on finding the Etalon-Analog field was applied [(Martazinova, 2005).

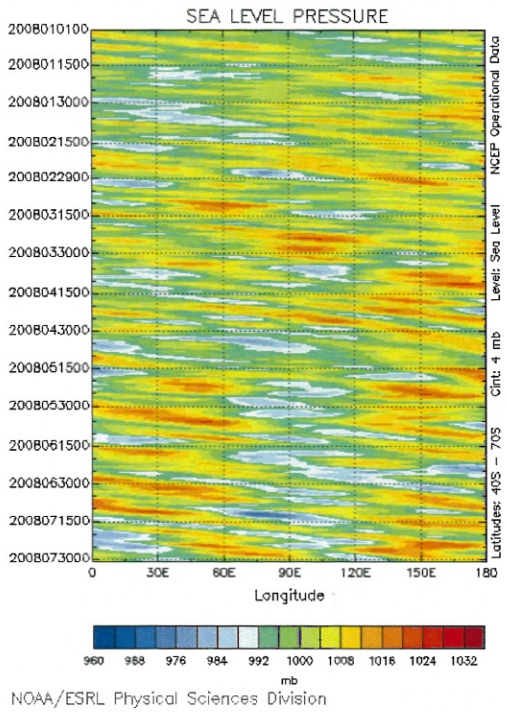

In Fig. 3 Longitude-time Diagram (Hovmoller) of the MSLP from 1 January to 30 July 2008

One of the most effective criteria that allow to geometrically juxtaposing MSLP fields is the geometric similarity criterion calculated on the basis of sign of anomaly of MSLP fields (Bagrov, 1969):

$$\rho_{ij} = (n_{+ij} - n_{-ij}) / N , \qquad (1)$$

Where n_+ is a number of points with coinciding anomalies in pressure fields,

n_- is a number of points with non-coinciding anomalies, N – total number of gridpoints, i,j – gridpoints in the field.

Like correlation coefficient, $-1 \le \rho \le 1$. Criterion ρ can be transformed to correlation coefficient R as follows: $R = 1.57 \rho$ (for $|\rho| < 0.4$). If $\rho = 0.30$ it means that 65% of gridpoints are similar by the sign of anomaly; if $\rho = 0.70$ it means that 90% gridpoints are similar and MSLP fields are identical on10% significance level.

Another traditional criterion is mean squared distance between fields (gridpoints).

Investigation into the periodicities in the troposphere has been made by means of the assessment of the similarities of any given day ("initial field", MSLP or any geopotential height) with subsequent days on seasonal time scale. Degree of similarity also implies the temporal stability of the initial field. For a given period of time the geometric similarity criterion was calculated between fields with time lag τ, resembling calculation of autocorrelation:

$$\overline{\rho}(\tau) = \frac{1}{K - \tau} \sum_{t=1}^{K-\tau} \rho(t, t + \tau), \qquad (2)$$

where ρ is calculated as shown in (1)
and *K – number of geopotential fields,*
τ - time lag (days)

We select the following sectors for MSLP fields: 200-360 degW and 40-75 degS; for upper levels higher 500 hPa all the circumpolar area has been considered south of 50S.

Let's check the periodicity in the troposphere by means of analysis of correlations of any selected initial MSLP field with other fields on seasonal time scale. It was detected that similarity is better in warm year than in cold one (fig. 1).

The similarity criterion of the initial MSLP fields in the first days sharply drops down to 0,30, reflecting evolution of synoptic systems within the synoptic period (Fig. 4). In the warm 1998 (one of the warmest in AP) a significant maximum is registered at 12-14th day however no maximum is seen in colder year. Another peak (greater than 0.50) is detected in 1998 at 2-monthly lag, close to 70th day; it is important for seasonal forecast. First "synoptic" maximum in ρ in warm year imply similarity in MSLP fields related with series of cyclones and second one is longer-range implying circumpolar displacement of cyclone(s).

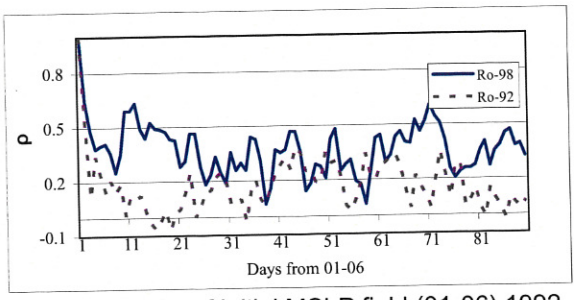

Fig. 4. Similarity of initial MSLP field (01-06) 1992 (cold) and 1998 (warm) with subsequent fields at seasonal scale.

Doing the same but for all fields during winter season with 90days shift we can see a smoother variability but with maxima in ρ on the monthly-and-half time scale (Fig. 5) We recognized such peaks in all seasons however summer (DJF) peak corresponds to 55-60th day, and winter (JJA) one is a bit longer. So winter periodicity is longer than in summer. Such peaks in the atmospheric circulation are evidences for the low frequency oscillation related with circumpolar displacement of the planetary waves.

Anomalies at 500 hPa level should be taken from the axis line of the planetary frontal zone, which has seasonal shift.

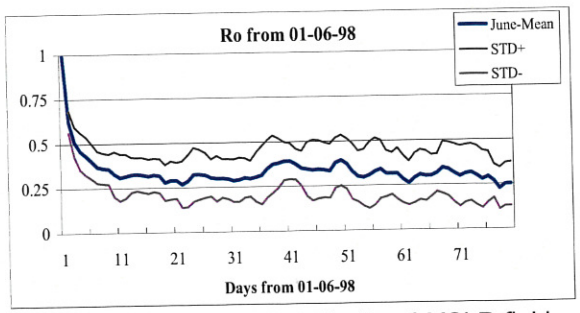

Fig. 5. Mean citerion of similarity of MSLP fields from (01-06) 1998 with subsequent fields at seasonal scale; Initial field is shifted 1 day. Confidence interval ± σ.

Our experience has shown that when selecting analogues in MSLP or upper-level field the best results is reached when displacement of the field including positions of individual synoptic systems within the area of interest is taken into account.

Typically there is some shift between atmospheric fields at a few degrees both in latitude and longitude. This shift has been named as "floating", to get best matching between the atmospheric fields the similarity should be assessed accounting for "floating" in the MSLP field, we showed for the Northern Hemisphere.

Floating means application of the method of finding the most accurate matching in meteorological fields by shifts by longitude and latitude. Floating of any field within two-month interval was restricted by a limit of 5 deg E and W, and N-S, which is determined by the distance between the individual highs and lows and seasonal shifts. At each (daily) time step a maximum similarity matrix ρ (max) of synoptic processes in the Southern Hemisphere has been calculated, taking into account shift both in latitude $\pm\Delta\varphi$ and longitude $\pm\Delta\lambda$.

$$\rho_{(max)} = \begin{pmatrix} 1 & \rho_{12(max)} & \rho_{13(max)} & \cdots\rho_{1K(max)} \\ & 1 & \rho_{23(max)} & \cdots\rho_{2K(max)} \\ & & \cdots & \cdots\cdots \\ & & & 1 \end{pmatrix} \quad (3)$$

where ρ_{ij} (max) - the best measure of the similarity of the initial synoptic fields with the subsequent one with time step j = 1,2,. . ., .

For example ρ_{13}(max) shows the best similarity of the MSLP field of the first and third days.

So the main task in this research is to find a maximum similarity matrix and to obtain the displacement of the initial MSLP field. Matrices were calculated for all months of each year.

4. SCHEME OF THE LONG-RANGE FORECAST OF MEAN MONTHLY AIR TEMPERATURE

Based on detected quasi periodicity in the atmospheric circulation a forecasting scheme of the anomaly of mean monthly air temperature 2 month in advance ($\Delta T\, t_{+2}$) has been developed for the Antarctic Peninsula region. General linear regression scheme (least squared method) for summer and winter in application to Vernadsky data is as follows:

$$\Delta T\, t_{+2} = 2{,}4\, \Delta T_t \; -1{,}57, \quad (4 - \text{Winter})$$
$$\Delta T\, t_{+2} = 0{,}71\, \Delta T_t \; +0{,}57 \; (4 - \text{Summer})$$

where as a predictor (ΔT_t) the anomaly of the mean SAT in the winter season (June-September) or summer months (DJF).

The regression coefficients are different for warm and cold season due to the different daily

and monthly air temperature ranges; in winter it is significantly larger.

Evaluation of prognostic schemes was carried out by the dependent and independent data of individual years 1991-2010, months of cold and warm seasons. When testing the method it was found that the sign of the anomaly in the second month from the initial one is successfully predicted, with a probability of 75% during the cold period and larger than 80% during the warm period. It should be noted that the temperature anomalies close to 1°C are predicted well in the range of error ± 0,5°C, but this method has poor predictability for the major anomalies of 2-4°C, and thus lowers the success in this prediction method.

Taking into account greater variability in SAT in winter months some correction has been made to the scheme including the mean square difference between the predicted and the actual temperature.

A new linear regression equation was obtained, allowing to calculate the extreme values of anomalies:

$$\Delta T_{t+2} = \varepsilon(\alpha \Delta T_t + b) \qquad (5)$$

Where predictor ΔT_t as above (4), and,

ε – coefficient of extremality, calculated as follows:

$$\varepsilon = \sqrt{\frac{\sum_{k=1}^{N} \Delta T_{kp}^2}{\sum_{k=1}^{N} \Delta \hat{T}_{kp}^2}}, \qquad (6)$$

where ΔT_{kr} - factual anomaly in the average monthly air temperature in the second month from the initial;

$\Delta \hat{T}_{kp}$ - predicted monthly anomaly of air temperature in the second month.

However, this improvement in the prediction scheme has achieved at the expense of some neglecting of small deviations in monthly SAT anomaly however skill probability of the sign anomaly remains high.

Future work will include consideration of the phenomenon El-Nino as it contributed greatly to regional climate at seasonal and annual scales.

CONCLUSIONS

This work describes current state in the regional climate, discusses needs for future measurements from viewpoint of the further study in the regional and local climates.

Future plans include research at the Antarctic Peninsula glaciers along with installation of automatic weather stations, at seaside just opposite Vernadsky station (location of Rasmussen Hut) and at some point further (at higher elevation) at AP. The state of AP glaciers should be assessed and the role of local circulations in the regional climates. This is particularly important at the moment when the temperature anomaly peaked at the region of AP and further projections are not clear

Method of the seasonal forecast for the region of Antarctic Peninsula is presented; in the further development it can be used for the entire Antarctica.

References

Bagrov N.A., 1969: Classification of synoptic situations. J. Meteorologiya and Hydrologiya 5, 3-12 (in Russian)

Carleton A.M., 1981: Climatology of the "Instant Occlusion" phenomenon for the Southern Hemisphere winter. Mon. Wea. Review, N 109, 177-181.

van Lipzig N.P.M., King J.C., Lachlan-Cope T.A., 2004: Precipitation, sublimation, and snow drift in the Antarctic Peninsula region from a regional atmospheric model. J. of Geoph. Res., vol. 109, D 24106-D24112.

Martazinova V., 2005: The Classification of Synoptic Patterns by Method of Analogs. J. Environ. Sci. Eng., 7, 61-65.

Martazinova V., Tymofeyev V., 2007: Interdecadal changes of tropospehric circulation in Southern extratropics during the recent warming in the Antarctic Peninsula (U.S. Geological Survey and The National Academies; USGS OF-2007-1047). Extended Abstract.067.

Meteorology of Falkland Islands and Dependencies. Roy. London, 1954, 250 p.

Marshall G.J., Orr a., van Lipzig N.P.M., King J.C., 2006 The impact of changing Southern Hemisphere Annular Mode on Antarctic Peninsula summer temperatures, J. of Climate, 19, 5388-5404

Turner J., Colwell S., Marshall G., Lachlan-Cope T., Carleton A., Jones P., Lagun V., Reid F., Iagovkina S: Antarctic climate during the last 50 years. Int. J. Climatol., 2005, 25, 279-294.

Evaluation of the Antarctic Mesoscale Prediction System (AMPS) in the Ross Island Region Based on a Comparison to Automatic Weather Station (AWS) Observations

Michael Tice[1] and Mark Seefeldt[1,2]

[1]Department of Engineering – Physics – Systems, Providence College, Providence, RI
[2]Cooperative Institute for Research in Environmental Sciences (CIRES), University of Colorado, Boulder, CO

The Antarctic Mesoscale Prediction System (AMPS) provides a robust and consistent data source for meteorological studies across Antarctica. The Ross Island region is home to McMurdo Station and is the primary logistical hub for the United States Antarctic Program. An evaluation of the AMPS 15 km and 1.67 km domains is performed in comparison to automatic weather station (AWS) observations across the Ross Island region. The evaluation covers the years 2009 – 2011 and includes 10 AWS sites in the region. The 12 - 23 hour AMPS forecasts from successive model runs are concatenated together forming a continuous time series. The AMPS values for 2 m temperature, station pressure, wind speed, and wind direction are evaluated in comparison to the AWS observations through a statistical model evaluation analysis, as well as in comparing time series plots. The results provide confidence that AMPS provides an accurate representation of the atmospheric state in the Ross Island region. An upcoming application of the AMPS products is in the analysis of the meteorology and atmospheric transport in analyzing ozone depletion events in the Ross Island region.

An Analysis of 10-years (2001-2010) of Automatic Weather Station (AWS) Observations in the Ross Island Region

Allison Burg[1] and Mark Seefeldt[1,2]

[1]Department of Engineering – Physics – Systems, Providence College, Providence, RI
[2]Cooperative Institute for Research in Environmental Sciences (CIRES), University of Colorado, Boulder, CO

An analysis of 10-years of automatic weather station (AWS) observations from the Ross Island region highlights the meteorology and climatology of this region with widely varying topography. The Ross Island region has long been one of the more heavily meteorological instrumented locations of Antarctica. This is due in part to the less demanding field logistics for the installation and maintenance of the AWS, and to support the operational meteorology forecasting of the United States Antarctic Program. Observations of ten AWS sites, spanning the years 2002-2011, is completed to characterize the meteorology and climatology of the region. Monthly analyses of temperature, pressure, wind speed, and wind direction are completed to produce monthly and annual averages and extremes. The resulting analyses provide a more complete understanding of the meteorology in the region. Such an improved understanding will be particularly valuable for a current study observing the surface level ozone of the region with an emphasis on ozone depletion events during the austral spring.

Validation of the Diurnal Cycles in Atmospheric Reanalyses over Antarctic Sea Ice

Esa-Matti Tastula, University of South Florida
Timo Vihma, Finnish Meteorological Institute
Edgar L Andreas, Northwest Research Associates
Boris Galperin, University of South Florida

Atmospheric reanalyses are widely applied in Earth sciences and thus need to be comprehensively validated. In the previous studies concentrating on the performance of different reanalyses, the results have been given as seasonal, monthly, or daily error statistics. For many applications it is, however, important to know how well the reanalyses perform with respect to the diurnal cycle. Conditions at high latitudes are particularly challenging for modeling of the diurnal cycle due to the small diurnal range of the solar zenith angle and the stable stratification of the atmospheric boundary layer. To test how well the most widely used reanalysis products (ERA-Interim, ERA-40, JRA-25, NASA-MERRA, NCEP-CFSR, and NCEP-DOE) manage to reproduce the diurnal cycle in such conditions, we use observations from the Ice Station Weddell (ISW), 26 Feb 00 UTC – 28 May 18 UTC (93 days). The quantities considered are incoming and outgoing shortwave and longwave radiation, fluxes and sensible and latent heat, cloud cover fraction, near-surface temperature, specific humidity, and wind speed. The average cycles are calculated based on the values at 00, 06, 12, and 18 UTC. Because the local time at ISW is four hours behind the UTC-time, the obtained cycles do not represent the true cycle but an approximation based on the four available values. To assess how these cycles evolve on seasonal scale, separate analyses for three 31-day subsets are also carried out. The uncertainty of an average diurnal cycle for the 95% confidence level is determined based on Monte Carlo simulations with red noise time series obtained by fitting an AR(1) model to the spectra of the residuals of the diurnal cycle fit.

The results demonstrate that there is a great variability among the diurnal cycles of the flux quantities given by different reanalyses. Shortwave radiation is problematic for ERA-Interim and ERA-40 during the first two subperiods during which these two model products yield too small a range. In contrast, NCEP-CFSR and NCEP-DOE struggle with the last subset where the former underestimates the cycle whereas the latter overestimates it, as does JRA-25 as well. The shape of the cycles is distorded in NASA-MERRA and NCEP-DOE: both give 8.00 LST (local sun time) values too large compared to the 14 LST ones. JRA-25 also underestimates 8.00 LST values. Overall, the diurnal cycle of the outgoing shortwave radiation is poorly captured by the reanalyses.

The problems associated with the shape of the cycle are not limited to shortwave radiation alone: none of the reanalyses succeeds with the observed shape of the diurnal cycle of the incoming longwave radiation, either, with a 14 LST minimum and an 8 LST maximum. Due to missing values, the average diurnal cycles could not be calculated for sensible and latent heat fluxes. There are, however, a few discernible cycles in the observations that compare well with the ones given by NASA-MERRA and NCEP-CFSR. The most curious feature about the diurnal cycle of sensible and latent heat fluxes is the tiny amplitude yielded by ERA-Interim and ERA-40.

Cloud cover fraction and near-surface temperature, specific humidity, and wind speed all feature small diurnal ranges, which, in most cases, fall within the uncertainties of the observed cycle. Yet, there is a statistically significant, albeit weak, diurnal cycle in the observed cloud cover fraction. This cycle is poorly captured by the reanalyses.

To better distinguish which one of the reanalyses is the most competent in reproducing the diurnal cycles at ISW, we apply a skill score approach. A reanalysis is awarded a point, if it accurately gives the range and the shape of the diurnal cycle of the studied quantities. The highest score goes to NCEP-CFSR, closely followed by ERA-Interim. There is a significant gap between the amount of

points received by these two and the amount given to the remaining four. A part of the shortcomings is due to the failure to capture the diurnal cycle in cloud cover fraction, which leads to errors in other quantities as well.